Escola de Camins
Escola Tècnica Superior d'Enginyeria de Camins, Canals i Ports
UPC BARCELONATECH

MASTER THESIS

Master

CIVIL ENGINEERING

Title

NUMERICAL ANALYSIS OF CANTILEVER AND ANCHORED SHEET PILE WALLS AT FAILURE AND COMPARISON WITH CLASSICAL METHODS

Author

ALEJO GONZÁLEZ TORRABADELLA

Tutors

ALEJANDRO JOSA GARCÍA-TORNEL
SEBASTIÀ OLIVELLA PASTALLE

Speciality

GEOTECHNICS

Date

JANUARY 2013

Acknowledgments. ***Agradecimientos***

Gracias a mi familia, a mis compañeros y a mis amigos. Gracias a mi madre por apoyarme, no sólo en esta tesina, sino en todo lo que he hecho. Gracias a Guille por compartir tantas horas de biblioteca. Gracias a Jose, por tu ayuda y también por las horas compartidas. Gracias a todos los compañeros de máster por la buena sintonía. Gracias a Agustín: esta tesina es la continuación de la tuya y he pretendido estar a la altura de un listón que dejaste alto. Gracias por estar siempre disponible y por tu inestimable ayuda.

Por último gracias a mis tutores, Alejandro y Sebastià, no sólo por su papel crucial en la dirección de este estudio, también por las lecciones aprendidas en los años de Obras Públicas.

INDEX

1. INTRODUCTION AND OBJECTIVES

1.1. Introduction

Concrete sheet pile walls were seldom designed before de beginning of the 20th Century, dating the first design methods from the early 1900's. It was in the 1950's, when sheet pile walls were broadly established as a solution to solve problems associated with deep excavations near buildings, subterranean structures or below the water table. Since then, the growing need to use scarce land efficiently, along with the improvement and development of specialized machinery with a greater efficiency, have led to an increase in the use of sheet pile walls.

Although design methods have been constantly reviewed and improved, these have not changed much in the last 50 years. Its usage is fully extended due to its simplicity and reliability. Despite the development of numerical methods in the last decades applied to geotechnical engineering the "classical" analytical methods are still broadly used.

This Master Thesis is framed into a wider study of the behaviour of sheet pile walls at failure. In particular, it is the continuation of a previous work by Cuadrado (2010) *[Stress-strain analysis at failure and safety conditions in cantilever and anchored sheet pile walls. Comparison with classical methods]*. In this study the author developed a detailed assessment of the classical methods for cantilever and single-anchored sheet pile walls and compared them with the Finite Element method. Additionally, that work included a contribution on safety practices, consisting of increasing the embedment depth by 20% and reducing the passive resistance.

The first motivation of this Master Thesis is the elaboration of a scientific paper based on the previous work of Cuadrado (2010). To do so, several weak points of this study had to be reviewed. As a first step, the sate of knowledge had to be reviewed in depth. The contribution of this master thesis has been to study the influence of some parameters whose influence was previously missed. The analysis has been focused on observing changes in the behaviour of sheet pile walls when those parameters or most significant data are changed. The main findings are that the initial stress state of the soil has an influence into the cantilever sheet pile wall behaviour. For K_0 (at-rest coefficient) values between 0.7 and 0.9 the minimum wall movements are registered.

The second motivation of this Master Thesis is the extension of the sheet pile wall modelization to the multiple-anchored case. For that case, the effects of increasing the anchor force and the staged excavation are analysed. Results show that when increasing the anchor force the movement of the wall is limited. In the staged excavation study, it may be seen that larger movements are registered with a late installation of the anchors. The effect of the early pre-stressing of the anchor is then to reduce the movements, particularly at the top of the wall.

1.2. Objectives

As mentioned, the main objectives of this Master Thesis are the elaboration of a paper towards the publication in a specialized journal, and to extend the previous studies to multiple-anchored sheet pile walls. Additionally, and as previous steps, this work thoroughly reviews the existing literature and validates the previous results.

The process has consisted of the following chronological steps:

- In-depth bibliographic review of published papers and all the available literature related to sheet pile walls. This review has included design limit equilibrium methods, numerical methods and theoretical or applied studies that have been widely treated since the middle 20th century.

- Review and appraisal of the previous results focused on cantilever and single-anchored sheet pile walls. Cases have been replicated and the influence of previously determined parameters has been studied in depth.

- Elaboration of a scientific paper, in order to be published according to a standardized layout.

- Extension of the previous study to multiple-anchored sheet pile walls. Resolution of the cases proposed through the Finite Element program Plaxis and analysis of the results.

1.3. Contents

This document can be seen as a collection of several fairly independent studies, which however constitute the parts of a total single body.

This master thesis is organized as follows:

The second chapter is named Background and includes a general description of sheet pile walls. It introduces the reader into the background of the sheet pile wall design, starting from the grounds, the earth pressure calculation and the classical methods.

The third chapter contains a review of the state of knowledge, from the first publications related to sheet pile walls until the most recent papers published in geotechnical journals. Some publications are merely mentioned, some others are reviewed in depth.

The fourth chapter describes the general use of the commercial software Plaxis and presents the model used.

The fifth chapter is born from the previous work of Cuadrado (2010), and discusses the influence of the initial stress state on sheet pile walls behaviour.

The sixth chapter presents the study of a two-level-anchored sheet pile wall. A discussion of the construction procedure and the anchor load is presented. This chapter includes the modelization of a three-level-anchored sheet pile wall, and results are compared with the two-level-anchored one.

Finally, the seventh chapter presents the conclusions of the study.

2. BACKGROUND

2.1. First sight on sheet pile walls

Retaining structures are commonly divided into two families:

- Rigid retaining structures, where the stability is provided by the use of a large volume of mass. Only rigid body movements can occur.

- Flexible retaining structures, where other properties of the materials, such as stiffness, strength and wall thickness are exploited in order to provide the stability. Bending and rigid body movements are found.

Sheet pile walls are classified as flexible retaining structures. The stability is provided through an embedment of the wall on the ground working as a cantilever structure (see Figure 2.1) and eventually a system of anchors (see Figure 2.2), so the wall is subject to shear stresses and bending moments. One of the main benefits is the minimization of used material, in contrast to the needs of rigid retaining structures.

Sheet pile walls are in essence walls built before excavating, with the double aim of resisting the earth pressure generated by the excavation, and limiting or preventing the water inlet. The execution of a sheet pile wall consists on an excavation of a trench, large and deep, without the need of shoring, but usually stabilized with bentonite slurries. Then, reinforcement bars are placed and the concrete is laid, or prefabricated elements are placed instead.

Sheet pile walls are not only able to resist earth pressures and prevent the water inlet, but also to receive vertical loads transmitted by other structural elements. Moreover, sheet pile walls are an efficient solution to limit ground movements associated with the excavation. Thus, there are four main functions that can be carried out by a sheet pile wall (Jiménez Salas, 1980):

i) Resist the thrust generated by the excavation.
ii) Limit the movements in the back of the wall, in the unexcavated zone.
iii) Prevent from the water inlet.
iv) Support vertical loads.

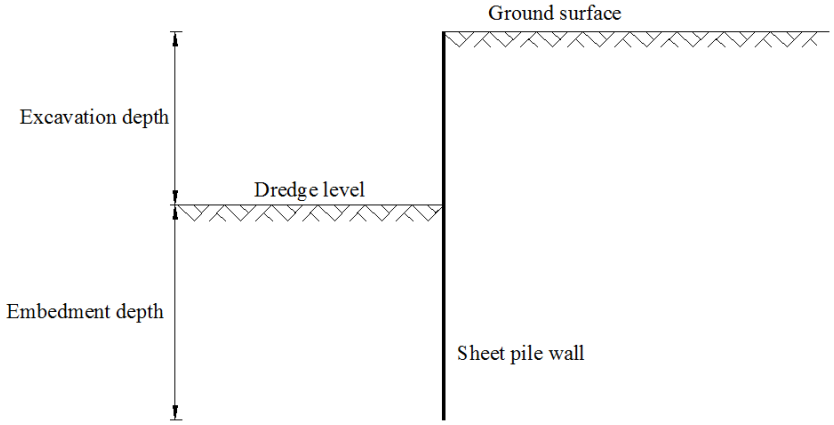

Figure 2.1 Cantilever sheet pile wall

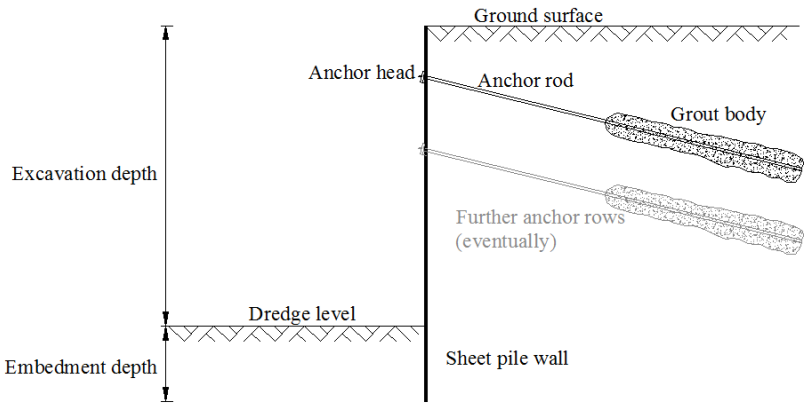

Figure 2.2 Anchored sheet pile wall. At first sight, lesser embedment is needed

2.2. Global mechanical behaviour

The main feature of an embedded retaining structure is the contribution on stability of the embedded zone. Hence, the main unknown parameter to define is the embedment depth, which depends on the magnitude and distribution of the earth pressures over the wall. Earth pressure acting on the sheet pile wall depends, at the same time, on:

- The type of earth pressure distribution
- Geometry
- Flexibility of the sheet pile wall
- Soil-structure interaction
- Construction method

2.2.1. Stress state

The stress state in each point of the sheet pile wall depends on the movement produced. In order to define the earth pressure at failure conditions, the Rankine states are used. Supposing a horizontal soil surface, with no external loads, the effective horizontal and vertical stress increase linearly with depth, and its relation is known as at-rest coefficient (K_0):

$$\boldsymbol{K_0 = \frac{\sigma_h}{\sigma_v}} \qquad \textbf{(2.1)}$$

When a sheet pile wall is introduced and an excavation is done, the earth pressure generated can be produced in two ways:

- Active pressure (K_a): The soil exerts a pressure against the wall. The wall moves to the excavation and the horizontal stress decreases, as the vertical stress remains unchanged. A decompression in the horizontal stress occurs. In a limit situation, a failure wedge is formed, producing a plastic regime. The earth pressure is lower than in the at-rest state.
- Passive pressure (K_p): The wall exerts a pressure against the soil. In this case the horizontal stress increases, while the vertical stress remains unchanged. Therefore, the earth pressure is higher than in the at-rest state. In a limit situation, a failure wedge is formed as well, but with greater dimensions than in the active case.

Figure 2.3 shows the horizontal thrust acting on the sheet pile wall. The ordinate axis can be replaced by K_0 by dividing by σ'_v, according to eq. 2.1, the bigger the movement

is, the higher the horizontal stress is, and so the earth pressure depends essentially on the strain. The asymptotes represent the active and the passive limit states, known as Rankine limit states. Normally, K_0 is closer to K_a than K_p, always meeting the following condition:

$$K_a < K_0 < K_p \tag{2.2}$$

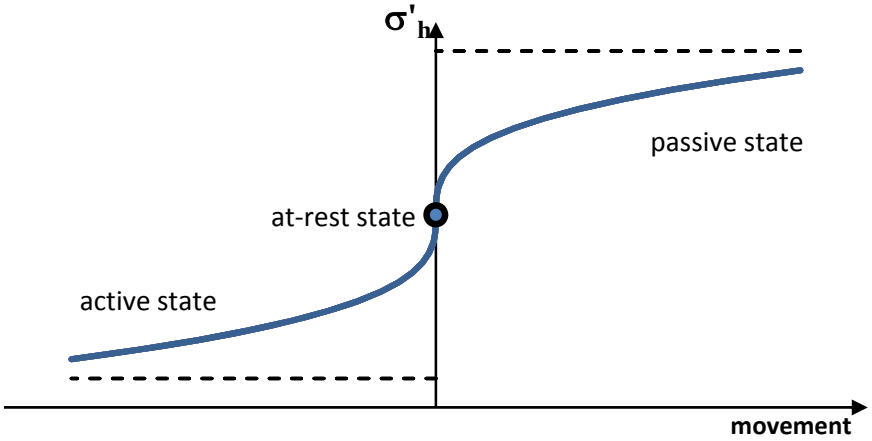

Figure 2.3 Basic scheme of horizontal stress depending on the movement. The vertical axis may be replaced by K_0 by dividing by σ_v

The three-dimensional stress state in one point may be represented by Mohr's circle, a two-dimensional graphical representation (see Figure 2.4). The stress state in one point may be broken in two components, the normal stress (ordinate σ_n), and the shear stress (abscissa τ). Principal stresses are σ_I (major) and σ_{III} (minor). The third principal stress σ_{II}, not represented, is assumed to be equal to σ_{III}. The circumference of the circle is the range of points that represent the state of stress on individual planes at all their orientations. The major and minor normal stresses are given when the shear stress is zero. The failure occurs when the linear envelope of Mohr Coulomb is surpassed (eq. 2.3). As seen in eq. 2.3 and Figure 2.4, the effect of cohesion is always favourable.

$$\tau = c + \sigma \cdot \tan\phi' \tag{2.3}$$

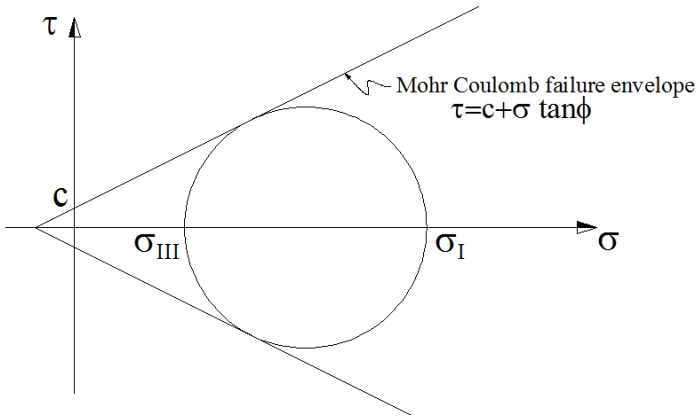

Figure 2.4 Mohr's circle. In this case, the failure criterion of Mohr Coulomb has been reached.

2.3. Earth pressures

In addition to the stress state in each point, estimating the earth pressure distribution is critical in order to design a retaining structure. Regarding this point, different theories are available. The theory applied to rigid structures can be applied, generally, to sheet pile walls as well. The back of the wall is, in every case, vertical. However, in sheet pile walls the passive pressure is more significant. Theories of Coulomb and Rankine are reviewed below. Both are commonly accepted for calculating earth pressures. The first dates from 1776 and the second from 1857. The general equations developed for both theories are based on the fundamental assumptions that the retained soil is cohesionless, homogeneous and drained.

2.3.1. Coulomb Theory

The main hypothesis of Coulomb is the creation of a flat failure surface of the soil that produces a slippage plane. This assumption is appropriate only in the active case, whereas in the passive case a significant error is found. Other hypotheses are the homogeneity of the soil, with a soil friction angle and the fulfilment of the Mohr-Coulomb failure criterion in the slippage plane. In addition, the method requires a sufficient rotation or yielding of the wall in order to engage the entire shear strength. The method is essentially based on the equilibrium of wedges at failure. In the active case, a maximum wedge to engage the maximum thrust is formed (see Figure 2.5), whereas in the passive case it is a wedge to provide the minimum thrust. Under conditions of homogeneous, cohesionless and drained soil, a linear earth pressure law is considered corresponding to the active case (eq. 2.4).

$$\sigma_h = K_a \gamma z \tag{2.4}$$

Where K_a is:

$$K_a = \frac{\sin^2(\alpha+\phi)}{\sin^2\alpha \, \sin(\alpha-\delta)\left[1+\sqrt{\frac{\sin(\phi+\delta)\sin(\phi-\beta)}{\cos(\alpha-\delta)\cos(\alpha+\beta)}}\right]} \tag{2.5}$$

Where the angles α, β and δ, as seen in Figure 2.5, represent:

α: Inclination of the wall from the horizontal.

β: Inclination of the ground in the back of the wall.

δ: Friction angle between the wall and the soil.

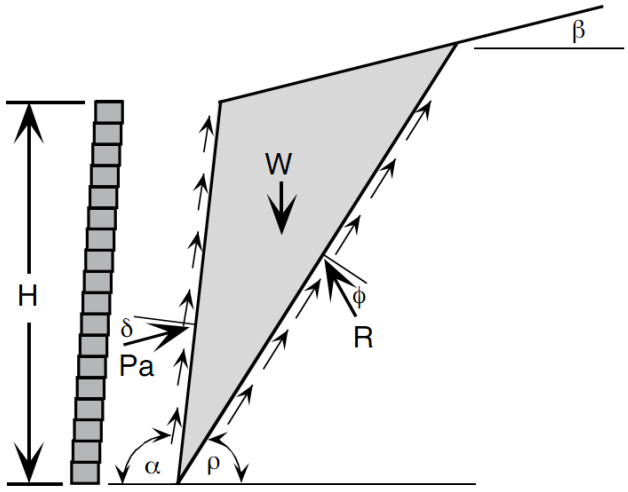

Figure 2.5 Coulomb wedge analysis

Notice that the interaction ground-structure promotes stability. The thrust magnitude is calculated through the equilibrium of forces involved at failure, and its direction depends directly on the angle δ adopted. The application point is assumed to be the centre of mass of the multiple unitary thrusts in the back of the wall.

The Coulomb theory is appropriate for the active case, and it is known to be slightly conservative. On the other hand, it is unsuitable for the passive case, especially for high values of δ and ϕ, and that makes it critical for sheet pile walls. Its greatest benefit is the versatility for complex geometries.

2.3.2. Rankine Theory

The main hypothesis of this theory is the condition of the soil to be in a Rankine limit state. A Rankine limit state is a stress state of plastic equilibrium, where failure surfaces are found in only two directions. In these surfaces the soil has reached the Mohr-Coulomb failure criterion (eq. 2.3).

As said, the failure surfaces in two directions define the size of the wedge produced. In the passive case, the failure involves much more volume of mass than in the active case, as seen in Figure 2.6.

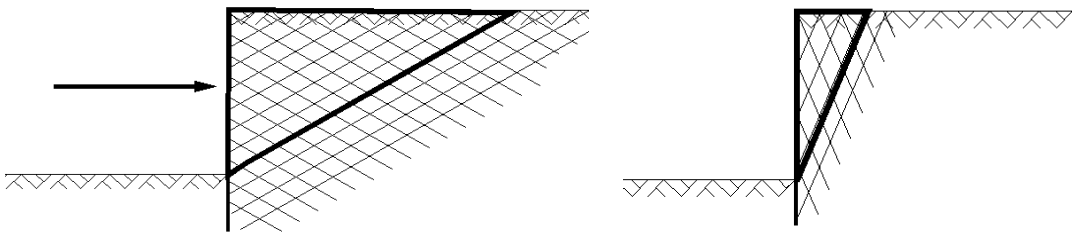

a B

Figure 2.6 Failure wedges. a) Passive limit state. b) Active limit sate.

Under this criterion, the failure occurs with only two soil friction angles, for respectively active and passive limit state, as shown in Figure 2.7. These angles determine the failure wedge formed, that will be different, as said, for the active and the passive limit state. Notice that in the active state, the minor stress σ_{III} corresponds to the

horizontal stress σ_h, and the major stress σ_I corresponds to the vertical stress σ_v. Accordingly, in the passive state, $\sigma_I=\sigma_h$ and $\sigma_{III}=\sigma_v$. The failure surface in Figure 2.7 is found by drawing a line from the pole to the point where the failure envelope is reached.

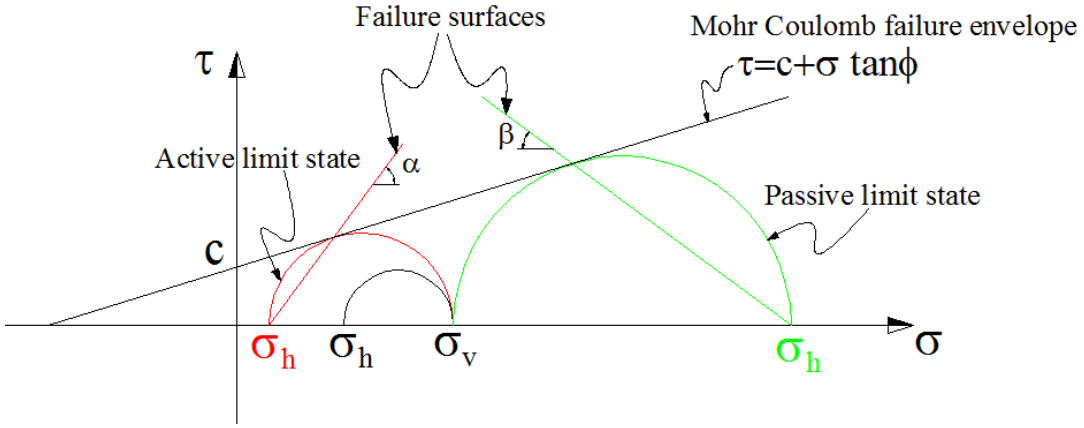

Figure 2.7 Mohr-Coulomb failure criterion. The black circle represents an initial stress state where $\sigma_v>\sigma_h$. A cohesion *c* has been considered

The failure state can be reached therefore from either active or passive state. The effective stress for each point of the soil, considering a horizontal ground surface, is:

$$\sigma'_H = \sigma'_V K_a - 2c\sqrt{K_a} \quad \textbf{(Active case)} \tag{2.6}$$

$$\sigma'_H = \sigma'_V K_p + 2c\sqrt{K_p} \quad \textbf{(Passive case)} \tag{2.7}$$

After a geometrical procedure, it can be proved that the angle of the failure surface, in Figure 2.7, depends only on the soil friction angle (ϕ), being $\alpha = \frac{\pi}{4} - \frac{\phi}{2}$ and $\beta = \frac{\pi}{4} + \frac{\phi}{2}$ for the active and passive limit state respectively. Coefficients K_a and K_p depend as well on the soil friction angle (ϕ). Under conditions of homogeneous soil and horizontal surface, its values are:

$$K_a = \tan^2\left(\frac{\pi}{4} - \frac{\phi}{2}\right) \tag{2.8}$$

$$K_p = \tan^2\left(\frac{\pi}{4} + \frac{\phi}{2}\right) \tag{2.9}$$

The Rankine theory is suitable for the active state, and it is known to be slightly conservative. It is, nonetheless, inadequate for the passive state. Its greatest benefit is the simplification achieved, especially for simple cases.

2.4. Classical design methods

There are several design methods for sheet pile walls. The original proposals date back from the first half of the 20th century, and have been constantly reviewed. Some of them are still reviewed and studied nowadays.

Analytical methods can be found under the name “classical methods” or “limit-stage design methods” (King, 1995). Regardless the name adopted, geotechnical design calculations in either cantilever or anchored sheet pile walls establish equilibrium of

horizontal forces and moments to define the failure state and the reference embedment below the dredge line (before applying the safety factor). The main analytical methods are presented below.

2.4.1. Cantilever walls

In cantilever walls, a reaction force appears at the bottom of the wall, allowing stability, as shown in Figure 2.8. When the embedment depth is increased, further reaction appears in the opposite direction, but this is strictly unnecessary to guarantee stability.

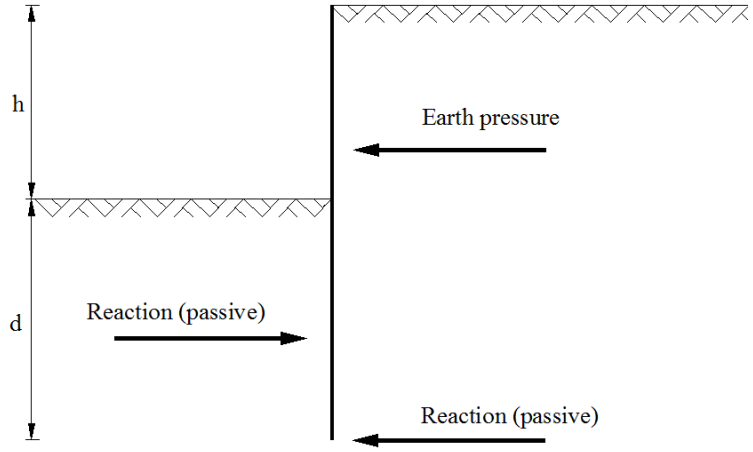

Figure 2.8 Schematic vision of the net earth pressure in a cantilever wall

Stability in cantilever sheet pile walls depends on an adequate embedment below the dredge line. The classical limit equilibrium methods attempt to model the sheet pile walls at failure conditions, and differ from each other in several assumptions, but being a common feature the reach of the failure state in the whole length of the wall.

The main analytical methods for cantilever walls (full method, simplified method and gradual method) are reviewed below.

Full method

This method, shown in Figure 2.9 and known as UK method as well, has been fully described by Padfield & Mair (1984) and gets its name in contrast to the simplified method, described later. The active limit state is assumed to be reached in the back of the wall above the rotation point, and the passive limit state is assumed to be reached in front of the wall between the dredge line and the rotation point. An overturn in the normal pressure direction is supposed to be produced at the rotation point, below which the full passive pressure is moved behind the wall and the active to the front, so there is a sudden jump in the earth pressure distribution which is needed to prescribe moment equilibrium.

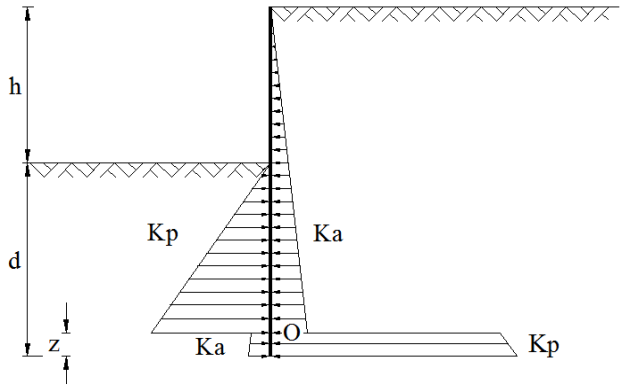

Figure 2.9 Full method. Note the sudden change in the earth pressure distribution

Simplified method

Due to the complexity of the full method, a simplification is recommended (Padfield & Mair, 1984). As shown in Figure 2.10, the earth pressure below the rotation point can be replaced by an equivalent concentrated force acting on point O, represented as R.

The value of *d* calculated is considerably lower than the one calculated from the full method. The common practice is to increase it by 20%, being therefore the reference embedment length equal to *1,2d*. The zone below the rotation point is assumed to receive the passive earth pressure, simplified as *R*, and a verification must be done in order to ensure that the additional length *0,2d* is able to generate the value of *R*.

The simplified method is slightly more conservative than the other methods, although it leads to appreciably similar results (Padfield & Mair, 1984). Its greatest benefit is the simplicity achieved on the traditional system of equations ($\Sigma F_H = 0, \Sigma M = 0$).

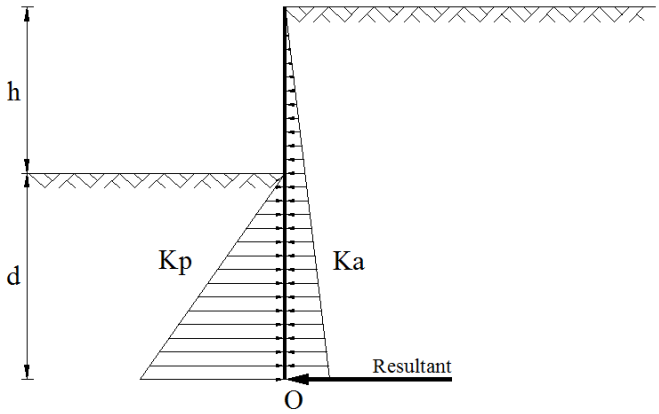

Figure 2.10 Simplified method. The thrust below the rotation point O is replaced by a concentrated force R

Gradual method

A slightly different approach was made by Krey (1932), and later reviewed by Bowles (1988), which does not involve the hypothesis of a sudden change in the earth pressure distribution. The assumption made in this method is to consider a transition zone where the net earth pressure gradually changes its direction from the front to the back of the wall, as shown in Figure 2.11. This transition occurs around the rotation point and is assumed to be linear. The earth pressure at the bottom of the wall is known (see Fig.4),

so the incognita to obtain the embedment depth is the height *z*. The gradual method is known as USA method (Day, 1999; Škrabl, 2006) or general rectilinear net pressure method as well (Day, 2001). All of them consist of modern versions of the method initially proposed by Krey in 1932.

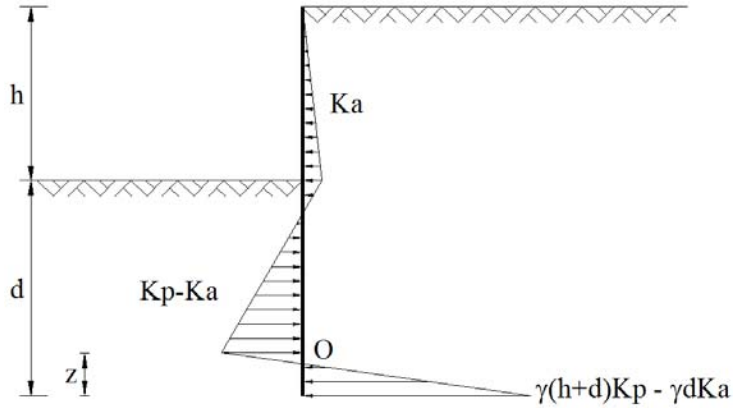

Figure 2.11 Gradual method, shown in net pressures

2.4.2. Single-anchored walls

Anchored walls (or tied-back walls) with a single row of anchors are able to achieve the equilibrium without considering a passive reaction at the bottom of the back of the wall, as seen in Figure 2.12. However, this reaction may be considered depending on the design method. The tie rod position, its inclination and its load are the subject of continuous studies.

The main advantage of an anchored sheet pile wall, against those cantilevered, is the ability to reduce the embedment depth. In other words, it has the ability to increase the excavation depth, which makes the structure more profitable. Some disadvantages are found as well, related to higher amount of unknowns in the problem. Although the excavation depth may be increased thanks to the existence of the anchor, it should not be forgotten, that until the anchor is placed, the structure behaves as a cantilever sheet pile wall.

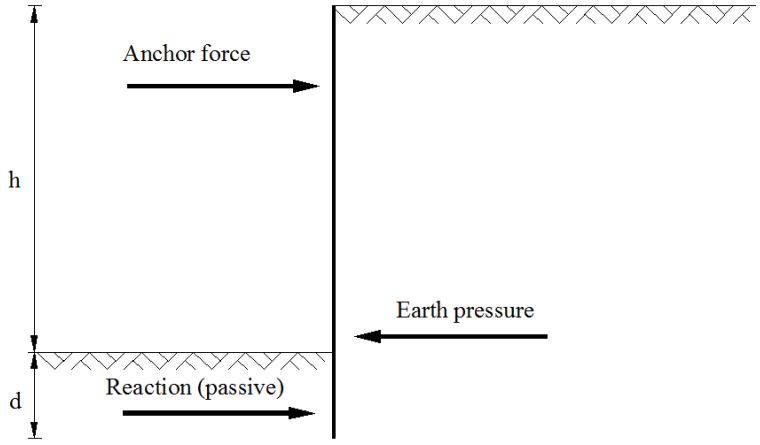

Figure 2.12 Schematic vision of the net earth pressure in an anchored wall

The main analytical methods for anchored walls are presented below, the free earth support method and the fixed earth support method, which differ on the hypotheses adopted.

Free earth support method

This method is based on the assumption that movements on the embedded zone of the wall are sufficient to mobilize the active and passive thrust behind and in front of the wall respectively. The passive pressure is assumed to act only in front of the wall through the depth *d* (Figure 2.13). The bottom of the wall has therefore free movement, and a minimum reference embedment depth, to satisfy equilibrium, is obtained.

The equilibrium is fulfilled between the passive and active pressures, and the anchor force, for obtaining the embedment depth. The way to proceed is to take moments respect the point of application of the anchor (the anchor head) and then equating this expression to zero. This equation provides the minimum embedment depth *d* to provide equilibrium.

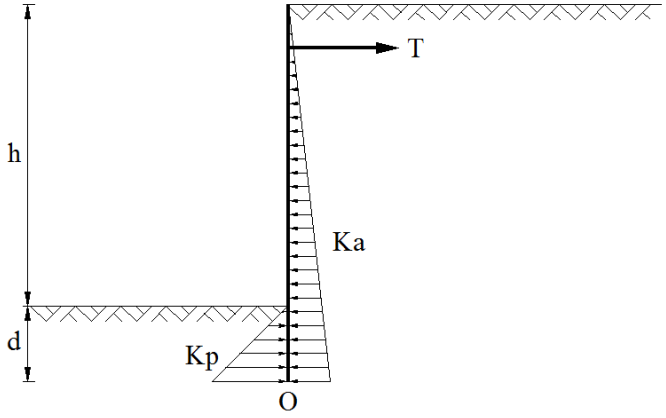

Figure 2.13 Free earth support method. The equilibrium involves movement of the bottom

Fixed earth support method

By increasing the embedment depth, an overturn in the normal earth pressure is achieved, until the deflected shape at the bottom becomes approximately vertical. Hence, the earth pressure distribution is essentially equal to the cantilever case (Figure 2.14), and the wall behaves like a partially built-in beam subjected to bending moments (United States Steel, 1984).

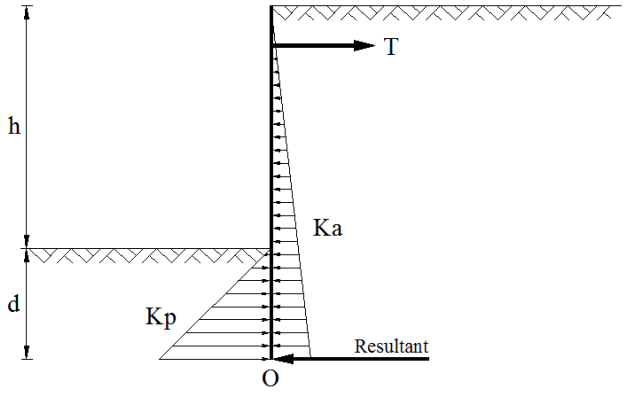

Figure 2.14 Fixed earth support method

This method leads to a maximum reference embedment depth. It requires an additional equation which is usually defined estimating where the zero net pressure (inflection point *O*; zero bending moment) is located. It is frequent to locate such point in the middle of the embedment depth, though other assumptions have been proposed. Blum (1931) showed a dependence relation between the distance from the inflection point to the dredge level and K_a.

The procedure to find the embedment depth is known as Blum's equivalent beam (shown in Figure 2.15), which consists of treating the sheet pile wall as a beam, and dividing it in an upper beam, where net earth pressures act against the back of the wall; and a lower beam, where net earth pressures act against the front of the wall. In the upper beam, equilibrium of moments may be taken at the anchor point to find R_b. Then, in the lower beam, moments are taken at the bottom to find the embedment depth, which must be increased in order to ensure that a reaction R_c is able to be engaged.

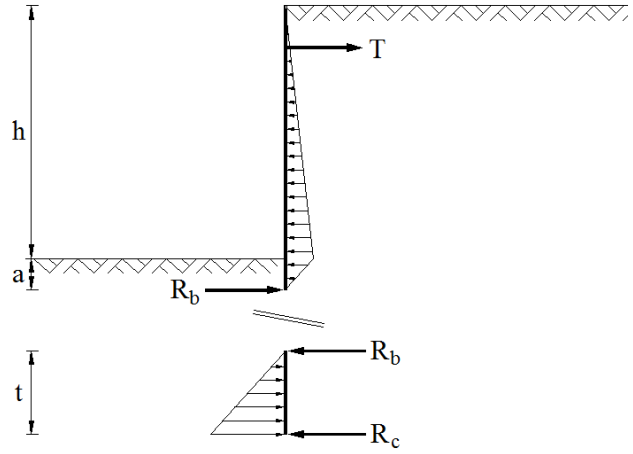

Figure 2.15 Blum's equivalent beam for the design of anchored sheet pile walls

2.4.3. Multiple-anchored walls

Multiple-anchored sheet pile walls represent a totally different geotechnical subject. The complexity of the problem is increased as the number of anchors grows. In fact, no analytical methods exist for the design of multi-anchored sheet pile walls. However, and despite the inexistence of analytical methods, the use of this kind of structures has been widely used. Owing to this, some analytical data are available, which contributes to a better understanding of the behaviour of multiple-anchored sheet pile walls.

By anchoring the free height of the wall in multiple rows, the embedment depth may be reduced significantly, which represents the most important advantage of this structure. Being strict, no embedment depth is needed to guarantee the stability. The action of the anchors is sufficient to provide equilibrium. However, by decreasing the embedment depth may appear other problems, as global instability or instability of the bottom of the excavation.

The design process consists of calculating the sheet pile wall as whether it was a continuous beam. The earth pressure adopted is corresponding to the stress distribution under the hypothesis of free earth support. All the anchors must receive tensile stress, and never of compression. Whether compression occurs, a new location of the anchors must be adopted. Frequently, trials must be done in an iterative process in order to optimize the distribution of moments and anchor loads.

Even in the absence of analytical methods, an implicit hypothesis must be considered: the absence of passive pressure in the zone of anchors. Otherwise, the structure must be treated as a propped wall. As in single-anchored sheet pile walls, it should not be forgotten that stability must be guaranteed in all the temporary phases during the construction, and not only in the final situation.

There are some specific calculation procedures, as that proposed by Caquot, based on locating the anchors in order to receive the same load, and exploiting the bending strength of the sheet pile wall. This solution creates a non uniform distribution of the anchors, where the spacing increases with the height. Other solutions involve the arbitrary location of the anchors or its inclination.

Few literatures have been published in relation to multiple-anchored sheet pile walls. Plant (1972) showed a series of tests in a multiple-anchored sheet pile wall. The effect of the anchor inclination on wall movement, sand subsidence, anchor load changes and earth pressure distribution were studied. A reduced model of sheet pile wall of 1 m high with 3 rows of pre-stressed anchors was used (shown in Figure 2.16). The material used was dry sand. The main conclusions from this study were (Plant, 1972):

- The behaviour of a multi-anchored retaining wall is complex and is related to the interaction between the wall, the soil and the anchors.
- The effect of increasing the anchors inclination is to magnify the wall and soil movements.
- The equivalent earth pressure coefficient[1] at full excavation became smaller as the anchor inclination increased.
- Consideration should be given to having the middle and lower levels of anchors less steeply inclined than the upper level to provide a more “rigid” integrated structural system in order to reduce movements.

Plant (1972) noticed the need to develop “analytical methods”, referring to finite elements, applied to sheet pile walls for the first time.

[1] The equivalent earth pressure coefficient $\left(K_e = \frac{E_b}{\frac{1}{2}\gamma H^2 L}\right)$ is an average relation between the horizontal pressure acting against the back of the wall and the horizontal theoretical thrust. In this ratio, the numerator is variable with the anchor inclination and the denominator remains unchanged.

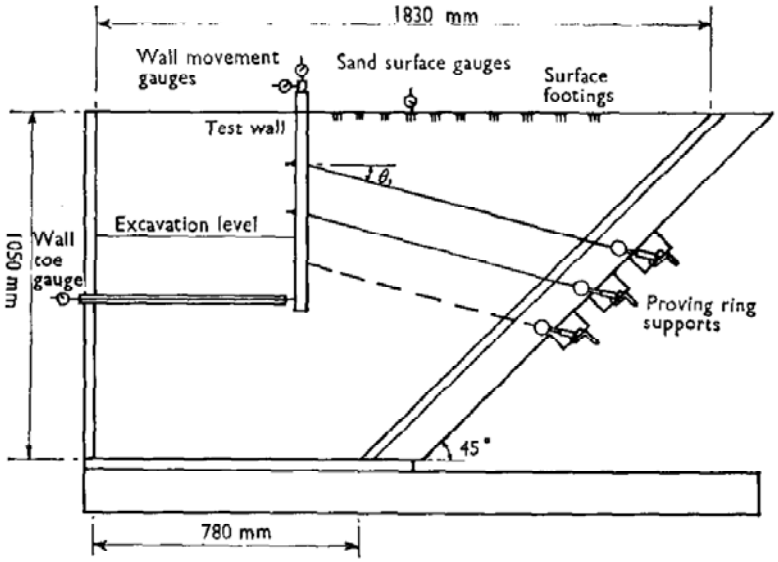

Figure 2.16 Model of multi-anchored sheet pile wall carried out by Plant

3. BIBLIOGRAPHIC REVIEW

Literature referred to sheet pile walls is diverse and may confuse the reader. First publications date from the early 20th century. Several authors have studied both anchored and cantilever sheet pile walls, in the same or in different publications. However, a distinction has been made in this study by separating the literature referred to cantilever, anchored and multi-anchored sheet pile walls. After a deep survey, the most relevant literature is summarized in Annex II. The main sources have been journals such as Géotechnique, Proceedings of Institution of Civil Engineering, Canadian Geotechnical Journal, Computers and Geotechnics; and on second term other less known journals, some essential books and proceedings from international workshops.

3.1. Free embedded cantilever sheet pile walls

Engel's method

Cantilever sheet pile walls were seldom designed before the beginning of the 20th century. One of the first design methods was introduced by Engels (1903), based on experimental observations. A parabolic net earth pressure distribution over the whole depth of embedment (Figure 3.1) was proposed, and the calculation of the reference embedment depth was done by equilibrium of horizontal forces and moments.

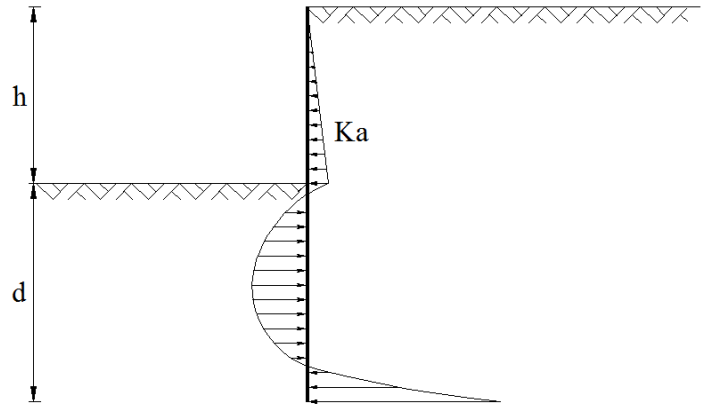

Figure 3.1 Engel's method. Parabolic earth net pressure distribution

A large number of limit equilibrium design methods were developed along similar lines (see Annex II), but differing with respect to:

- The shape of the earth pressure distributions
- The method of computing the equilibrium of the wall
- The theories used in derivation of earth pressure coefficients
- The definition and magnitude of a factor of safety
- The assumed distribution and direction of wall friction
- The method of obtaining the internal friction angle of the soil.

Krey's method

Krey (1932) proposed a rectilinear net earth pressure distribution (Figure 3.2) where the active earth pressure in the back of the wall above the dredge line and passive earth pressure in front of the wall immediately below the dredge line were fully mobilized

even before failure (Bica & Clayton, 1989), which was showed later by many other authors. The design depth of penetration was calculated by finding *z*, corresponding to the maximum net earth pressure in front of the wall, satisfying both equilibrium of horizontal forces and moments about the bottom of the wall. Krey's method became the basis of the most used method nowadays.

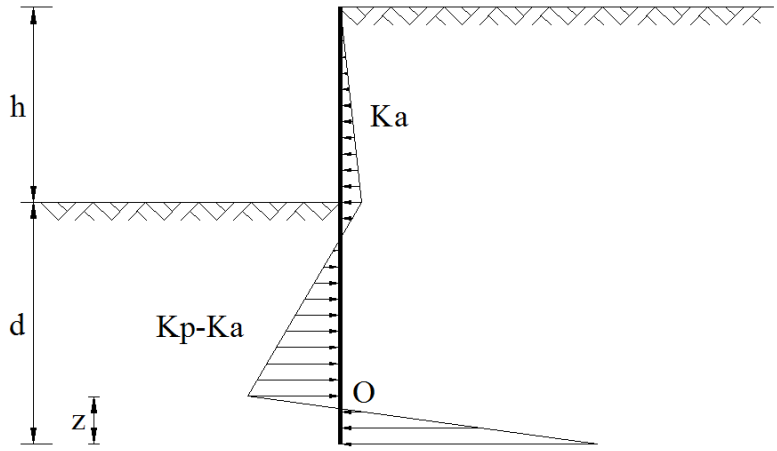

Figure 3.2 Krey's method. Rectilinear earth pressure distribution. This was originally separated into two diagrams, for both upper and lower part of the wall from the dredge level.

Blum's method

A modification on Krey's method was proposed by Blum (1931), resulting in a simplification of the previous methods. The earth pressure in the lower part of the wall was replaced by a fictitious force *R* acting on point *O*, as shown in Figure 3.3. The embedment depth was calculated by taking moments about point *O*. It was later when the practice of increasing the calculated embedment depth by 0.2*d* was introduced (Bica & Clayton, 1989), being the first Schmidt (1942). The final design embedment depth was therefore 1,2*d*. Nonetheless, the safety provided by this practice was unknown (Cuadrado, 2010).

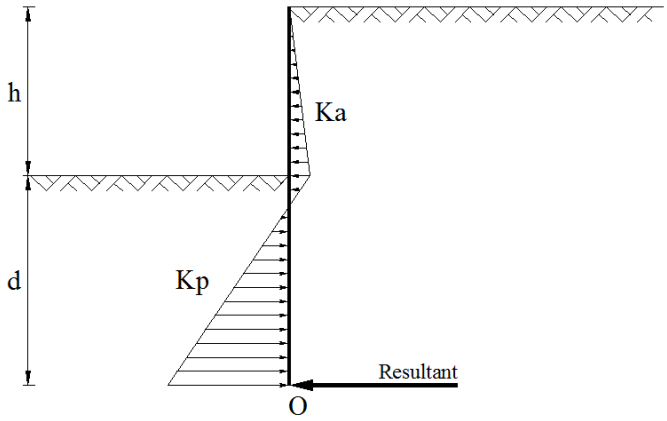

Figure 3.3 Rectilinear earth net pressure distribution from Blum's method. Note the fictitious force R

Rowe's method

Rowe (1951) carried out a comprehensive series of tests on model walls in loose and dense sand. Starting from these, introduced an empirical design method. A factor of reduction of 1.5 on the passive earth pressure and an angle of friction of the wall equal to zero were considered in order to obtain the design depth of penetration, by taking moments about the point of application of *R*. Equilibrium of horizontal forces was verified as well, but Rowe did not consider (as Blum had done) the extension of the wall below the point of application of *R*. To obtain the reference depth of penetration *d*, an angle of wall friction equal to 2ϕ/3 was considered, and the passive earth pressure remained unfactored. In fact, Rowe distinguished between the design embedment (no wall-soil friction, reduction of K_p) and the equilibrium embedment (soil friction factored 2/3, K_p not reduced). The calculated depth of penetration was not increased by any factor. The maximum bending moment was evaluated at the point of zero shear force from a different net earth pressure distribution (shown in Figure 3.4 a), using the design depth of penetration. However, now full mobilization was assumed of passive earth pressures (calculated with an angle of wall friction of 2ϕ/3) immediately below the dredge level and partial mobilization for depths below the depth to the maximum net earth pressure t (Figure 3.4 b). An important feature in this method was an empirical correction for the effect of wall flexibility on the maximum bending moment. Rowe's method was later simplified, by assuming a single net earth pressure distribution which resembled Blum's method, and by including factors of safety on shear strength parameters when evaluating passive earth pressure.

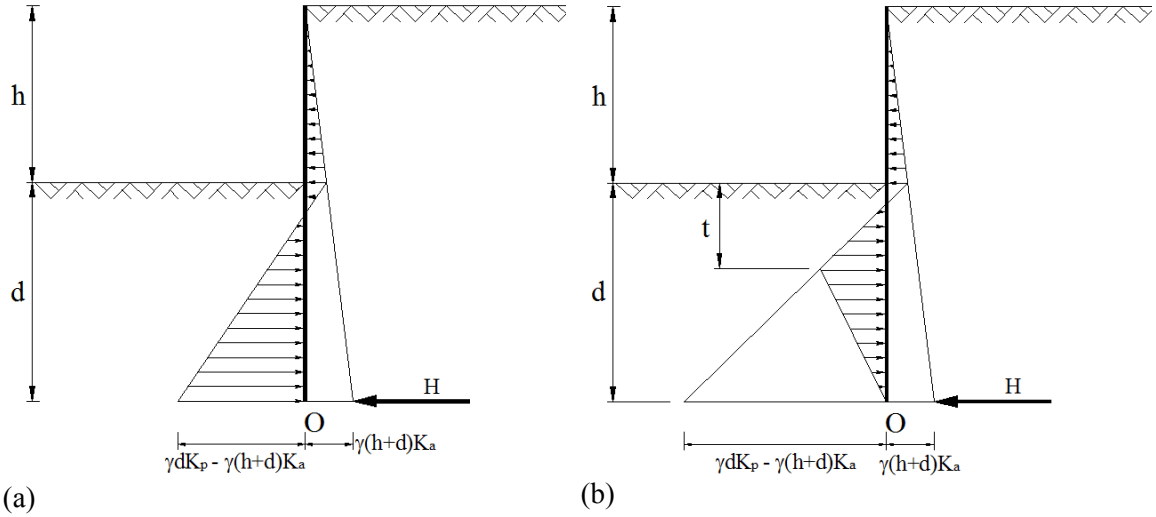

Figure 3.4 Rectilinear net earth pressure distribution from Rowe's method: (a) For determining limit and design depths of penetration. (b) For bending moments at design depths of penetration.

Brinch Hansen's method

A more refined design method was introduced by Brinch Hansen in 1953. Unlike previous methods, the Brinch Hansen method obtained a solution to the problem by satisfying all plane equilibrium conditions, together with approximate kinematic compatibility conditions between the wall and the rupture surface. This method was extremely complex, and so an approximate step by step routine was recommended which assumed a simplified earth pressure distribution (Figure 3.5). Brinch Hansen used earth pressure coefficients derived on the basis of a factor of safety on *c'* and tanϕ', and

the position of the rotation centre relative to the depth at which the pressure was to be calculated. The maximum bending moment was first determined, at the point of zero shear force on this distribution. The depth of penetration was then obtained by requiring equilibrium of horizontal forces and moments for the lower part of the wall, including the unbalanced moment at the point of zero shear force. The additional depth of penetration Δd was calculated using empirical equations. The lateral pressures were assumed to be constant below the point of zero shear force; however Brinch Hansen showed that this gave a solution within a few per cent of that achieved by the more complex, full analysis.

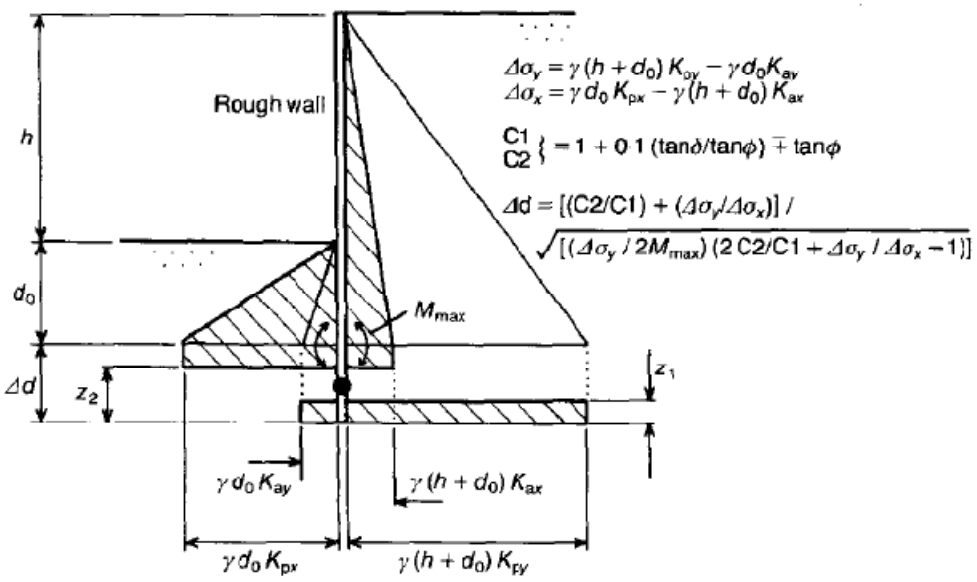

Figure 3.5 Earth pressure distribution as assumed in Brinch Hansen's method

Application of X-ray method

Bransby & Milligan (1975) presented an experimental study of the soil deformations in laboratory-scale cantilever flexible sheet pile walls in dry sand. The wall was 30cm high, embedded in 37 cm of dense sand, within a glass-sided tank. The study simulated plane strain conditions. The X-ray technique was used to determine movements on the soil around the wall and to observe the rupture surfaces in the sand. An analytical method was presented, which linked soil deformations with deflexions of the wall.

The X-ray method was commonly used to measure deformations. In essence, the method consists of burying a rectangular planar grid of lead markers within the sand and the exposing radiographs of the sample at different stages of the test. The position of each marker on the radiograph may be measured and so the displacements of the marker, and hence of the soil, between exposures may be determined. An example of results is shown on Figure 3.6.

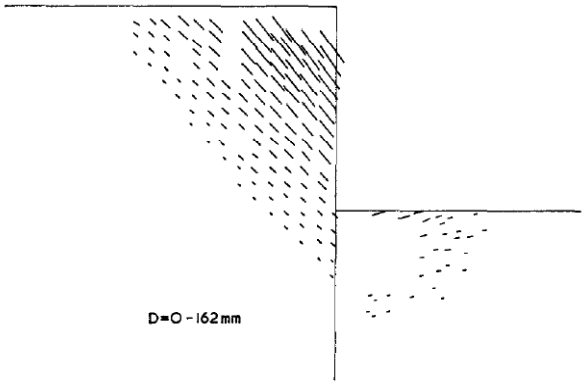

Figure 3.6 Displacements in sand using the X-ray method in a test carried out by Bransby & Milligan (1975)

The effect of wall roughness on deformation behaviour seems to be small. The method proposed assumes that the increments of strain at points along any β line (rupture surface) are equal, and determined only by the incremental angle of rotation of the wall. This method is found to give good predictions of the behaviour, and should make it possible to estimate the magnitude and extent of surface settlements behind the wall (Bransby & Milligan, 1975).

CIRIA Report 104

Padfield & Mair (1984) presented Design of retaining walls embedded in stiff clay, also known as CIRIA Report 104, which has become one of the most referred publications related to sheet pile walls. This report covers the design of singly propped or cantilever walls embedded in stiff overconsolidated clay. An introduction to the earth pressure calculation was included, and methods for both anchored and cantilever walls were summarised (free-earth and fixed-earth conditions, full method and simplified method). Various methods of assessing the factor of safety against overall stability were compared, and four of them recommended. These were a factor on embedment, on strength parameters, on moments and on passive pressure. Applied examples were included as well.

Finite Element application

First applications of the Finite Element method date from early 1980's. The discretizations of the geometry were coarse, and the results were limited.

Fourie & Potts (1989) presented a comparison of finite element and limit equilibrium analysis for a cantilever wall. The soil behaviour was modelled through an elasto-plastic constitutive law, under drained conditions. The classical methods used were the full method and the simplified method, described in CIRIA Report 104. In the finite element model, Young's modulus is considered to increase linearly with depth. Drained conditions, with zero pore water pressures everywhere, zero cohesion and a single soil friction angle of 25º were considered. The domain was discretised by 165 eight-noded isoparametric elements (see Figure 3.7). The effect of the initial stress was studied as well. Two extreme cases, with K_0=0.5 and K_0=2 were performed.

Results showed that larger horizontal movement of the wall occurs with K_0=2, than with K_0=0.5, for the same depth of excavation (see Figure 3.8). This figure shows a horizontal asymptote, representing the maximum excavation depth allowed with this geometry and these strength parameters, and therefore corresponds to the limit state. The maximum excavation depth was 10.6m, with a wall height of 20m, which means an embedment depth of 9.4m. Further results of the comparison indicated that both the limit equilibrium method used in the Paper and the finite element approach give similar predictions of the embedment depth required to ensure stability. The finite element analysis justifies the 20% increase in embedment depth arbitrarily assumed in the limit equilibrium approach, which was showed again by Cuadrado (2010). Results showed as well, that in excavations with low K_0 values, limit equilibrium methods overestimate the maximum bending moments in almost 50%. Some reduction of the bending moment must therefore be guaranteed.

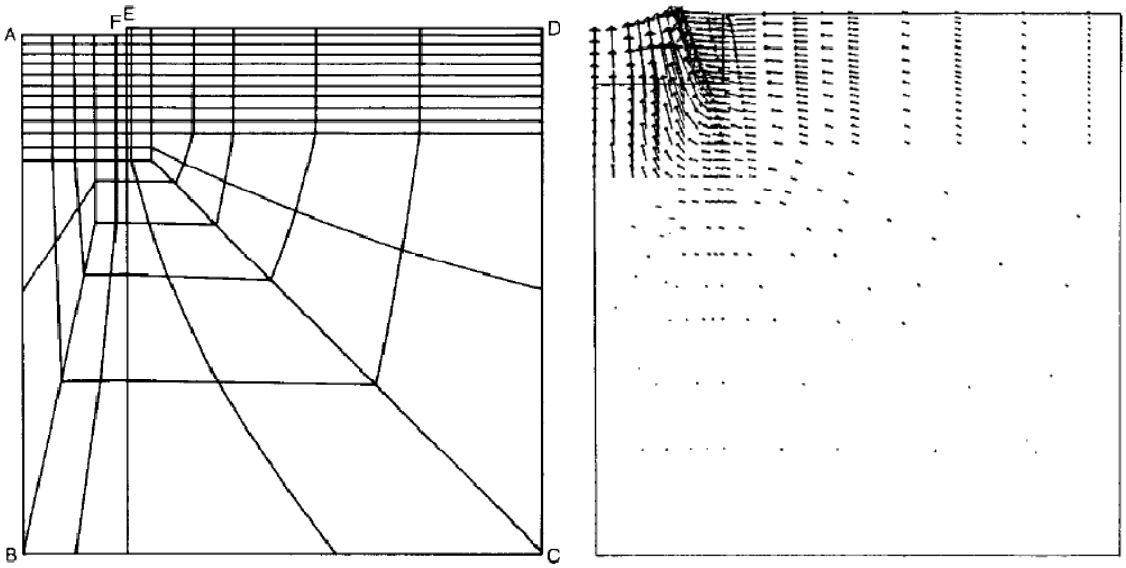

Figure 3.7 (a) Finite element mesh performed by Fourie & Potts (1989). The square-shaped geometry has 100m side. (b) Displacements with K_0=2.

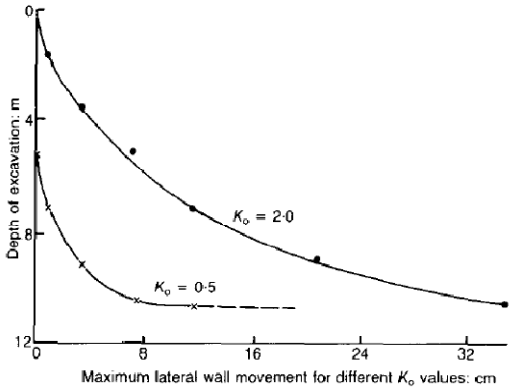

Figure 3.8 Results of horizontal displacement vs. depth of excavation for two K_0 values.

Day & Potts (1993) showed that while working with a Finite Element model, beam elements are appropriate to represent sheet pile walls. However, since the effect of wall element type is significant, beam elements are not recommended for the analyses of thick concrete retaining walls (referring to rigid structures); in which 2-D elements are appropriate as they more accurately describe the geometry of the structure.

Review of analytical methods

Bica & Clayton (1989) presented an in-depth review of the analytical methods available until then. 25 methods were described and compared with each other and with experimental data. The authors concluded that limit equilibrium methods may be capable of providing good estimates of the equilibrium depth of embedment and maximum bending moment. However, this will only occur if there are subtle compensations for the errors inherent in their extremely simplified assumptions. The authors mentioned as well the need to develop further research, primarily focused on acquiring more experimental data on the behaviour of sheet pile walls.

King's method

A new analytical method for the analysis and design of sheet pile walls at failure conditions was proposed by King (1995). This method has become relatively popular and is frequently referred. The method essentially consists of a semi-empirical procedure, since it is based on limit equilibrium, and at the same time a parameter is taken from a graph. It represents an alternative to the current limit state methods, not requiring the geometrical simplifications of the earth pressure distribution. According to this method, equilibrium can be established without assuming the limit state in the passive region. On the other hand, the method is dependent on an empirical parameter determined from the results of centrifuge tests. The applicability of this method has been verified by Day (1999), proving its conservative prediction and proposing a new value for the empirical parameter.

The active pressure is mobilised in the back of the wall above the dredge level, as normally (see Figure 3.9). The rest of points on the graph can not be solved, although they are related to each other. Starting from predetermined values of h and ε, y and x (respectively, maximum pressure in front of the wall and depth of zero net pressure) can be calculated. Below the dredge level, the slope of the net pressure law is unknown at service conditions, but known at limit conditions. Then, x and P (active pressure at the dredge level) may be related. The ratio x/P at failure conditions is known to be equal to$1/(K_p-K_a)\gamma$. By substituting P by $K_a\gamma h$ a ratio x/h at failure is obtained, and equal to $(K_p/K_a -1)^{-1}$. The safety factor is expressed as the ratio x/h at service conditions to $(x/h)_c$ at failure conditions.

When designing for a predetermined safety factor, an embedment depth is calculated following the procedure below. First of all, the ratio $(x/h)_c$ is calculated (at failure conditions). It depends only onϕ. Then, x/h is calculated at service conditions through the safety factor. Finally, h/d is obtained from Figure 3.10 using ε'=0.35 curve. Since h is known from the start, the embedment depth d is obtained.

When checking the safety factor, the inverse procedure must be followed.

The recommendation to use ε'=0.35 curve was based on centrifuge tests. Later, Day (1999) showed that King's recommendation of ε'=0.35 is generally conservative, more than both the UK and the USA methods. This value must be therefore slightly lower.

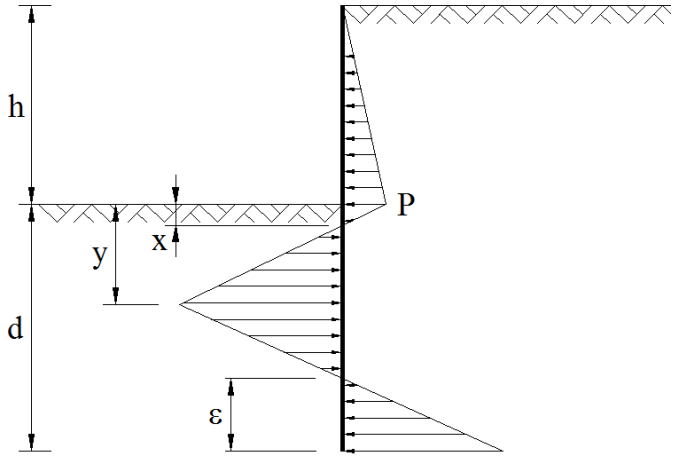

Figure 3.9 Assumed net pressure diagram for King's method

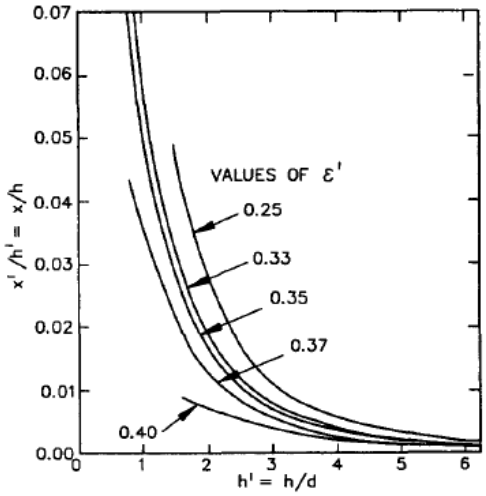

Figure 3.10 Obtention of the embedment depth *d* in King's method. ε'=0.35 curve must be used.

King compares his method with the gradual method (called *A* in the paper) and the full method (called *B*), and it is found to give critical depths of excavation closer to those observed in centrifuge tests than the current methods. The main feature and benefit of this method is the non-use of the currently assumed passive pressures in depth.

Powrie (1996) presented one of the few studies considering non-drained conditions.

Day's method

Day (1999) presented a Finite Element study where the net earth pressure over the sheet pile wall was examined. The mesh used (showed in Figure 3.11) presented some improvements with respect to those used in previous papers. In the Finite Element Day chose a wall height of 10 m and considered 5 cases with soil friction angles within 20º and 50º, with variable excavation depth. Results are shown on Figure 3.12. The study showed that the point of zero net earth pressure for the appropriate rectilinear

approximation is dependent on the ratio between the active and passive earth pressure distributions at limiting conditions.

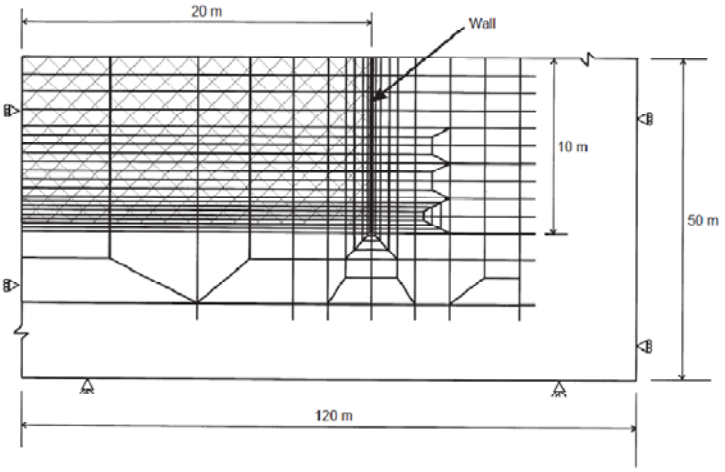

Figure 3.11 Finite Element mesh developed by Day (1999)

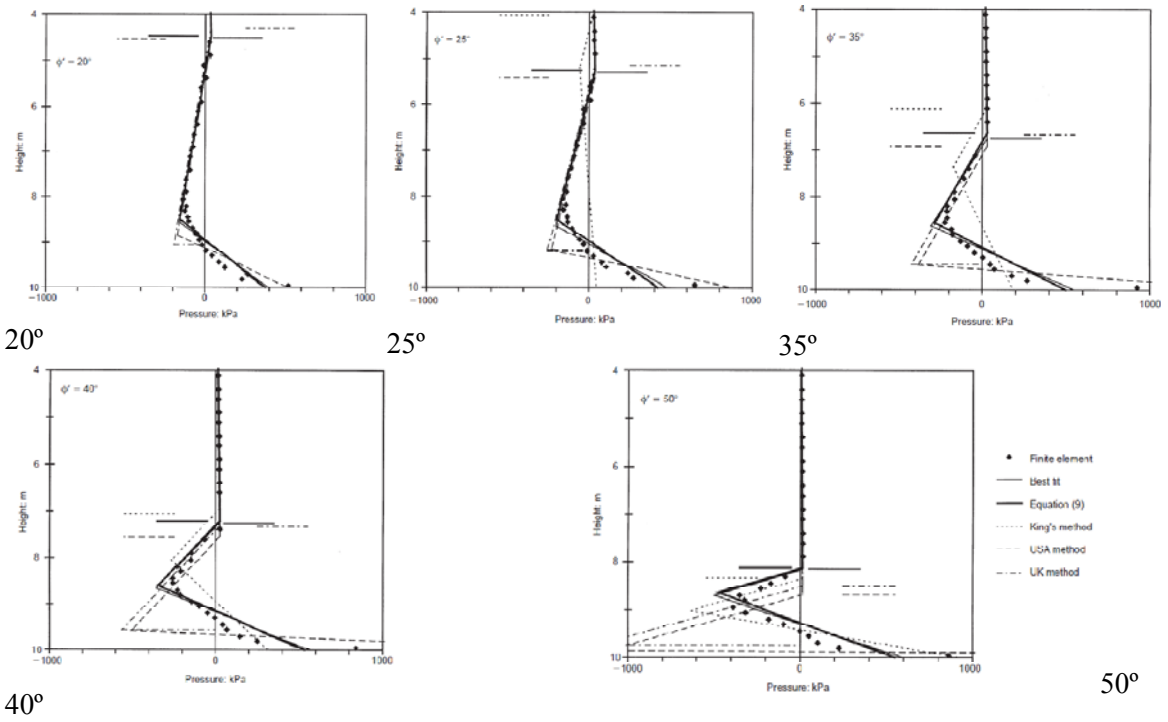

20º 25º 35º

40º 50º

Figure 3.12 Cases studied by Day (1999)

Day proposed an equation in order to define the point of zero pressure (see Figure 3.13). This equation proposed a linear relation between the position of the point of zero pressure and the ratio K_a to K_p. Starting form this, and according to Day (1999), the proposal by King (1995) that ε'=0.35 is generally conservative. The predicted retained height and maximum bending moment are generally less than indicated by the Finite Element data. Results from the Day's equation were found to be in excellent agreement with the finite element predictions and with centrifuge model data.

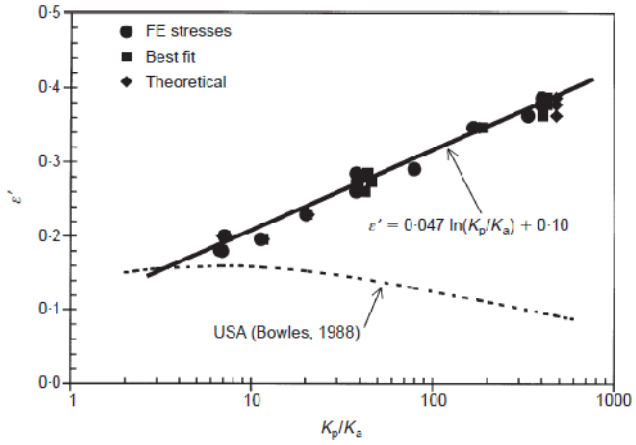

Figure 3.13 Point of zero net earth pressure, presented by Day (1999)

On later studies, the same author explained that the value *ε'* is known at all stages of excavation but is not necessarily constant. Remember that *ε'* is the quotient between the distance from the toe of the wall and the point of zero net pressure *ε* and the embedment depth *d*. The value of *ε'* is given by the equation 3.1 (Day, 1999):

$$\varepsilon' = 0.047 ln\left(\frac{K_p}{K_a}\right) + 0.10 \quad (3.1)$$

The value *ε'* may be constant only under the assumptions of linear earth pressure distribution, which is reasonably true on the back of the wall, but it is not in front of the wall.

On a newer paper released in 2001, Day showed the results of 30 cases using the same geometry and mesh, comprising a range of conditions with soil friction angles within 20º and 50º and K_0 values of 0.5 and 2.0. The author notes that for practical cantilever walls, the active and passive earth pressure coefficients can be assumed to be at the theoretical limiting values of methods such as Caquot and Kerisel. Day (2001) verified and noted the very good predictions give by the Padfield and Mair's CIRIA Report 104. The maximum bending moment is dependent only in the net pressure above that point, and so the maximum bending moment may be calculated directly using the assumption that the passive pressure is fully mobilised. The expression of the maximum bending moment may be therefore simplified as shown in 3.2.

$$M_{max} = \frac{1}{6} K_a \gamma (a + h)^3 + \frac{1}{6} K_p \gamma a^3 \quad (3.2)$$

Where,

$$a = \frac{h}{\sqrt{\frac{K_p}{K_a}} - 1} \quad (3.3)$$

Mobilizable Strength Design method

Osman and Bolton (2004) presented a new method for the design of cantilever sheet pile walls by introducing the concept of mobilizable soil strength. The motivation was the need to address the real and non-linear behaviour of the soil (Osman & Bolton,

2004). The objective was to satisfy both serviceability and safety in a single step of calculation.

The concept of mobilizable strength refers to the shear stress τ in undrained conditions of clays. Clays that remain undrained during the excavation stages must deform only in shear. Figure 3.14 shows the idealised earth pressure distribution from which, starting from a known geometry, strength and pivot position may be determined by solving force and moment equilibrium.

An especially interesting tip in this study is the ratio of the height of the rotation point above the toe and the total height of the wall, for different excavation depths. The graph shows a maximum where the height of the rotation point is always less tan 2.5% of the total height of the wall (see Figure 3.15).

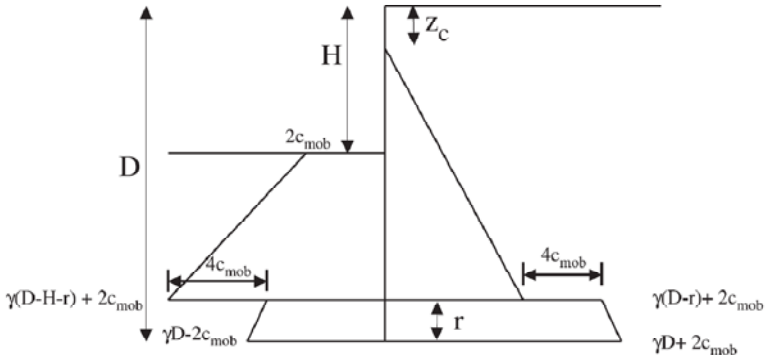

Figure 3.14 Lateral earth pressure distribution under undrained conditions. C_{mob} refers to the mobilizable soil strength (Osman & Bolton, 2004)

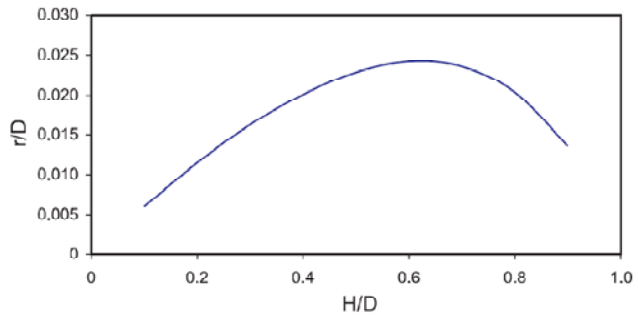

Figure 3.15 Height of rotation point above the toe. H = excavation depth, D = total wall height. (Osman & Bolton, 2004)

Limit equilibrium methods do not exist in isolation. Each of the limit equilibrium design methods was originally associated with particular earth pressure coefficients, methods for determining angles of friction, safety factors, etc. These design facets are at least as important as the fundamentals of the limit equilibrium calculations.

Bearing in mind that the equilibrium calculations most commonly used (those of Krey and Blum) pre-date the widespread use of effective stress, of triaxial testing, and of the standard penetration test, it is hardly surprising that a large element of adaptation has occurred. The survey of the literature carried out by Bica & Clayton (1989) produced about 25 different methods of design, and almost every one of those was based on either

Krey's or Blum's methods. Since then, many other methods have been presented, such as King's method or Day's method. The principal variations within these methods are in earth pressure coefficients, factors of safety, shear strength parameters and the influence of construction methods.

3.2. Anchored sheet pile walls

Rowe's experiments

In 1952, Rowe presented the results from fifteen models of flexible walls retaining cohesionless soil (see Figure 3.16). The influence of surcharge, anchor yield, dredge level, soil type and state, pile flexibility and anchor level were studied. Rowe presented a chart for the design of anchored pile walls. One of the conclusions was that the anchor load is generally close to the free earth support value, which is a common procedure for the design of anchored sheet pile walls. The design procedure consisted on entering into the chart with the soil friction angle and the parameter β (see Fig.3.2.1). The last was the quotient between the depth to the anchor level and thetotal wall height. The chart provided the penetration depth indirectly, from the parameter α, which was equal to $1 - \frac{D}{H}$.

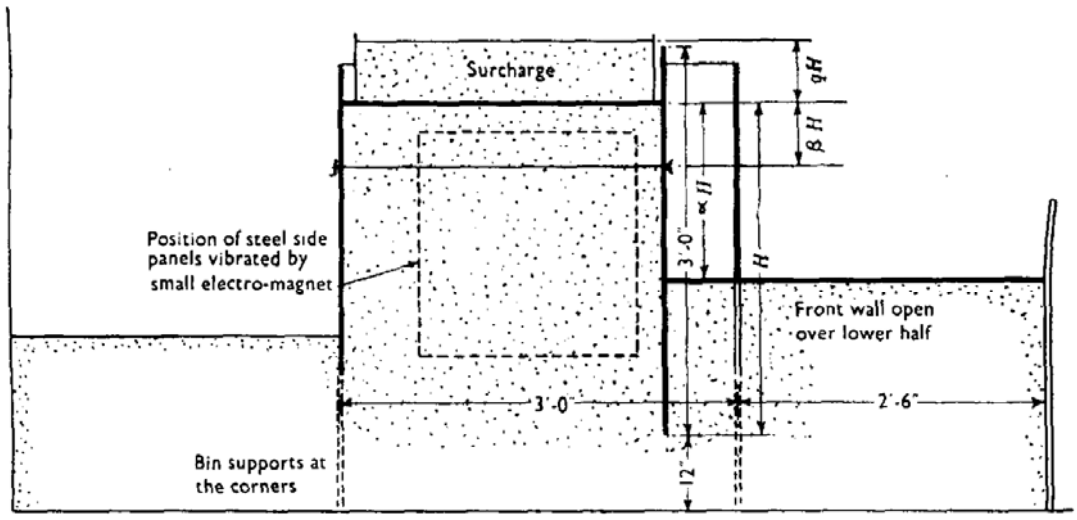

APPARATUS FOR FLEXIBILITY TESTS

Figure 3.16 Anchored sheet pile wall modeled by Rowe (1952)

These design procedure was based on experimental data of reduced models. The anchor inclination was horizontal. The different tie-rod levels and dredge levels provided different curves β.

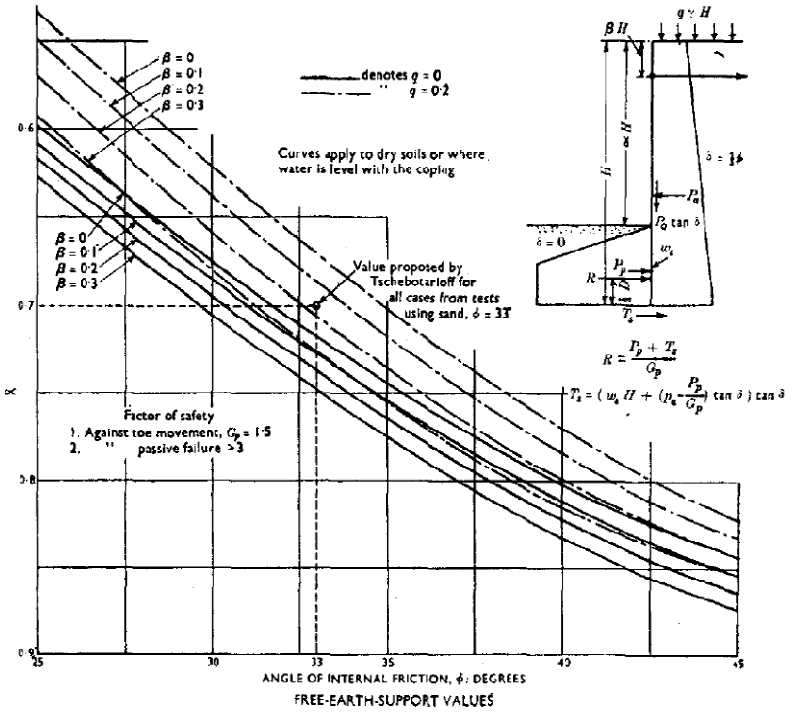

Fig.3.2.1. Chart presented by Rowe (1952) for the design of anchored sheet pile walls

First studies of anchor inclination

In 1972, Plant presented a study of the anchor inclination on multi-anchored sheet pile walls. The paper presented the results of tests with a scale-model sheet pile wall of 0,6m height retaining dry sand (see Fig.3.2.2). The three anchor rods were inclined 0º, 15º, 30º and 45º. In a second series, the two lower levels remained horizontal, while the upper level was inclined successively 30º, 45º and 60º.

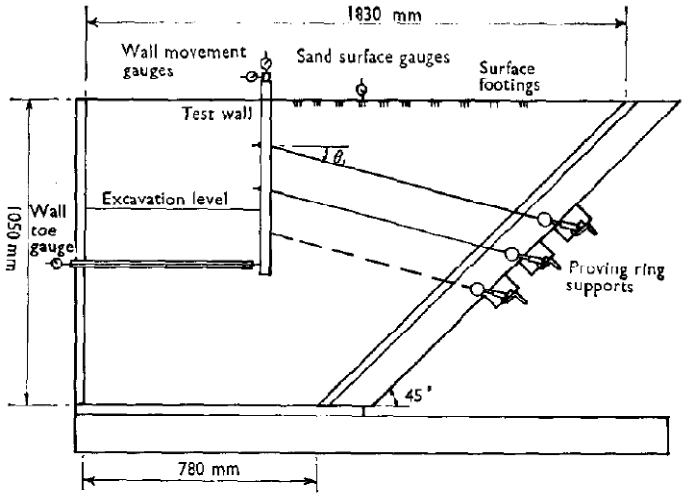

Fig.3.2.2. Sheet pile wall scale-model developed by Plant (1972)

Plant noted the complexity of the behaviour of the overall system soil-wall-anchor. Plant showed that when increasing the anchor inclination, the wall and soil movements were enlarged. Movement of the wall may not be eliminated but reduced by selecting an

appropriate anchor inclination. Additionally, having the lower level of anchors less inclined than the upper level provides a more rigid integrated structural system that reduces movements. In this publication, Plant noted the need of developing the Finite Element method, which is one of the earliest mentioning to do so.

The main contribution of this study was to provide experimental data, which has a great value, especially nowadays.

Radiographic method

Milligan (1983) presented an experimental study on sheet pile walls anchored near the top where displacements were measured by the radiographic method, as done by Bransby& Milligan in 1975 for cantilever sheet pile walls. The behaviour of the wall was found to be, as expected, much more complex than in cantilever case. Model walls for this study were 30 cm height retaining dry and dense sand. The dredge level was changed successively, resembling a staged excavation. The roughness of the wall was changed as well in different series.

As done in cantilever walls by the same author, the X-ray method consisted in burying a grid within the sand and then exposing the sample to X-rays. The lead markers show the movement of each point of the grid, as shown in Fig.3.2.3. Displacements measured by the X-ray method in a staged excavation (Milligan, 1983). The location of failure surfaces may be possible, where the contours of incremental shear strain show a narrow zone of a very high strain gradient (see Fig.3.2.4).

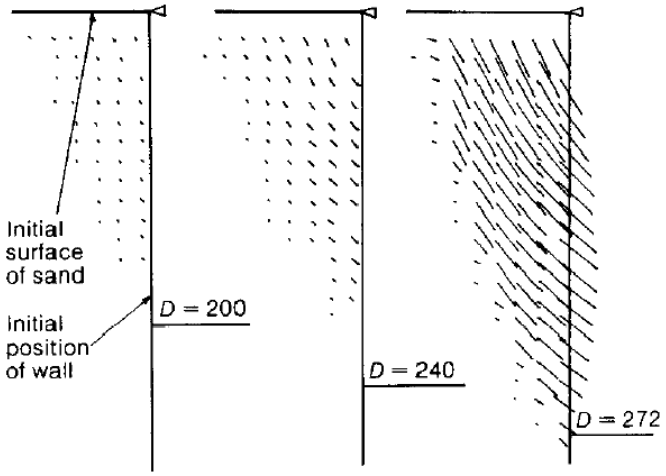

Fig.3.2.3. Displacements measured by the X-ray method in a staged excavation (Milligan, 1983)

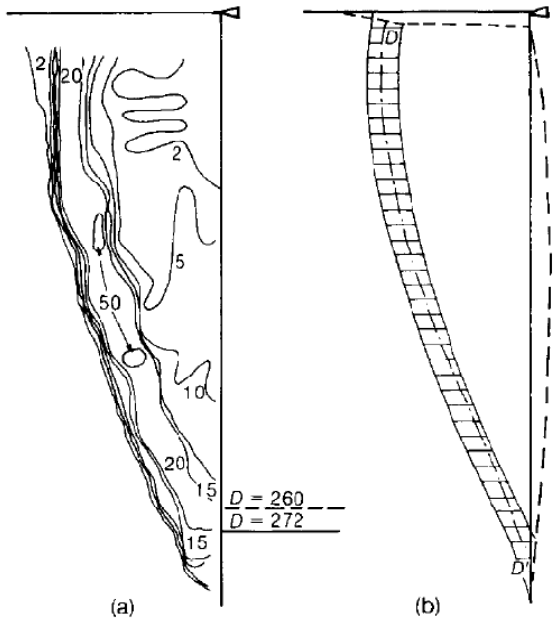

Fig.3.2.4. Location of failure surfaces (Milligan, 1983)

The study was focused on the measurement of the movement behind the wall, and not in front of this. Studies of measurements of movements in front of the wall could not be found for this study.

Propped walls

Richards & Powrie (1994) developed a study supported on the finite element method. The mesh used can be seen in Figure 3.17. The objective was the study of the effects of construction sequence and pre-excavation lateral earth pressures on the behaviour of a sheet pile wall propped –not anchored– at both crest and dredge level. Results showed minimum wall movements occurred with top down construction (single excavation stage) with temporary props. Minimum bending moments occurred with construction in open cut (see Figure 3.18). The study concludes that maximum bending moments and at the same time minimum movements occur in the case of top down construction with temporary props, because the temporary prop takes comparatively lesser compressive load.

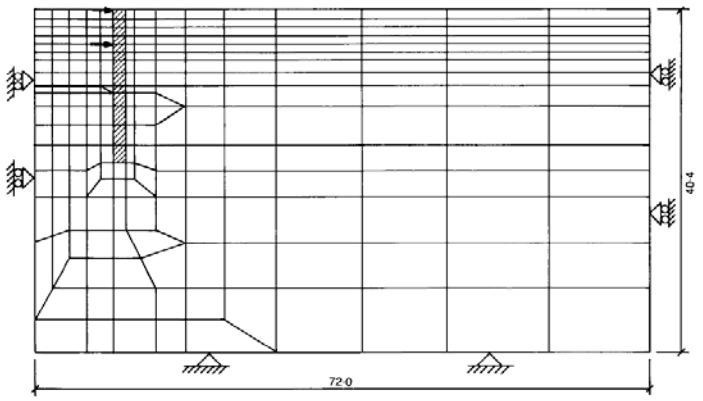

Figure 3.17 Mesh used by Richards & Powrie (1994)

This study included two cases of initial earth pressure coefficient: K=1 and K=2. The effect of increasing the earth pressure coefficient was, according to Richards & Powrie (1994) that the magnitudes of the reverse bending moments, which occur at later stages towards the bottom of the wall, are increased.

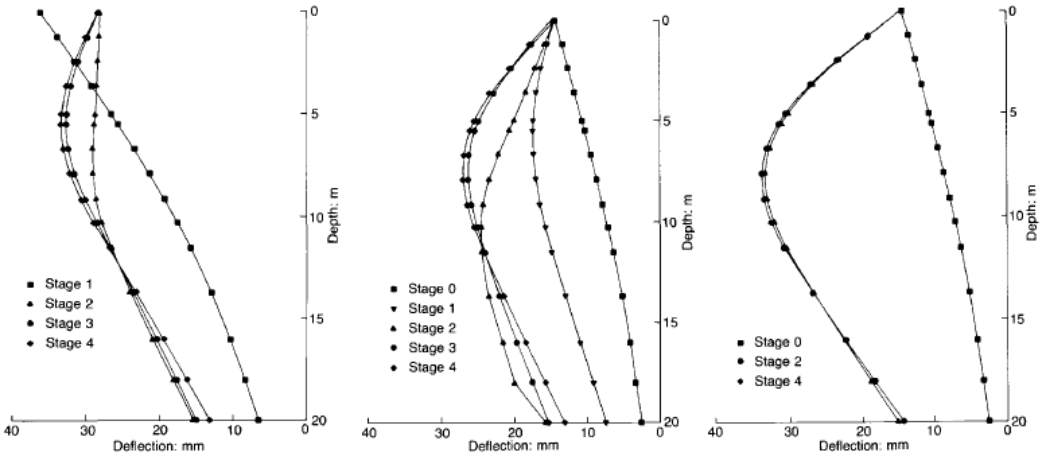

a b c

Figure 3.18 Wall deflections for K_0=1 with (a) two temporary props, (b) one temporary prop and (c) no temporary props.

First publications related to sheet pile walls were essentially results from experimental tests, normally compared with theoretical design methods. On a second period, theoretical developments led to several new methods. Nowadays, is much more difficult to find results from experimental studies on recent papers, as these are usually focused on the Finite Element method. In the early 80's , with the development of numerical methods, the experimental studies started a trend to disappear, as opposite to Finite Element studies, which are somehow more effective or more accessible, in terms of simplicity, and essentially, in invested time.

4. NUMERICAL MODEL

4.1. Introduction

This chapter has the double aim of introducing a general scheme of the usage of the commercial software used (Plaxis) and explaining the performance of the model used.

PLAXIS is a special purpose two-dimensional Finite Element computer program used to perform deformation and stability analysis for many types of geotechnical applications. Real situations may be modelled either by a plane strain or an axisymmetric model. The user interface consists of four sub-programs (Input, Calculations, Output and Curves) which are performed to be used successively in a geotechnical modelling. These sub-programs can be treated one by one, forming a logical and complete methodology in order to undertake a geotechnical problem.

The operation of each sub-program is briefly described below.

Input program

To carry out a finite element analysis using Plaxis, the user has to create a finite element model and specify the material properties and boundary conditions. This is done in this sub-program. The user must create a two-dimensional geometry model composed of points, lines and other components, in the x-y plane. The generation of an appropriate finite element mesh and the generation of properties and boundary conditions on an element level is automatically performed by the Plaxis mesh generator based on the input of the geometry model. Finally, the initial effective stresses are generated to set the initial state. The procedure scheme is showed below.

General settings: Specify a filename, the model (axisymmetry or plane strain), the size of the domain, type of element (6 or 15 nodes), units, etc.

Geometry: Creation of the geometry using points, lines, plates, geogrids, interfaces or anchors.

Loads and boundary conditions: Specify distributed or point loads, prescribed displacements, drains, wells and fixities.

Material properties: Specify the general properties of the soil and structures. Soils can be modelled either through a user-defined model or one of the predetermined (Mohr-Coulomb, soft soil, hardening soil, jointed rock). Properties are applied to each element of the geometry.

Mesh: The mesh is the composition of finite elements in which the geometry is discretised. The basic type of element is the 6-node or the 15-node triangular element. Plaxis allows for a fully automatic generation of the mesh, resulting on an "unstructured" mesh. This mesh may look disorderly, but the numerical performance of these meshes is usually better than for regular (structured) meshes. Users may also customise the finite element mesh in order to gain optimum performance.
The element used in this study is the 15-node triangular element, which provides an interpolation of fourth-degree order for the displacements, with twelve points of Gauss's numerical integration where stresses are evaluated. The 15-node triangular

element provides better exactitude, although it leads to a major consumption of memory, and lower values of efficiency.

Initial conditions: Initial water pressures are generated by drawing the water table. Then, the initial effective stress field is generated by selecting the K_0 coefficient for each cluster, not taking into account of the structural elements.

Calculations program

One the geometry model has been created, the mesh has been generated and the initial conditions have been created, it is necessary to define what kind of calculations must be realised. The calculations program differentiates plastic calculations, consolidation, phi-reduction and dynamic. The project may be divided in phases in order to simulate construction stages, for instance, the activation of a surcharge or a staged excavation.

Choosing plastic calculation, as used in all the cases studied, leads to non linear equations which have to be solved in each calculation phase in a series of load steps. In Plaxis, there are diverse proceedings to solve non linear plasticity problems, based all of them on the selection of the load step. The selection of the correct configuration is automatically done by the program, to ensure the optimal results. This proceeding is controlled by a certain parameters that preserve the equilibrium between the exactitude, efficiency and hardiness. However, these can be manually selected in order to closely monitor the exactitude and the load steps.

Output program

In the Output program the user may easily view the results and elaborate results lists from the values originated from the calculation process. The main results from a finite element are the node displacements and the stresses, including the stresses against the structural elements if present.

Results may be checked through shadings, contours, lines, arrows or other representations. As said, results can be given in tables, with a structure that resemble to Windows environment, so these can be easily exported to the main Office applications (usually Excel) in order to handle and study them appropriately.

Curves program

The Curves program contains all facilities to generate load-displacement curves, stress-strain diagrams or stress paths in pre-selected points of the geometry.

This sub-program has been not used in this study, inasmuch as the diagrams provided are limited to previously selected points, and taking into account that results have been fairly handled, it has proved not to be a useful tool for the development of this study.

4.2. Modelling sheet pile walls

Modelling sheet pile walls in a finite element program as Plaxis involves a large amount of parameters, including those for the soil, for structures or for loads, all necessary to complete a calculation.

This chapter is devoted to the explanation of all geometrical and geotechnical data adopted for the design of sheet pile walls used in this study.

4.2.1. Geometry

The first step consists of the creation of the geometry of the model. On the general settings window, shown in Figure 4.1, the user can select the general model used (plane strain), the element type (15-node triangle) and the dimensions. The size of the geometry depends on the case studied (cantilever or anchored walls), the excavation height and the embedment depth. In each case the influence of the excavation may be different. Two considerations related to the geometry size must be taken into account:

- Too large size of geometry leads to a major computational cost. Besides, the results given on distant points may be not relevant, since these are out of the influence range of the excavation.
- Too small size of geometry may lead to wrong results, as these are under the influence of the boundary conditions.

It has been proved that the same sheet pile wall modelled with a different geometry size gives different results from each other. In order to review and verify previous results, an equal geometry has been used as in the previous study, when running the cases for a second time.

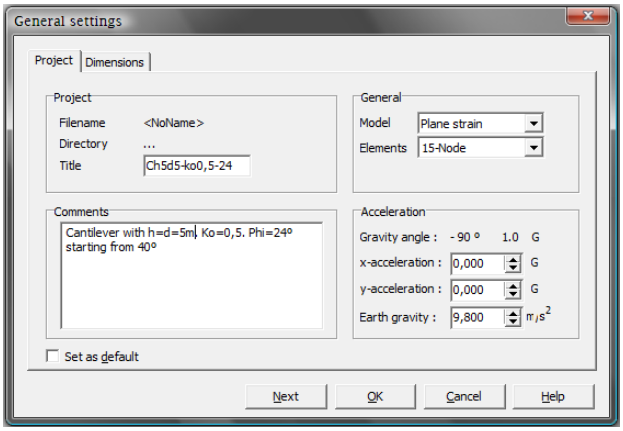

Figure 4.1 General settings window

Modelling the ground

The ground is represented by a set of independent lines. When a set of lines form a closed polygonal an independent cluster is created, where the soil properties can be applied. Diverse clusters can be created in order to model, for instance a stratified soil or the ground layers that will be successively excavated in a staged progress.

Modelling sheet pile walls and interfaces

Sheet pile walls may be modelled through the element “plate”. Plates are geometrical lines as well. Consequently when placing a plate, a back and a front of the wall are quickly created.

Plates represent structural elements, resembling to a beam, and therefore a bending stiffness (EI) and an axial stiffness (EI) must be introduced. The equivalent plate thickness is calculated through the following transformation:

$$d_{eq} = \sqrt{12 \frac{EI}{EA}} \quad \textbf{(4.1)}$$

The usage of the element plate avoids using a dense discretization through the mesh for modelling the sheet pile wall.

Alongside the wall, the element “interface” has been used with a double aim. The interface pretends to eliminate the stress and deformation peaks produced in the corner of a structure. At the same time, the soil structure interaction is simulated by decreasing the soil resistance in this contact. Each interface has assigned to it a virtual thickness, which is an imaginary dimension used to define the material properties of the interface. The higher the virtual thickness is, the more elastic deformations are generated.

Modelling ground anchors

Geogrids may be used in combination with node-to-node elements to simulate a ground anchor. The geogrid is used to model the grout body and the node-to-node anchor is used to model the anchor rod (free length).

The anchor rod, which crosses the failure wedge, is usually made up of cord or steel cable whose function is to transmit from the anchor point until the bulb, situated outside the failure wedge, the stresses supported by the wall.

The anchor bulb consists of the cord enclosed by a grout body, usually of cement slurry, due to its length and diameter (depending on terrain and load). The forces transmitted by the anchor rod, and hence the earth thrust, are resisted by friction.

Plaxis element "node-to-node anchor", which simulates the free length of the anchor, is an elastic element that allows the transmission of load from one to another element, simulating the free length of the anchor. The node-to-node anchor consists of two points where the stress is concentrated, since the intermediate length that separates only acts as a transmitter of loads, and therefore the bulb is not well represented. Due to this, the grout body has been simulated using the element "geogrid".

The geogrid fixed to the end of the node-to-node anchor can represent a linear element on which to distribute the loads transferred by the free length. The diameter of the bulb may not be simulated by the mechanism described. However, a good approximation has been found by assigning a value of stiffness to the geotextile equivalent to that of steel cable. Because this simulation, two important phenomena in the design of anchors can not be reproduced: slippage bulb-cord and slippage bulb-ground. Both checks should be carried out afterwards.

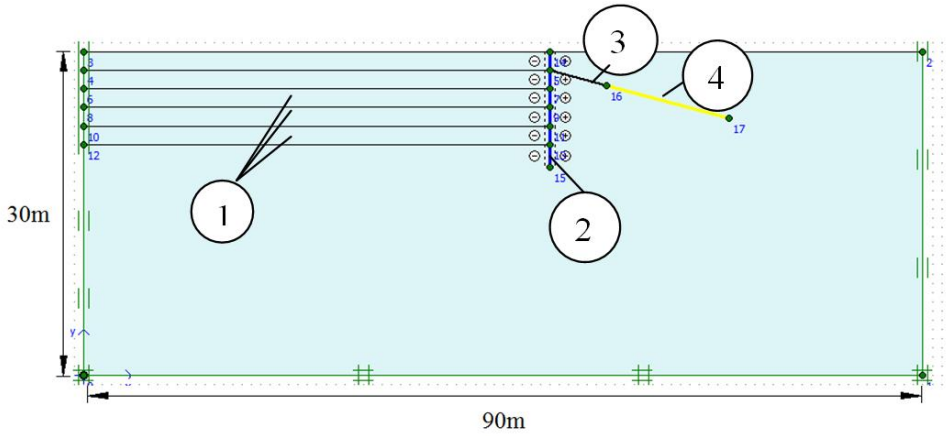

Figure 4.2 Geometry of the model. (1) Clusters. (2) Sheet pile wall. (3) Anchor rod. (4) Grout body

4.2.2. Loads and boundary conditions

Plaxis allows entering into the model boundary conditions and known loads. Of all the options available, only the "standard fixities" option has been used . This boundary condition is used in many geotechnical problems, as a quick and comfortable application. In the case of sheet pile walls it has been very useful because it fits the needs of the analysis in the following ways:

- To the vertical lines corresponding to the X coordinate that constitute a boundary of the model, a horizontal fixity is assigned in which the lateral displacement is zero ($U_x = 0$).
- To the geometric lines that constitute the lower boundary of the model, a zero displacement in both vertical and horizontal axis is assigned ($U_x = U_y = 0$).

Plaxis external loads are of two types: point and distributed. Loads must be activated in the calculations program only when desired.

4.2.3. Material properties

The application of the constitutive equations of finite element model requires the use of a number of parameters or previous data, depending on the type of material, so that the problem can be solved. These soil properties are usually obtained from geotechnical studies.

The computational power of finite element management is accompanied by several variables that need a numeric value. The main difficulty regarding these variables lies in knowing the precise meaning of each of them, often invisible in the classical analytical methods, and taking magnitudes that are coherent with each other to provide consistency to the model.

This thesis is the continuation of a previous thesis. The contribution of this master thesis has been to study the influence of some parameters whose influence was previously missed. The analysis has been focused on observing changes in the behaviour of sheet pile walls when those parameters or most significant data are changed. That would allow making the comparison with analytical calculation methods.

The main parameters that have been analysed are: friction angle, cohesion, rigidity of sheet pile walls and anchors, and anchor tensioning force. Before addressing the calculation methodology adopted it is useful to know the input value required by the program for each material.

Material sets for soil

Most of the material data has been chosen to be identical as in the previous thesis, so that the study to be relevant and comparable. Material properties are introduced in Plaxis within three categories:

1) General (see Figure 4.3):

Material model: The material model used in all cases has been Mohr-Coulomb, a one-dimensional approximation to the real behaviour of the soil.

Material type: In all cases a drained material has been selected, so the soil friction angle and the cohesion are involved.

Specific weight (γ_{unsat}): 20 kN/m^3. The saturated specific weight has been considered to be the same, as it is not relevant in a drained study.

The pore index and the permeability are not relevant, since it is a drained study.

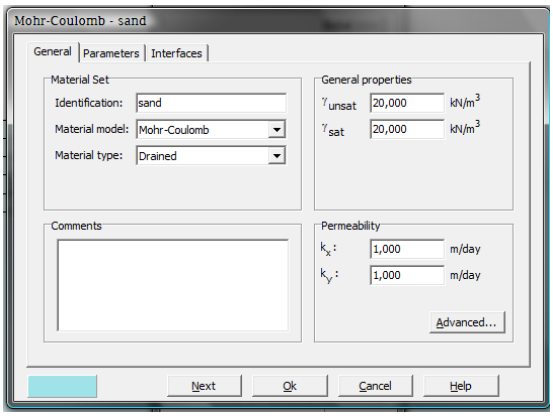

Figure 4.3 General window for material sets

2) Parameters (see Figure 4.4):

Young modulus (E): The value chosen represents an average value for soils, $1.3 \cdot 10^5$kN/m^2. This value is consistent with the stress and the paths expected for the cases analysed. The influence of this parameter has been studied in the previous thesis, and the findings showed that too large or too small values of *E* may cause numerical problems.

Poisson's coefficient (ν): A value of 0.3 has been adopted, which is consequently with drained conditions. Usually this value is adopted for drained soils, when variations in the volume are significant.

Cohesion (c_{ref}): For the cases analysed, a value of zero has been adopted. When considered, a value of 10 kN/m^2 has been adopted.

Soil friction angle (φ in Plaxis, ϕ in the thesis): The main strength parameter of the soil. Its value is variable in this study and constitutes the element in which this study is focused.

Dilatancy angle (ψ): Has not been taken into account in this study, because its usage is limited to strongly overconsolidated soils.

Alternative stiffness parameters: These parameters are automatically calculated from the Young modulus and the Poisson's ratio.

Advanced parameters: This option allows the elimination of tensile stresses (tension cut-off), through which the soil has zero tensile strength. This option has been used in all the cases studied and is perfectly in accordance with the behaviour of the sheet pile walls studied.

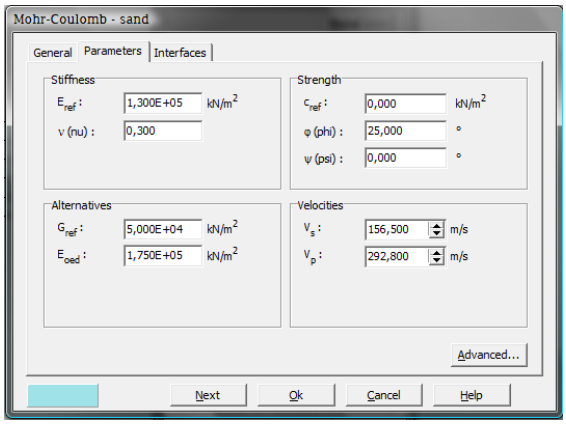

Figure 4.4 Parameters window for material sets

3) Interfaces

Through this window the strength of the interface is selected. The "rigid" option has been selected, in order not to decrease the resistance of the soil between the wall and the ground. Thereby, the same hypothesis as in the classical methods is fulfilled.

Once the material sets are competed, the user must apply the material properties to each cluster. The at-rest coefficient is manually introduced in the phase of initial stress generation (see chapter 4.2.4).

Material sets for plates (sheet pile walls)

The data for plates is summarised in one window (see Figure 4.5).

Material type: The constitutive model which governs the relation stress-strain has been selected "elastic" for all the cases analysed. This selection simplifies the calculations and is in accordance with the reality, since sheet pile walls are designed to have an elastic response.

Axial and bending stiffness (EA), (EI): An elastic modulus of $35 \cdot 10^6$ kN/m^2, characteristic of a current concrete used in sheet pile walls, and an area and an inertia corresponding to a thickness of 40 cm have been considered.

Weight (w): Is obtained by multiplying the unit weight of the plate material by the thickness of the plate. Therefore, it has units of force per unit area.

Poisson's coefficient (ν): For thin and flexible structures a value of zero is recommended for the direction normal to the plane.

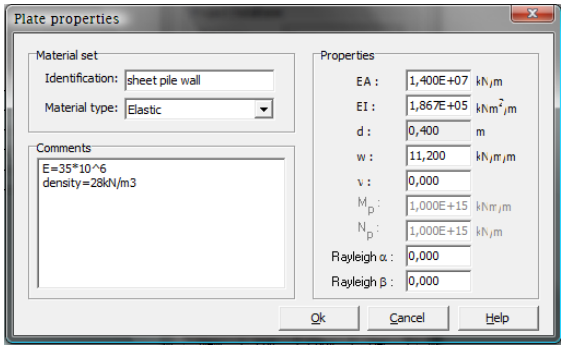

Figure 4.5 Window of plate properties

Material sets for geogrids (anchor bulb)

Geogrids represent geotextile elastic material extending in the direction perpendicular to the plane and are only able to resist tensile stress. Its elastic behaviour is modelled by the axial stiffness value:

$EA=3.3\cdot10^4$ kN/m

This value is calculated by dividing the node-to-node anchor value by the distance between anchors, to provide an equivalent stiffness to the bulb.

Material sets for node-to-node anchors (anchor rod)

The proceeding for this tool is identical to the geogrid (see Figure 4.6). An elastic behaviour without plastification has been specified (for the same reasons given in the case of the plates). The axial stiffness value is the same as that used in the geogrid and corresponding to a steel cable obtained form the design of the anchor.

The difference with the geogrid is the introduction of the spacing of anchors to automatically obtain the equivalent stiffness.

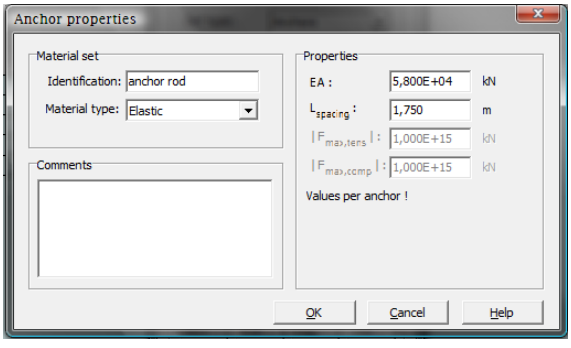

Figure 4.6 Window for node-to-node anchor properties

4.2.4. Mesh and initial stresses generation

The division of the finite element domain in which to perform the subsequent calculations is the discretization of the problem and is represented by the mesh.

The mesh has been generated by a preliminary analysis that uses a coarse mesh (few elements). Then, points or areas with concentrations of stress are found, or strain or phenomena where better accuracy is desired. The global mesh of the model in these areas is adjusted, to take into account possible local phenomena, maintaining a certain balance with the time consuming calculation.

It has been found that despite a very fine mesh provides better accuracy of results, the consumption of computing time increases and therefore a decision has been made to sacrifice accuracy to achieve a better balance over time.

The elements requiring special attention such as sheet pile walls or anchors, which have demanded greater precision of the results for further analysis, the mesh is refined by local refinement factor that reduces the size of the elements in proportion to the value introduced. In general, the overall level of refinement type is "fine" with a local refinement in displays and anchors between 0.25 and 0.5.

Having established the optimal mesh, the last step before proceeding with the calculations is to establish the initial conditions for the water flow and stresses.

When setting the initial stresses the program switch off by default all the different elements to the soil type, as a starting point of the tensions of the soil prior to any action. At all times it has been assumed normally consolidated soil represented by a zero value of OCR and POP parameters corresponding to the degree of overconsolidation and preconsolidation pressure respectively.

The at-rest coefficient may be introduced manually (see Figure 4.7), and then assigned to each cluster. Whether not, the program automatically introduces a value of the coefficient calculated from Jacky's formula by default:

$$K_0 = 1 - \sin\phi \tag{4.2}$$

After this step, the initial stresses are generated in the model (see Figure 4.8).

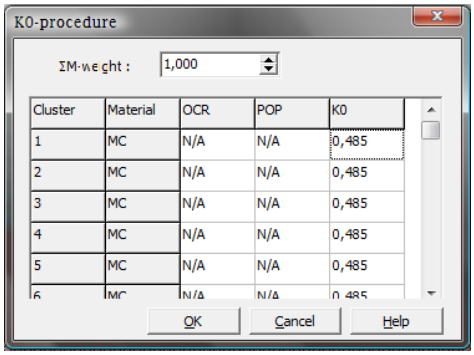

Figure 4.7 Window for entering K_0

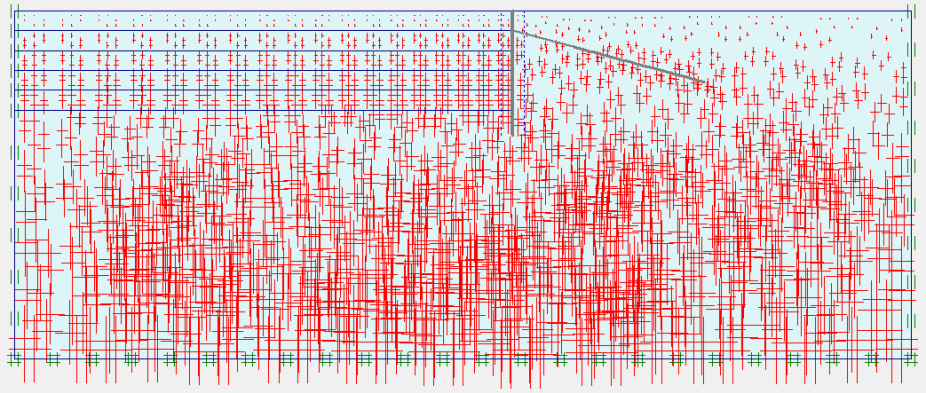

Figure 4.8 Initial effective stresses

5. INFLUENCE OF THE INITIAL STRESS STATE

The initial stresses in a soil body depend on the weight of the material and the history of its formation. At the initial moment, the stress state is characterised by a vertical effective stress (σ'_{v0}). The horizontal earth pressure is determined by the lateral earth pressure (or at-rest) coefficient (K_0).

The influence of initial stress conditions has been studied through a finite element model by Fourie & Potts (1989). In this study, the geometry of 100X100 m was discretised by 165 eight-noded isoparametric elements. Two values of K_0, 0.5 and 2, considered to be extreme, were used and a single soil friction angle (ϕ=25º) was considered. Nowadays, the development of finite element programs together with the improvement of calculation power of computers, allows extending the range of cases studied fairly easily.

The at-rest pressure is the initial thrust exerted by a horizontal-surface soil body before being excavated; or before a wall attached to it suffers any kind of movement. Whether the soil is homogeneous and the forces applied over it vertical or horizontal, this thrust will be, by symmetry, horizontal. The at-rest coefficient is therefore defined as the ratio horizontal to vertical effective earth pressure, as in eq. 5.1.

$$\boldsymbol{K_0 = \frac{\sigma'_h}{\sigma'_v}} \tag{5.1}$$

The finite element program Plaxis has an automatic procedure to introduce the value of the at-rest coefficient (K_0) when generating the initial stresses. By default, the parameter K_0 is calculated through the formula of Jacky (eq. 2.1). However, Plaxis allows introducing manually it instead. A consideration must be done in order to ensure that the soil is initially normally consolidated, since the formula of Jacky is appropriate only for normally consolidated soils. The possibility of having an overconsolidated soil involves the manual introduction of K_0 using eq. 5.2 or eq. 5.3 (Mayne & Kulhawy).

$$\boldsymbol{K_0 = K_0^{NC} OCR + \frac{1-\nu}{\nu}(1 - OCR)} \tag{5.2}$$

$$\boldsymbol{K_0 = K_0^{NC} OCR^{\sin\phi'}} \tag{5.3}$$

In normally consolidated soils, K_0 is constant and depends on the soil friction angle. In overconsolidated soils, K_0 is found to be much more variable with the variation of the soil friction angle. The methodology used in this study, consisting of a phi-reduction procedure, involves a different value of K_0 when initial stresses are generated, since the soil friction angle is different in each case. In order to make the results comparable, in the previous work of Cuadrado (2010) a criterion was established, consisting on generating the same initial stresses for all cases. That means introducing the same value of K_0 in the entire domain regardless of the soil friction angle with the purpose, as said, to establish a basis in which results may be comparable.

This study is focused on the influence of the initial K_0 value on the behaviour of the sheet pile wall. Results of the failure and the stress state for the same geometry were presented and analysed in the previous work of Cuadrado (2010). For this reason, results are not shown for a second time.

When introducing manually the value of K_0, the program Plaxis warns of selecting very high or very low K_0-values, since this values may cause initial plasticity. This effect will be explained forward.

5.1. Methodology

A phi-reduction procedure has been applied to two free embedded cantilever sheet pile walls. The procedure resembles to that developed by Cuadrado (2010), consisting of modelling the sheet pile wall on Plaxis and then calculating the equilibrium by reducing the soil friction angle successively until equilibrium is not reached. The soil friction angle corresponding to the limit state is assumed to be the last case immediately before collapse.

Near the limit state, numerical difficulties are found out, hindering the choice of the minimum soil friction angle supported. Eventually, equilibrium is achieved for a soil friction angle lower than in a case where it is not. Due to this, a criterion of choice has been established, based on selecting the first angle for which the equilibrium is not fulfilled, in a phi-reduction procedure. In most cases, the numerical difficulties are found to be related to the instantaneous excavation, which are, at least partially, solved with a staged excavation.

The methodology followed in the study of the influence of K_0 is presented below.

1) Model a cantilever sheet pile walls in Plaxis with a determined geometry: h=d=5m.
2) After pre-selecting a value of K_0, the limit state is found by reducing successively the soil friction angle (phi-reduction procedure) as explained above.
3) A new value of K_0 is adopted, and point 2 is repeated. The range of K_0 values used attempt to be realistic, within 0.5 and 2.
4) Interpretation and analysis of the results.

Cases considered

As said, the sheet pile wall modelled has a retained height of 5m and an embedment depth of 5m.

The phi-reduction procedure starts from a soil friction angle of 45º. The methodology based on assuming a K_0 value independently of the soil friction angle presents a difficulty. This is a "synthetic" situation, and therefore verification must be done in order to ensure the value of K_0 adopted to be within the values of K_a and K_p, according to relation 2.2. It should be not forgotten that K_a and K_p represent limit values, and therefore K_0 can not be lower as K_a or higher as K_p. In that case, the soil would be at failure in the initial state. Hence, the possible values of K_0 comprise a range as showed on Table 5.1. Taking into account that K_a increases as ϕ decreases, and K_p decreases withϕ (eq. 2.8 and 2.9), the soil friction angle considered in Table 5.1 is expected to be the minimum achieved in Plaxis for this geometry. According to this, K_0 may not be lower than 0.44 or higher than 2.28, which is in agreement with Fourie & Potts (1989), who considered two extreme values, 0.5 and 2. Thus, four values of K_0 have been selected for the study: 0.5, 0.75, 1, 1.5 and 2.

ϕ	K_a	Kp
23º	0.44	2.28

Table 5.1 Selection of the cases to study

5.2. Analytical methods

The sheet pile wall design usually starts from soil geotechnical data, basically the soil friction angle. Then, the embedment depth is calculated according to the classical analytical methods, seen in 2.4.1.

In this study, as in the previous work of Cuadrado (2010), the procedure has been the inverse as the common way to design a sheet pile wall. In other words, the way to proceed has been to start from a specified geometry (excavation and penetration depth) and then obtain the soil friction angle corresponding to the limit state of stability. The reason of this procedure is essentially practical. While working with the numerical model, a huge amount of cases are needed to be run, and it is much easier to change the soil properties than the geometry.

Table 5.2 shows the results for the case analysed.

CASE	ANALYTICAL METHOD	
	ϕ_s	ϕ_g
h=5m d=5m	28.5	30.1

Table 5.2 Soil friction angles resulting form the analytical methods. ϕ_s=simplified method. ϕ_g=gradual method.

5.3. Results analysis

A sheet pile wall with a retained height (h) of 5m and an embedment depth (d) of 5m has been modelled. In this chapter the results of the behaviour of the wall related to K_0 variation are explained in depth.

Movements of the sheet pile wall are mainly horizontal (see Figure 5.1). A vertical component almost always exists, which can be ascendant or descendant. However, the most part of the movement corresponds to a horizontal component. A rotation point is recognised near the bottom of the wall, such as classical methods predict.

The horizontal displacement at the top of the wall has been selected in order to assess the effect of K_0 parameter on the wall behaviour.

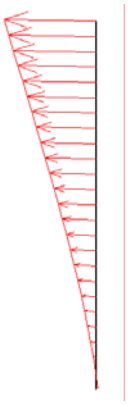

Figure 5.1 Displacements in the sheet pile wall, represented with arrows, near the limit state. A rotation point is recognised near the bottom of the wall.

Figure 5.2 shows the evolution of the horizontal movement at the top of the wall as the soil friction angle is decreased. This relation does not represent a physical process or evolution in time, but a set of results for the same geometry when the soil has successively poorer strength properties. At first sight, a non linear trend is recognised. The horizontal movement of the wall grows as the soil friction angle is reduced. Notice the vertical asymptote corresponding to the limit state, with strong similarity to results of Cuadrado (2010). Failure situations have not been represented.

K_0= 0.3 case has been represented as well (see Figure 5.2), but the sequence of phi-reduction has not been completed, since the soil is at failure conditions for values of ϕ below 35º. This case is therefore not representative.

Curves are in agreement with each other. These are nearly parallel and have the same asymptote, with the exception of K_0= 0.5 curve, which seems to have another trend. For K_0 values from 0.75 to 2, movements at the top of the wall grow with K_0, for the same soil friction angle (see Figure 5.2). This observation is in accordance to those showed by Potts & Fourie (1989). The difference on the wall horizontal displacement may be considerable, being able to reach the double value of displacement depending on the K_0. A different trend can be recognised for K_0 values below 0.75. In this case, horizontal displacement seems to grow as K_0 value decreases. Such fact involves the existence of a minimum displacement for a particular K_0 value.

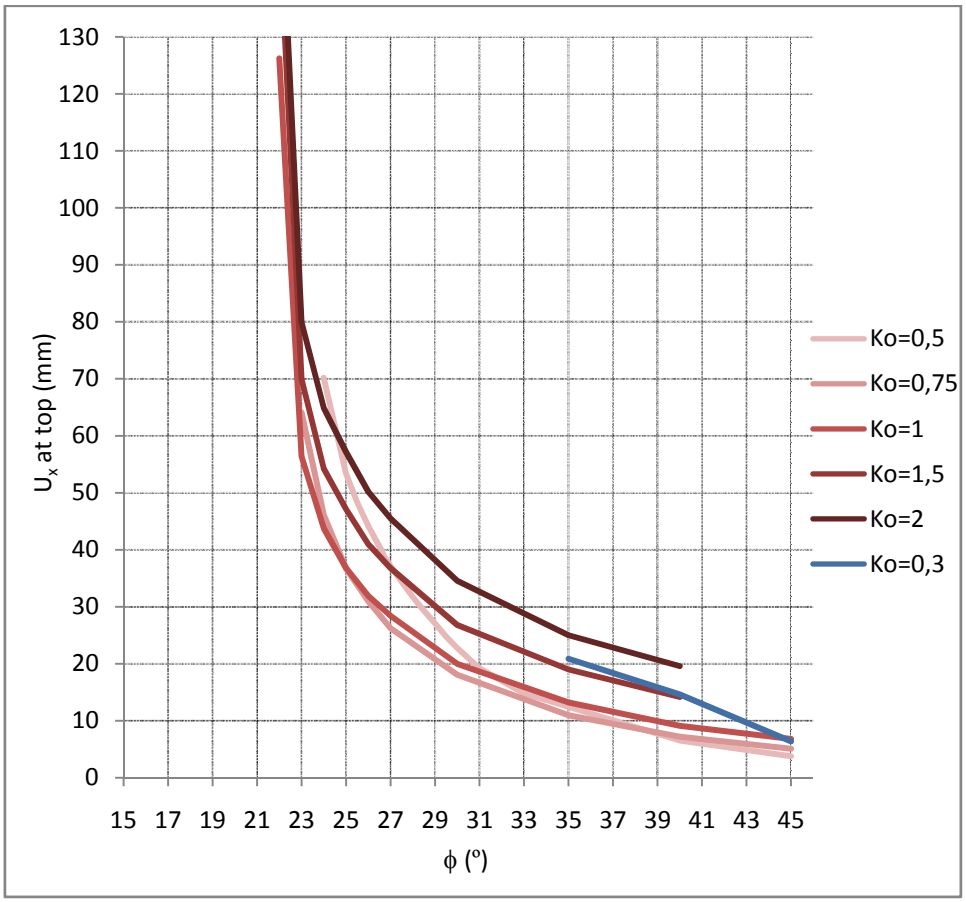

Figure 5.2 Evolution of the movement at the top of the wall with soil friction angle variation. Notice the vertical asymptote corresponding to the limit sate.

Figure 5.3 shows the horizontal displacement at the top of the wall, which is equivalent to a vertical cut on Figure 5.2. As seen above, a minimum value of horizontal displacement can be recognised for a particular value of K_0, especially near the limit state. This minimum is more recognisable, the closer from the limit state the soil is. The minimum movement is located for K_0 values between 0.7 and 0.9 depending on the soil friction angle. In a limit situation with a soil friction angle of 25º the minimum movement occurs with a K_0 value of 0.85. Movement may change up to 40% depending on the initial stress state.

In Figure 5.3, the right branch of the graph represents a rigid movement, with higher values of horizontal stress in relation to vertical stress; while the left branch shows a more deformable behaviour pattern.

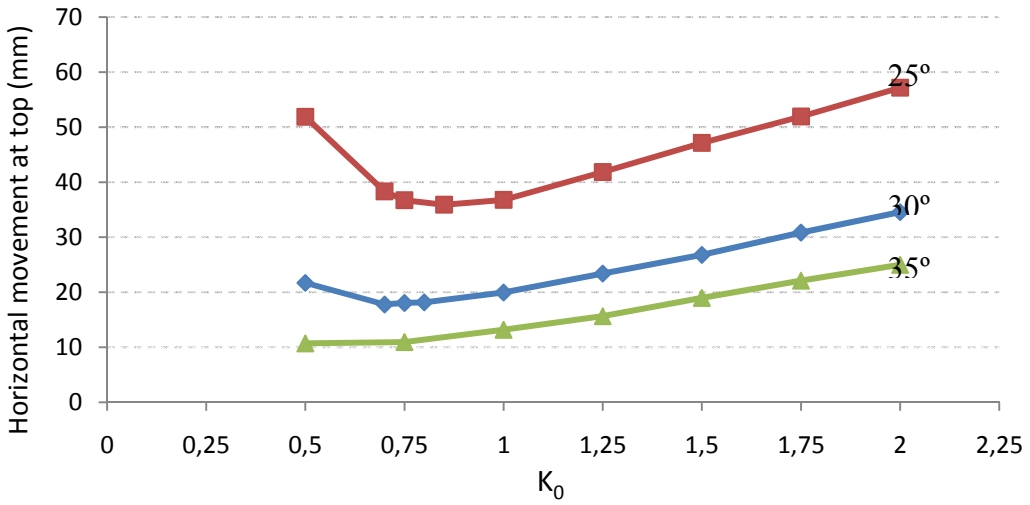

Figure 5.3 Evolution of the movement at the top of the wall with K_0 for different soil friction angles.

Numerical difficulties

Some numerical difficulties are found near the point of minimum displacement. When calculating this case, the maximum number of iterations is reached and the accuracy condition is not fulfilled.

6. MULTIPLE-ANCHORED SHEET PILE WALLS

6.1. Introduction

This chapter is devoted to the study of sheet pile walls anchored with multiple rows of anchors. The behaviour of single anchored sheet pile walls has been studied by Cuadrado (2010). This chapter pretends to be the broadening of this study to further anchor levels.

As seen in chapter 2.4.3, it can be stated that the complexity of the system soil-structure grows as the number of anchors is increased. The complex interaction between wall and soil own of the design of cantilever sheet pile wall by itself is increased by adding the effect of the anchors, which interact with both the wall and soil. The design of this kind of structures is based on the global experience. In fact, there may not be found any analytical method for the design of multiple-anchored sheet pile walls in the existing literature. All the studies performed so far are essentially experimental.

The object of the study is three fold. First, to evaluate the influence of the construction procedure in a two level-anchored sheet pile wall. Secondly, to evaluate the influence of the variation of the anchor load, and the variability of the bending moments depending on the moment in which the pre-stressing force is applied. And finally, a case of three-level-anchored sheet pile wall has been developed, in order to compare it with the two-level-anchored case and notice the advantages of a third row of anchors. These issues have been studied deeply in the past by authors such as Richars & Powrie (1994) for the case of propped –not anchored– sheet pile walls. A summary of this study can be found on chapter 3.2.

The wall-soil system response may differ greatly depending on the construction procedure. It is not the same applying the anchor load when the dredge level is at the anchor point, or applying the same load after finishing the excavation, with the entire sheet pile wall working as a cantilever structure. The bending moment law and the wall movement may differ depending on the cases explained.

The anchors may not be placed before the excavation takes place. The excavation at the anchor level must be achieved before placing the anchor and applying the pre-stressing force. In fact, further excavation depth must be achieved before placing the anchor due to constructive needs. Therefore, there is a lapse of time in which the sheet pile wall, or a particular height of it, behaves such as cantilever wall.

In the same way, the anchor position may be subject to an arbitrary location. The common practice is to locate the first row of anchors near the crest of the wall in order to reduce movements at the top. Bending moments and movements may differ as well when choosing the appropriate location.

The usual trend in the design is to reduce bending moments and movements. A lesser bending moment may permit the reduction of the wall section, which represents an economical and practical benefit. A reduced movement represents an important advantage at service conditions. In anchor load terms, the predictable response to the anchor load increase is to reduce the bending moment, which is the main motivation of anchoring sheet pile walls. This is preferable to reducing the anchor load and increasing the bending moment.

There are no geotechnical mechanisms for the failure of anchored sheet pile walls, but a global failure mechanism. This may occur specially with anchors with insufficient length, where the anchor does not overpass the Rankine failure wedge.

The inputs in this study are therefore the position and inclination of the anchor rows in the wall, the construction procedure, obviously the geometry, and the anchor load. The position of the anchor rows and the construction procedure are studied below. The geometry is the same for all the cases. The anchor load is explained below.

Anchor load

The anchor load applied to the rod in a single-anchored sheet pile wall has been studied by Cuadrado (2010). The anchor force of the tie rod may be determined by the analytical methods –free earth support or fixed earth support– but this value corresponds to the equilibrium at failure. However, this load will be different in service conditions and depends on the stages followed.

Cuadrado (2010) showed as well that regardless the anchor force applied, after the excavation is done, this trend to the theoretical value of the anchor force. In fact, the fictitious point to which the anchor load tend is slightly higher as the theoretical free earth support value. This behaviour may be seen on Figure 6.1.

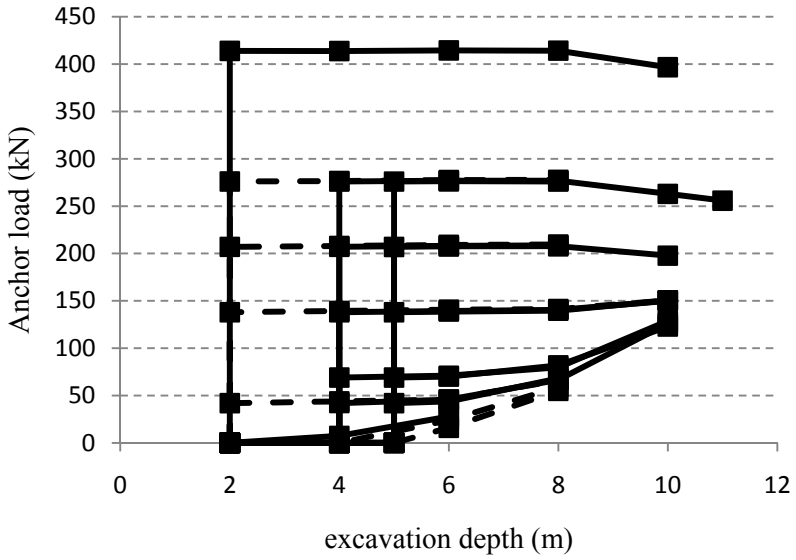

Figure 6.1 Variation of the anchor force as excavation takes place, for different prestressing loads (Cuadrado, 2010).

Further conclusions from Cuadrado (2010) where that the behaviour of the wall resembles to that predicted by the analytical methods only when applying to the anchor a force similar to the theoretical value. As the strain takes place in the anchor, the passive pressure is mobilized. In other cases –with other values of prestressing force– the failure mechanism is different from that predicted by the classical methods and the behaviour is not comparable.

The anchor load has been selected by basing on the free earth support method, and therefore assuming a single row of anchors, a force of 249,01 kN/m must be applied to the anchor in order to guarantee equilibrium. This force is supposed to be distributed in

both anchors. In order to simplify the cases, the same force is applied to each anchor and is equal to ½ the theoretical value for a single-level anchored sheet pile wall (124,5 kN/m). This value is rounded to 125 kN/m in order to guarantee the stability of the model.

6.2. Geometry and methodology

The geometry used consists of a sheet pile wall of 15 m total height and an embedment depth of 6 m. The retained height above the dredge level is therefore 16 m. This cantilever section is sustained by two rows of anchors with an inclination of 15º. The anchor length must be sufficient to overpass the Rankine failure wedge. Starting from a strict soil friction angle of 36º, an anchor length of 20 m fulfils this condition. The geometry of the model may be seen on Figure 6.2.

Total lenght	15 m
Embedment depth	3 m
Retained height	12 m
Anchor rows	2
Anchor inclination	15º
Anchor length	20 m
Soil friction angle	36º

Table 6.1 Sheet pile wall geometry

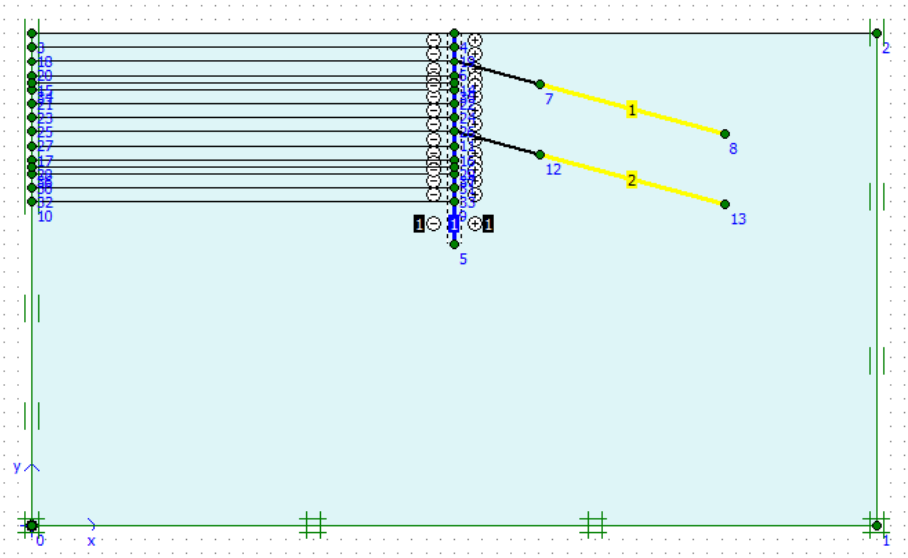

Figure 6.2 Geometry of the model for the double row-anchored sheet pile wall

6.2.1. Study of the influence of the construction procedure

For the study of the influence of the construction procedure a range of cases has been considered. The aim is to recognise a trend in the relation between the stages followed, the bending moment and wall movement. The methodology consists of the following steps:

i) Represent the geometry of the model which permits a staged excavation.
ii) Installation of the anchors when the anchor level is reached in the excavation.
iii) Steeply increase the excavation depth before placing the anchors and applying the load.

Cases considered

Case 1: Installation of the anchors when the anchor level is reached in the excavation.

Case 2 to 6: Late installation of the anchors with the maximum cantilever section as possible on case 6.

CASES	Excavation before placing 1st row of anchors		Excavation before placing 2nd row of anchors
CASE 1	2 m	17%	7 m
CASE 2	3 m	25%	8 m
CASE 3	4 m	33%	9 m
CASE 4	5 m	42%	10 m
CASE 5	6 m	50%	10 m
CASE 6	7 m	58%	11 m

Table 6.1 Cases considered

6.2.2. Study of anchor load variation

In this study, the starting point is case 3 mentioned above. A case has been selected where a certain wall defection occurs before placing the anchors. In this situation, an excavation of 2 m below the anchor level is completed before placing the anchors.

The anchor load is steeply increased from 0.5 to 3 times the theoretical value (125 kN/m) as seen on Table 6.2. Therefore, the second case (125 kN/m) corresponds to the case 3 mentioned above. The construction procedure is then the same as case 3, starting with 4 m of excavation -2 m beneath the anchor level- and the placing and pre-stressing of the upper anchor. Then the excavation continues until 2 m below the lower anchor. The lower anchor is placed and pre-stressed and finally the rest of the excavation -3 m- is completed. The construction procedure may be seen on Table 6.3.

Anchor load	
0.5 x theoretical value	62.5 kN/m
1 x theoretical value	125 kN/m
1.5 x theoretical value	187.5 kN/m
2 x theoretical value	250 kN/m
3 x theoretical value	375 kN/m

Table 6.2 Anchor load variation cases

STAGE 1	Excavation 1 m
STAGE 2	Excavation 1 m
STAGE 3	Excavation 1 m
STAGE 4	Excavation 1 m
STAGE 5	Pre-stress upper anchor
STAGE 6	Excavation 1 m
STAGE 7	Excavation 1 m
STAGE 8	Excavation 1 m
STAGE 9	Excavation 1 m
STAGE 10	Excavation 1 m
STAGE 11	Pre-stress lower anchor
STAGE 12	Excavation 1 m
STAGE 13	Excavation 1 m
STAGE 14	Excavation 1 m

Table 6.3 Stages followed in the anchor load variation study

6.2.3. Three-level-anchored sheet pile wall

A case of sheet pile wall with three rows of anchors has been developed. The objective is to notice the advantage of placing an additional anchor row in terms of wall movement and bending moment. To do so, a third row of anchors has been placed beneath the existing lower row, near the point with potentially higher values of bending moment. Geometry may be seen on Figure 6.3. The expected behaviour is similar to the double-row-anchored sheet pile wall case, but with lower values of the maximum bending moment and horizontal wall movement. The construction stages followed are summarized on Table 6.4.

STAGE 1	Excavation 1 m
STAGE 2	Excavation 1 m
STAGE 3	Excavation 1 m
STAGE 4	Pre-stress 125 kN/m upper anchor
STAGE 5	Excavation 1 m
STAGE 6	Excavation 1 m
STAGE 7	Excavation 1 m
STAGE 8	Excavation 1 m
STAGE 9	Excavation 1 m
STAGE 10	Pre-stress 125 kN/m middle anchor
STAGE 11	Excavation 1 m
STAGE 12	Excavation 1 m
STAGE 13	Excavation 1 m
STAGE 14	Pre-stress 125 kN/m lower anchor
STAGE 15	Excavation 1 m

Table 6.4 Stages followed in the 3-row-anchored sheet pile wall

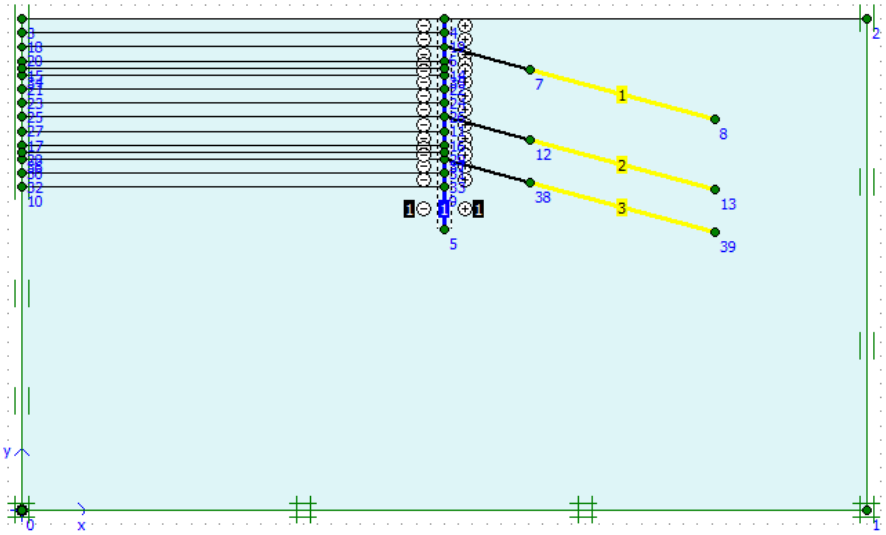

Figure 6.3 Geometry of the model for the three-level-anchored sheet pile wall

6.3. Results analysis

The wall horizontal displacement shows that all the length of the wall has moved to the excavation (see Figure 6.4), and although the displacement is lower at the bottom of the wall, the condition of the free earth support is fulfilled. The anchor load effect may be seen on the stress diagrams, where the shape of the bending moment and shear curves are modified with respect to the cantilever situation.

Figure 6.5 shows the final stress state for case 3, where the anchors have been placed when the excavation has reached 2 m below the anchor point. It may be seen that the passive pressure has been mobilised not only in front of the wall, but around the anchor points. This situation is far from failure.

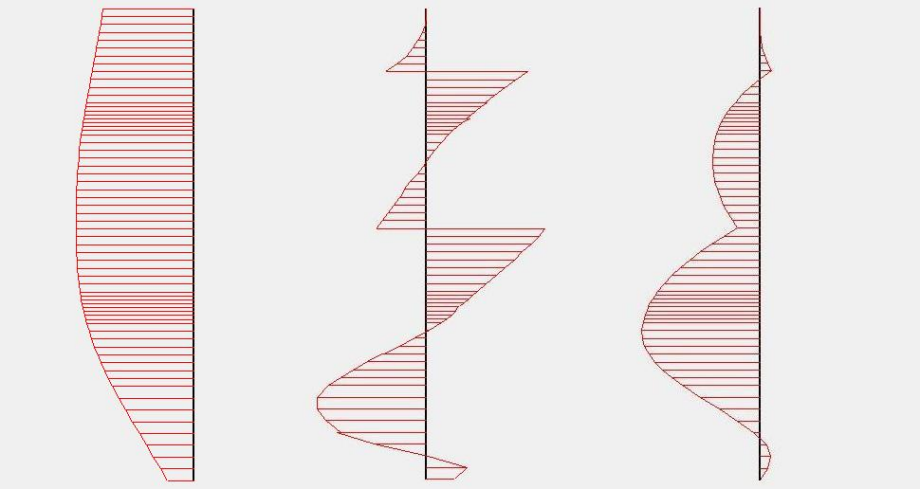

(a) (b) (c)

Figure 6.4 Sheet pile wall anchored in two rows with 200% of the theoretical anchor load. (a) Horizontal wall displacement. (b) Shear diagram. (c) Bending moment diagram

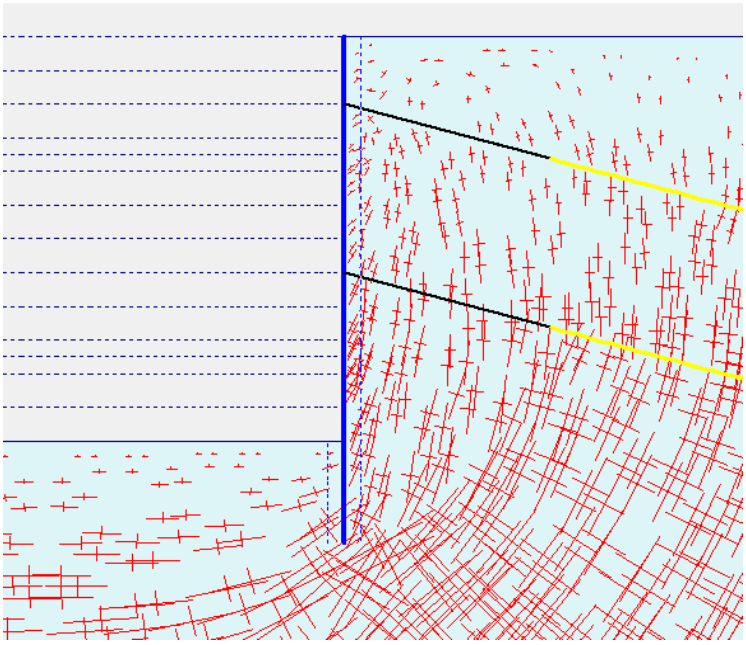

Figure 6.5 Main stress directions around the wall for case 3

Influence of the construction procedure

Table 6.5 Results for construction procedure cases shows the results for the 6 cases considered. The maximum horizontal displacement is minimum for the case 1 and maximum for the case 6. There is a recognisable trend to increase with the lately installation of the anchors (see Figure 6.6). This behaviour is not linear, but polynomial, so the displacement is greater when the more excavation is completed before placing the anchors. The effect of the early pre-stressing of the anchor is then to reduce the movements, particularly at the top of the wall. Oppositely, a larger movement of the wall takes place when lately applying the anchor pre-stress. A different behaviour may be seen for the bottom of the wall (see Figure 6.7). This point has roughly the same displacement independently from the stages followed. This behaviour is probably due to an excessive embedment depth, greater than needed.

CASE	% excv	M_{MAX} (kNm/m)	$Displ.Hzt._{MAX}$ (mm)	$Displ.Hzt._{TOP}$ (mm)	$Displ.Hzt._{TOE}$ (mm)	$M_{upper\ anchor}$ (kNm/m)	$M_{lower\ anchor}$ (kNm/m)
1	17	530,44	83,83	68	16,86	44	145,55
2	25	533,25	89,44	75,78	16,66	47,32	160,19
3	33	525,96	101,96	93,28	16,16	46,73	187,39
4	42	546,64	133,51	130,7	15,16	48,58	239,05
5	50	499,24	183,47	183,47	14,47	48,99	176,16
6	58	670,66	305,25	305,25	11,48	46,78	463,95

Table 6.5 Results for construction procedure cases

The maximum horizontal movement is not located in the top of the wall, but in a certain depth. Additionally, the later the anchor force is applied, the closer the maximum

horizontal movement is to the top of the wall. This occurs for cases 5 and 6 (see Table 6.5). This behaviour is predictable, as it resembles to cantilever behaviour.

In a hypothetic extreme situation, where the 100% of the excavation is completed before placing and pre-stressing the anchors, the entire wall is working as a cantilever structure in the lapse of time dedicated to the excavation. And so the maximum displacement would be at the top of the wall.

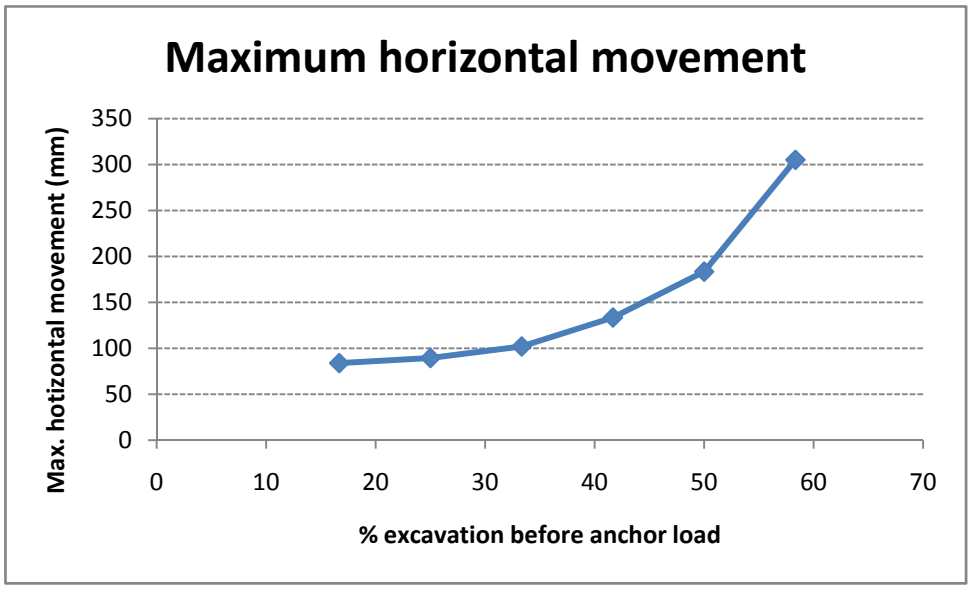

Figure 6.6 Maximum horizontal movement at the final stage for the 6 cases considered

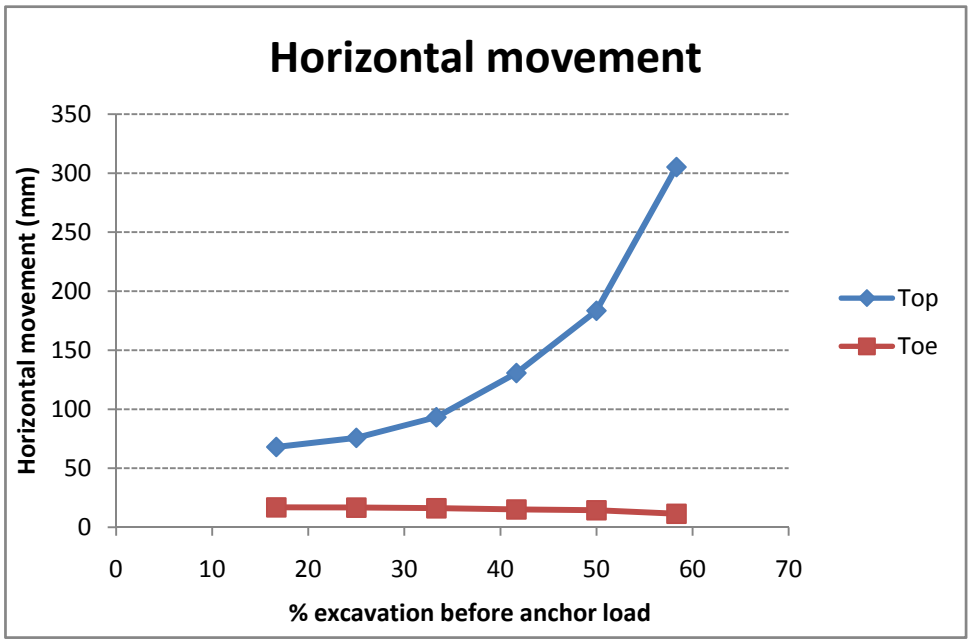

Figure 6.7 Horizontal displacement at the top and the bottom of the wall, at the final stage.

The shape of the bending moment distribution, and so the maximum bending moment, depend on the anchor load. A clear trend has not been found for the bending moment variation depending on the late application of the anchor load (see Figure 6.8). The

bending moment is supposed to be greater when the anchors are pre-stressed immediately after reaching the excavation level and lesser when a lapse of time runs before applying the load. This dependence has not been proved. The maximum bending moment takes place at 10 m from the top of the wall, but this distance is smaller for cases 5 and 6, where more deflection occurs before applying the anchor load. Note in Figure 6.9 that the bending moment at the lower part of the wall has roughly the same value, independently from the stages followed.

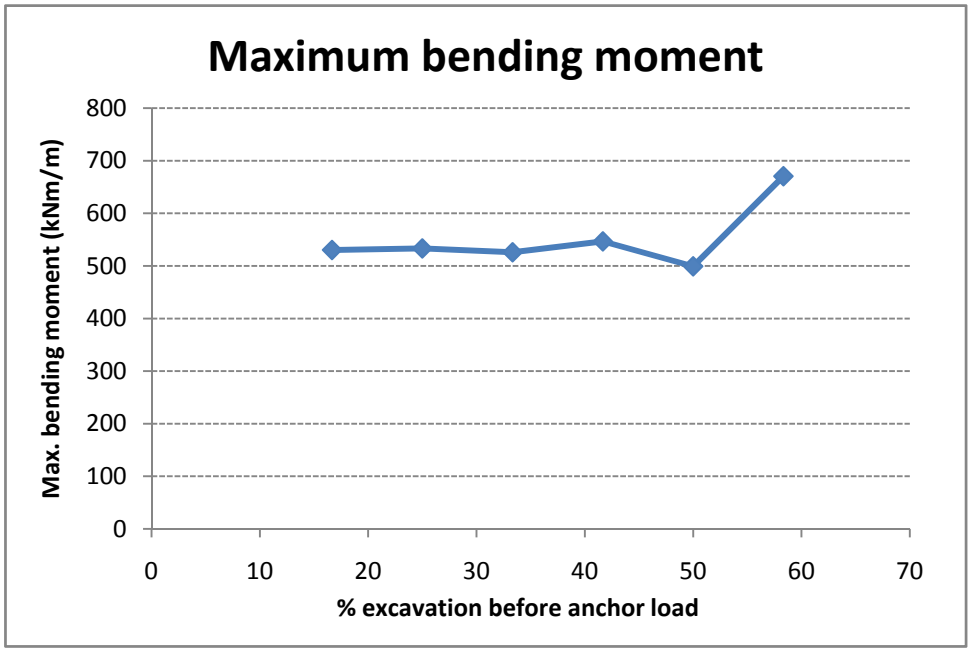

Figure 6.8 Maximum bending moment in the wall at the final stage

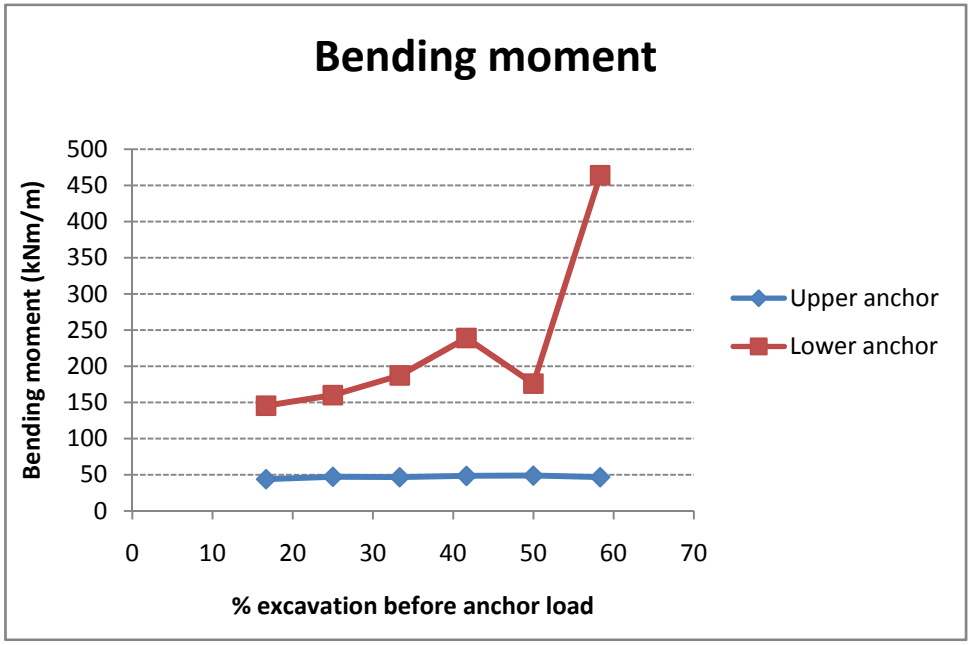

Figure 6.9 Bending moment at the anchor points, upper and lower anchors

Anchor load variation

Five cases have been run with the same geometry, and only changing the anchor load value. For the first case, a value of one half the theoretical anchor force has been considered, and then increasing the load for the next cases until three times the theoretical value in the last case.

Results on Table 6.6 show that the displacement decreases as the anchor load increases, with a nearly linear trend (see Figure 6.10), which is the predicted behaviour. As mentioned before, the top of the wall is more sensitive to the displacement variation depending on the anchor load variation (see Figure 6.11). The upper row of anchors is critical in order to reduce movements at the top.

% Over theoretical value (125kN/m)	Load (kN/m)	M_{MAX} (kNm/m)	Displ.Hzt.$_{MAX}$ (mm)	Displ.Hzt.$_{TOP}$ (mm)	Displ.Hzt.$_{TOE}$ (mm)	$M_{upper\ anchor}$ (kNm/m)	$M_{lower\ anchor}$ (kNm/m)
50%	62,5	539,12	119,13	115,25	15,58	47,56	224,56
100%	125,0	525,96	101,96	93,28	16,16	46,73	187,39
150%	187,5	518,35	87,62	74,42	16,80	48,53	141,63
200%	250,0	500,40	75,76	58,28	17,30	47,71	94,47
300%	375,0	448,28	52,83	37,91	18,34	86,91	8,50

Table 6.6 Results of anchor load variation

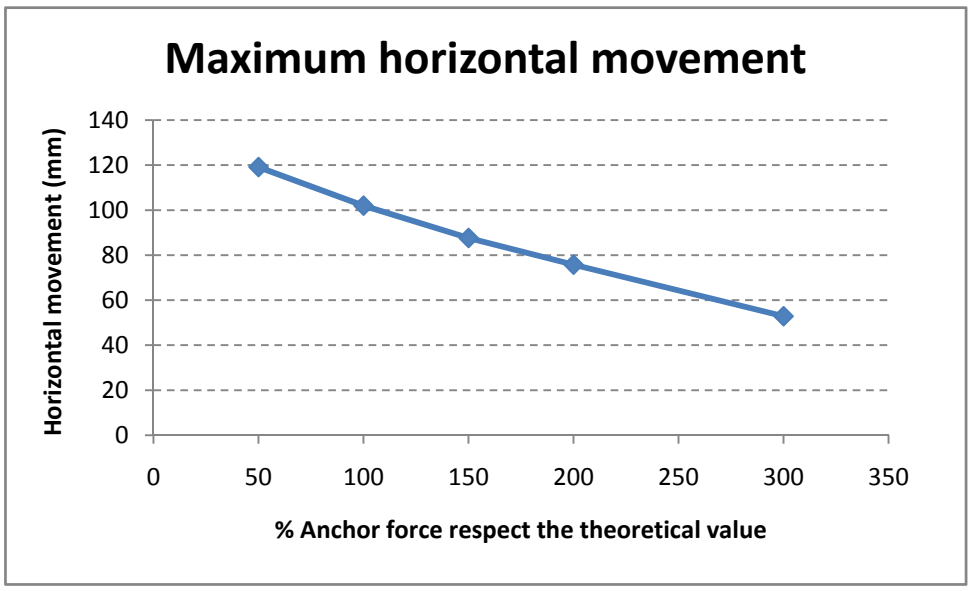

Figure 6.10 Maximum horizontal displacement while increasing anchor load

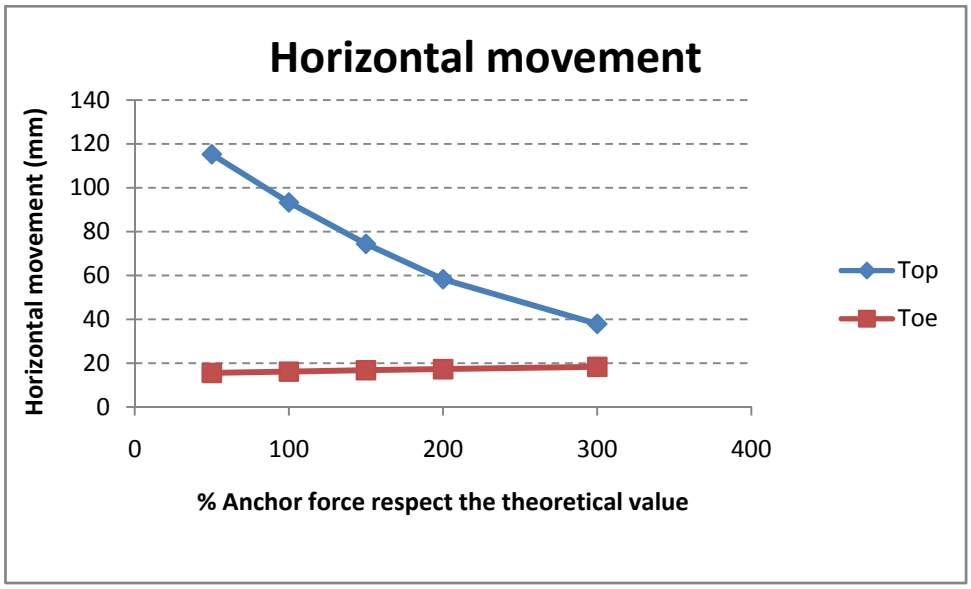

Figure 6.11 Horizontal displacement as anchor load is increased

In terms of bending moment, the expected behaviour is that a greater anchor load will lead to greater values of bending moment. This pattern has not been seen on the cases run. The bending moment, far from increasing, slightly decreases while the anchor load is multiplied (see Figure 6.12).

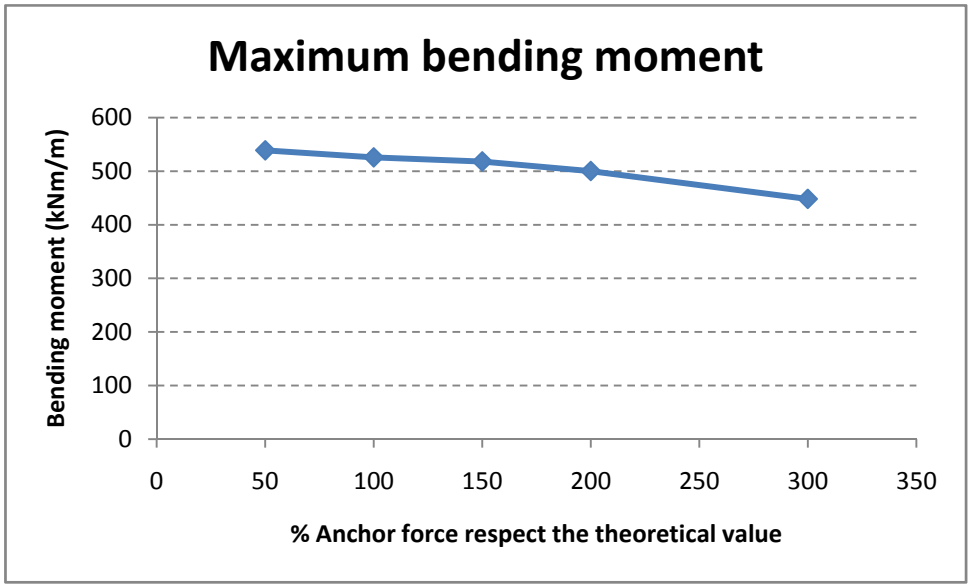

Figure 6.12 Maximum bending moment of the wall for different anchor loads

Three-row-anchored sheet pile wall

The results obtained are the expected in terms of bending moment and horizontal displacement. As seen in results Table 5.1 the maximum bending moment is significantly reduced when adding a third row of anchors. In this table, results have been compared with case 2 of the 2-row-anchored model, where the same excavation stages have been followed. The modification on the bending moment distribution shape may be seen on Figure 6.13. The effect of the lower anchor may be seen on the shear

distribution as well. In the same way, the maximum displacement is significantly reduced (see Table 6.7). Its location depends, as in the 2-row-anchored model, on the stages followed. When the anchors are placed after the whole excavation –or most of it– has been completed, the structure has been working as a cantilever wall in this lapse of time, and so the maximum displacement is registered at the top. The shape of the horizontal displacement does not differ much from the 2-row-anchored case.

The anchor load has been considered the same for the three levels. However, it seems that this practice may not be fully recommended. Anchor load may be adapted to the shear stress distribution, applying higher load to the lower rows and a lower load value to the upper anchor.

	M_{MAX} (kNm/m)	Displ.Hzt.$_{MAX}$ (mm)	Displ.Hzt.$_{TOP}$ (mm)	Displ.Hzt.$_{TOE}$ (mm)	$M_{upper\ anchor}$ (kNm/m)	$M_{middle\ anchor}$ (kNm/m)	$M_{lower\ anchor}$ (kNm/m)
3 rows	305,57	70,06	60,05	17,49	38,87	137,65	257,52
2 rows (Case 2)	533,25	89,44	75,78	16,66	47,32	-	160,19

Table 6.7 Comparison between results for 3-row-anchored and 2-row-anchored sheet pile walls

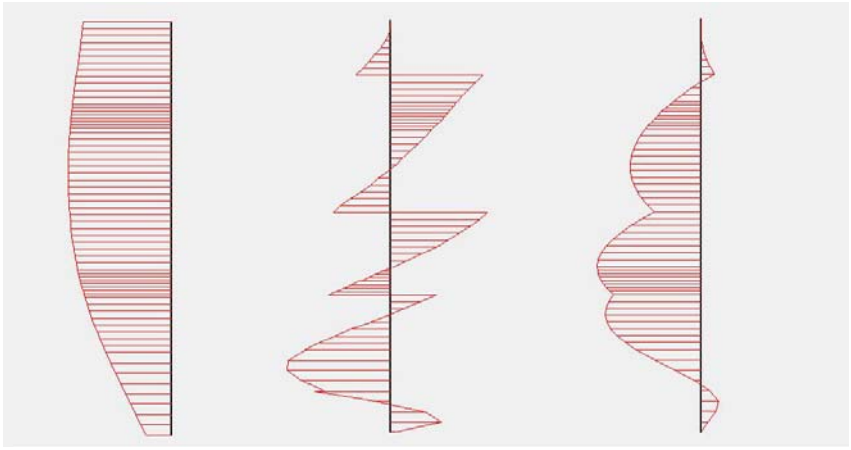

(a)

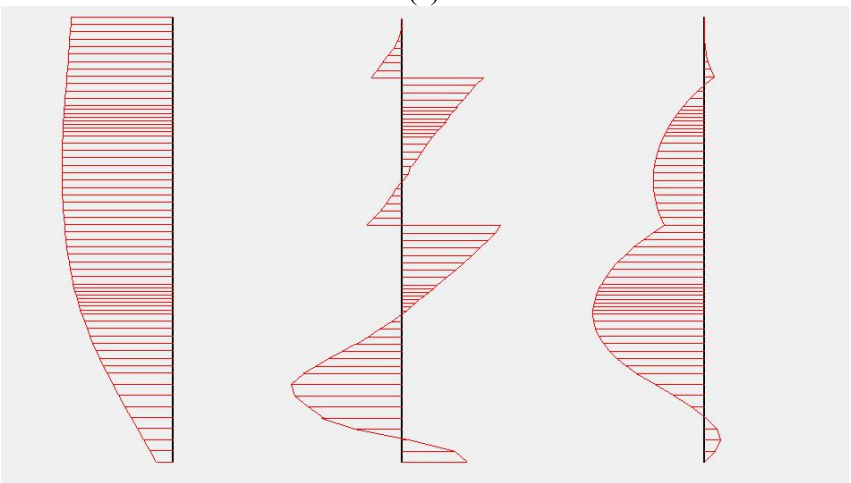

(b)

Figure 6.13 Comparison of diagrams, from left lo right, of horizontal displacement, shear and bending moment. (a) 3-row-anchored sheet pile wall. (b) 2-row-anchored sheet pile wall

7. CONCLUSIONS

The main conclusions of the study accomplished in this master thesis are presented below.

Bibliographic review

First publications related to sheet pile walls date from the early 20th century. These were essentially results from experimental tests, normally compared with theoretical design methods. On a second period, theoretical developments led to several new semi-empirical methods. Nowadays, after the relatively recent development of numerical methods, it is much more difficult to find results from experimental studies in recent papers. These are usually focused on the Finite Element method. In the early 80's, with the development of numerical methods, the experimental studies started a trend to disappear, oppositely to the Finite Element studies. These are somehow more effective or merely more accessible in terms of simplicity and, essentially, in terms of invested time.

Influence of the initial stress state K_0

Depending on the initial stress state, the difference on the wall horizontal displacement may be considerable, being able to reach the double value of displacement. This occurs not only near the failure state, but at service conditions as well. For K_0 values from 0.75 to 2, movements at the top of the wall grow with K_0, for the same soil friction angle. Oppositely, for K_0 values below 0.75 the horizontal displacement seems to grow as K_0 value decreases. This fact leads us to think that there is a particular K_0 value for which the displacement is minimal. This minimum is more recognisable, the closer from the limit state the soil is, or in other words, with lower soil friction angle values.

For K_0 values between 0.7 and 0.9 the minimum movement at the top is registered, depending on the soil friction angle. With a soil friction angle of 25º (close to the limit state) the minimum movement occurs with a K_0 value of 0.85. Movement may change up to 40% depending on the initial stress state.

Influence of the construction procedure

The construction procedure on two-level anchored sheet pile walls has a critical influence over the movement of the wall, particularly at the top. It may be stated that the later the anchors are placed and pre-stressed, the more deflection it occurs in the wall, and so larger movements are registered at the top. Oppositely, when the anchors are placed and pre-stressed immediately after reaching the anchor point, these absorb the movement and limit the wall strains.

In contrast to cantilever sheet pile walls, the maximum horizontal displacement is not located at the ground surface, but at a particular depth. However, it has been seen that when applying the anchor force when most of the excavation has been completed, the maximum displacement takes place at the top of the wall, instead of being at depth, and resembling to the cantilever behaviour.

Influence of the anchor load variation

The anchor force increment has a direct effect on the reduction of the wall horizontal displacement. When applying three times the theoretical anchor force, the maximum

displacement is reduced nearly times three. This reduction is particularly remarkable at the top of the wall, although it obviously depends on the position of the upper anchor. Oppositely, the lower section of the wall does not suffer this behaviour so closely. This part of the wall slightly reduces its movement when increasing the anchor force.

Three-level-anchored sheet pile walls

The effect of adding a third row of anchors is to reduce movements and bending moments. The upper row is preferable to be placed the near as possible to the top of the wall. Its position is critical in order to reduce movements. The other rows may be placed in arbitrary locations in order to reduce bending moment distribution.

It seems that applying the same load to both anchors is not the best practice. Anchor load may be adapted to the shear distribution, applying higher load to the lower anchors and less to the upper anchor.

This master thesis represents the continuation of the previous work of Cuadrado (2010). The main objectives have been fulfilled: the state of knowledge has been reviewed, cases have been run for a second time and new issues subject to review have been discussed. An introduction to the modelization of multiple-anchored sheet pile walls has been carried out and a scientific paper has been written in order to be published in a scientific journal. However, this master thesis could include many other issues already mentioned by Cuadrado (2010), such as un-drained conditions, presence of external loads, etc. These have been excluded due to excessive extension and time, but may be the subject of study in coming works.

8. REFERENCES

1. BARDEN, L. (1974) “Sheet pile wall design based on Rowe’s method”. Part III of “A comparison of quay wall design methods”. CIRIA Technical Note 54.

2. BICA, A. V. D. & CLAYTON, C. R. I. (1989) “Limit equilibrium design methods for free embedded cantilever walls in granular materials”. ICE Proceedings, Part 1, 86, 879-898.

3. BLUM, H. (1931) Einspannungsverhältnisse bei Bohlwerken. W. Ernst & Sohn. Berlin.

4. BOWLES, J. E. (1988) “Foundation analysis and design”. McGraw-Hill, 4th Edition. New York.

5. BRANSBY, P. L. & MILLIGAN, G. W. E. (1975) “Soil deformations near cantilever sheet pile walls”. Géotechnique 25, No. 2, 175-195.

6. CHERUBINI, C., GARRASI, A., PETROLLA, C. (1992) “The reliability of an anchored sheet pile wall embedded in a cohesionless soil”. Canadian Geotechnical Journal, 29, 426-435.

7. CHUGH, A. K. & LABUZ, J. F. (2011) “Numerical simulation of an instrumented cantilever wall”. Canadian Geotechnical Journal, 48, 1303-1313.

8. CUADRADO, A. (2010) “Análisis tenso-deformacional en rotura y condiciones de seguridad de pantallas en voladizo y ancladas. Comparación con métodos clásicos”. Universitat Politècnica de Catalunya. Thesis.

9. DAY, R. A. & POTTS, D. M. (1993) “Modelling sheet pile retaining walls”. Computers and Geotechnics, 15, 125- 143.

10. DAY, R. A. (1999) “Net pressure analysis of cantilever sheet pile walls”. Géotechnique, 49, No.2, 231-245.

11. DAY, R. A. (2001) “Earth pressure on cantiléver walls at design retained heights”. ICE Proceedings Geotechnical Engineering, 149, Issue 3, 167-176.

12. FOURIE, A. B. & POTTS, D. M. (1989) “Comparison of a finite element and limiting equilibrium analyses for an embedded cantilever retaining wall”. Géotechnique 39, No.2, 175-188.

13. HANNAH, T. H. (1987) “Ground anchorages: anchor testing - measuring absolute movement”. ICE Proceedings, 82, Part 1, 639-644.

14. KING, G. J. W. (1995) “Analysis of cantilever sheet-pile walls in cohesionless soil”. Journal of Geotechnical Engineering, Vol. 121, No.9.

15. MA, J., BERGGREN, B., BENGTSSON, P., STILLE, H., HINTZE, S. (2009) "Behaviour of anchored walls in soils overlying rock in Stockholm". International Journal of Geoengineering Case Histories Vol. 2, Issue 1, 1-23.

16. MILLIGAN, G. W. E. (1983) "Soil deformations near anchored sheet-pile walls". Géotechnique 33, No.1, 41-55.

17. OSMAN, A. S. & BOLTON, M. D. (2004) "A new design method for retaining walls in clay". Canadian Geotechnical Journal, 41, 451-466.

18. PADFIELD, C. J. &MAIR, R. J. (1984) "Design of retaining walls embedded in stiff clay". CIRIA Report 104.

19. PLANT, G. W. (1972) "Anchor inclination - its effect on the performance of a laboratory scale tied-back retaining wall". ICE Proceedings, Part 2.

20. Plaxis 8.2. (www.plaxis.nl)

21. POTTS, D. M. & FOURIE, A. B. (1984) "The behaviour of a propped retaining wall: results of a numerical experiment". Géotechnique 34, No.3, 383-404.

22. POWRIE, W. (1996) "Limit equilibrium analysis of embedded retaining walls". Géotechnique, 46, No.4, 709-723.

23. RICHARDS, D. J. & POWRIE, W. (1994) "Finite element analysis of construction sequences for propped retaining walls". ICE Proceedings, 107, 207-216.

24. ROWE, P. W. (1952) "Anchored sheet-pile walls". ICE Proceedings. Part I, Vol. I.

25. ROWE, P. W. (1955) "A theoretical and experimental analysis of sheet-pile walls". ICE Proceedings. Part I, Vol. I.

26. ROWE, P. W. (1955) "Sheet-pile walls encastré at the anchorage". ICE Proceedings. Part I, Vol. I.

27. ROWE, P. W. (1956) "Sheet-pile walls at failure". ICE Proceedings.

28. ROWE, P. W. (1957) "Sheet-pile walls subject to line resistance above the anchorage". ICE Proceedings.

29. ROWE, P. W. (1957) "Sheet-pile walls in clay". ICE Proceedings. Part I, Vol. I.

30. SCHRIVER, A. B. &VALSANGKAR, A. J. (1996) "Anchor rod forces and maximum bending moments in sheet pile walls using the factored strength approach". Canadian Geotechnical Journal, 33, 815-821.

31. SIMPSON, B. (2000) "Partial factors: where to apply them?" International Workshop on Limit State Design in Geotechnical Engineering. Melbourne, Australia.

32. ŠKRABL, S. (2006) “Interactional approach of cantilever pile walls analysis”. ActaGeotechnicaSlovenica, 2006/1.

33. USS (1975) “Steel Sheet Piling Design Manual”. United States Steel.

34. VALSANGKAR, A. J. &SCHRIVER, A. B. (1991) “Partial and total factors of safety in anchored sheet pile design”. Canadian Geotechnical Journal, 28, 812-817.

35. YOUSSEF, Y. G. (2003) “Berms for stabilizing earth retaining structures”. Faculty of Engineering of Cairo University. Fayoum, Egypt.

ANNEX I: PAPER

Safety assessment of limit equilibrium methods for the design of cantilever and anchored sheet pile walls

Alejo González, Agustín Cuadrado, Alejandro Josa, Sebastià Olivella

Abstract: The paper presents an accurate evaluation of the safety provided by the classical methods based on limit equilibrium for cantilever and anchored sheet pile walls. The most used of these methods are reviewed. The embedment depth increment of 20% and the earth pressure coefficient reduction are established nowadays as common practices, although the real safety provided by these is unknown. In order to compare the prediction of the classical methods, the Finite Element program Plaxis has been used. A decomposition of the safety factors has been developed in order to evaluate the contribution of each practice to the global safety. Results show some disagreements between the numerical solution and classical methods prediction. In cantilever walls, the passive state is not fully mobilised at the bottom of the wall. In anchored walls, the failure mechanism given by the Finite Element analysis suggests a failure statewhere the sheet pile wall describes a translation movement on the deep zone, and at the same time a rotation movement around the anchor point. The real safety factor comprises a range between 1.3 and 1.8 for cantilever walls and between 1.3 and 1.7 for anchored walls, depending on the method and the anchor force. The safety factor provided by the embedment increase of 20% is found to be 1.15 for cantilever walls, and lower for anchored walls.

Key words: sheet pile wall, design, finite element, safety factor.

Introduction

Limit equilibrium methods in sheet pile wall design are being used since a long time, even with the recent development of numerical methods, such as Finite Element analysis. The full method for cantilever sheet pile walls, shown in Figure 0.1(a), has been described by Padfield&Mair (1984), consisting on an idealised pressure distribution at limiting conditions, and assuming that there is a sudden reversal between the passive and active thrust at the rotation point. The complicated nature of this method leads in practice to an iteration process, reason why the simplified version, shown in Figure 0.1(b), is recommended (Padfield&Mair, 1984). A complete method, shown in Figure 0.1(c), has been introduced by Bowles (1988), which considers a transition zone around the rotation point where the thrust gradually changes its direction. Besides, a large number of analysis and design methods for embedded cantilever walls have been developed, being most of them based on classical limiting earth pressure distributions, and these have been reviewed by Bica and Clayton (1986). The three mentioned methods are well known as UK method, UK simplified method and USA method as well (Day, 1999; Škrabl, 2006), according to the simplifications of the assumed earth pressure distribution.

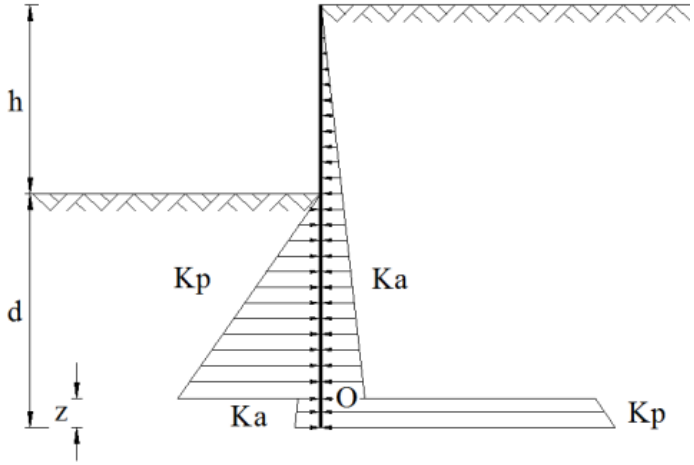

a) Full method or UK method

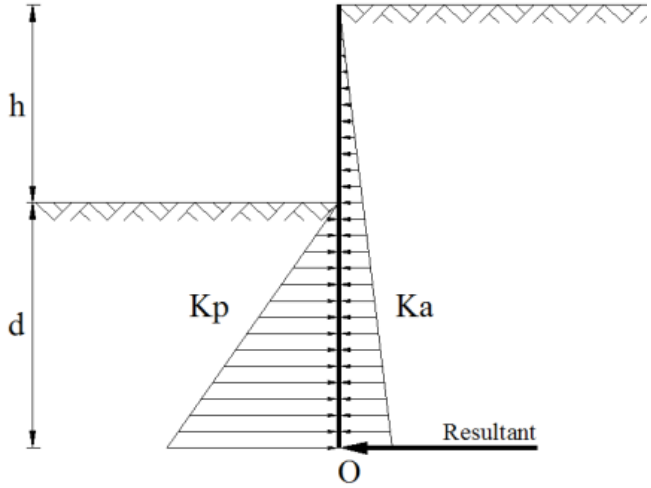

b) Simplified method or UK simplified method

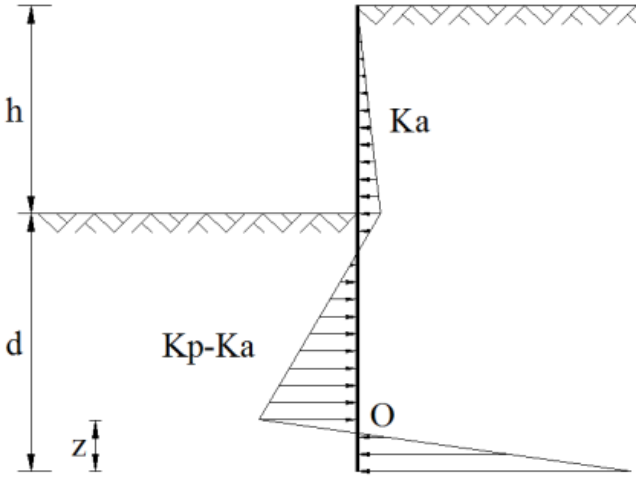

c) Gradual method or USA method

Figure 0.1. Limit equilibrium methods for cantilever sheet pile walls

The success of the extended use of the classical methods lies in its simplicity and its proved reliability. Many authors have analysed these methods, noting that the collapse of a cantilever sheet pile wall is in general well or slightly conservatively predicted (Potts &Fourie, 1984; Powrie, 1996; Day, 1999; Day, 2001). The methodology used has been diverse: centrifuge tests, laboratory-scale models, X-ray method, observations in real walls, as well as analytical and numerical analyses. A semi-empirical method at failure conditions has been proposed by King (1995): an alternative to the limit state methods, not requiring the geometrical simplifications of the earth pressure distribution. According to this method, equilibrium can be established without assuming the limit state in the passive region. On the other hand, the method is dependent on an empirical parameter determined from the results of centrifuge tests. The applicability of this method has been verified by Day (1999), proving its conservative prediction and proposing a new value for the empirical parameter. First comparisons between classical methods and Finite Element showed that the actual net pressure distribution can be well approximated through three lines (Day, 1999), which is in accordance with the methods seen above.

Few authors have analysed the classical methods applied to anchored walls. Valsangkar&Schriver (1991) showed the results of a parametric study, reviewed the existing methods and proposed values of safety factors for each method. The X-ray method has been commonly used to study experimentally the field of deformations near anchored walls, and the complex phenomenon known as arching has been observed by Milligan (1983). This refers to the state of stress existing in a zone of soil which is trying to deform between two zones of more rigid soil (Milligan, 1983). The behaviour of a sheet pile wall supported by multiple rows of anchors has been studied experimentally by Plant (1972), who first mentioned the need to develop the finite element analysis, and noted the complex behaviour of a multi-anchored retaining wall. Finite element analysis applied to propped walls has been carried out by Potts &Fourie (1984) and Richards &Powrie (1994), noting the first the relevance of K_0, and observing the second that the movements or the bending moments can be minimized by choosing the appropriate construction sequence.

When designing through limit equilibrium methods, a factor of safety must be introduced in order to take account of uncertainties, and to provide a safety margin. Modes to achieve a safety factor are to increase the obtained depth of by 20%; to decrease the two soil strength parameters c' and ϕ'; to establisha relationship between the restoring moments and the overturningmoments; as well as reducing the passive earth-pressure coefficient (Padfield&Mair, 1984), (King, 1995), (Day, 1999). The first practice is introduced as an attempt to take into account the simplification done when modifying the earth pressure law (see Figure 0.3), although it may be used as well in order to increase the global safety. It is found that the increase of 20% of the embedment depthyields a conservative prediction (Padfield&Mair, 1984), although the actual safety provided by the practices described is unknown.

The aim of this paper is to evaluate in detail the safety that these practices provide, through an analysis of the safety factors. The limit state is reached in the Finite Element program Plaxis by reducing successively the friction angle of the soil, represented by an elasto-plastic law, and the contribution of each practice (Kp reduction and embedment depth increment) is studied through a decomposition of the safety factors. The

simplified method and the gradual method are analysed in cantilever sheet pile walls, and free earth support and fixed earth support methods are analysed in anchored sheet pile walls.

Earth pressure distributions in cantilever walls

Stability in cantilever sheet pile walls depends on an adequate embedment below the dredge line. The classical limit equilibrium methods attempt to model the sheet pile walls at failure conditions, and differ from each other in several assumptions, but being a common feature the reach of the failure state in the whole (or in the most part of the) length of the wall.

Geotechnical design calculations in either cantilever or anchored sheet pile walls establish equilibrium of horizontal forces and moments to define the failure state and the reference embedment below the dredge line (before applying the safety factor).

Full method

This method, shown in Figure 0.2 and known as UK method as well, has been fully described by Padfield&Mair (1984) and gets its name in contrast to the simplified method, described later. The active limit state is assumed to be reached in the back of the wall above the rotation point, and the passive limit state is assumed to be reached in front of the wall between the dredge line and the rotation point. An overturn in the normal pressure direction is supposed to be produced at the rotation point, below which the full passive pressure is moved behind the wall and the active to the front, so there is a sudden jump in the earth pressure distribution which is needed to prescribe moment equilibrium.

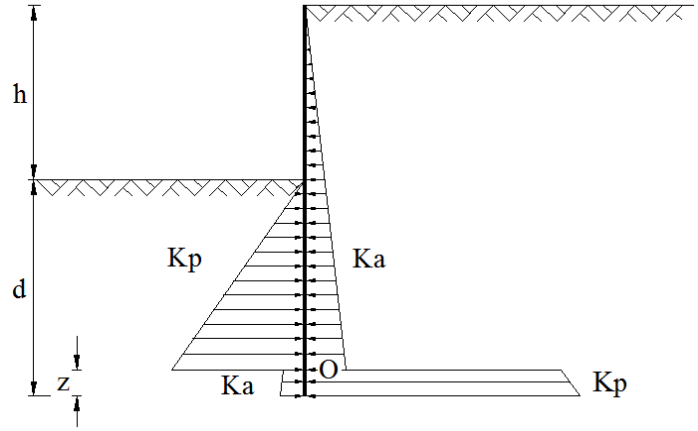

Figure 0.2.Full method. Note the sudden change in the earth pressure distribution

Simplified method

Due to the complexity of the full method, a simplification is recommended (Padfield&Mair, 1984). As shown in Figure 0.3, the earth pressure below the rotation point can be replaced by an equivalent concentrated force acting on point O, represented as R.

The value of *d* calculated is considerably lower than the one calculated from the full method. The common practice is to increase it by 20%, being therefore the reference embedment length equal to *1,2d*. The zone below the rotation point is assumed to receive the passive earth pressure, simplified as *R*, and a verification must be done in order to ensure that the additional length *0,2d* is able to generate the value of *R*.

The simplified method is slightly more conservative than the other methods, although it leads to appreciably similar results(Padfield&Mair, 1984). Its greatest benefit is the simplicity achieved on the traditional system of equations ($\Sigma F_H = 0, \Sigma M = 0$).

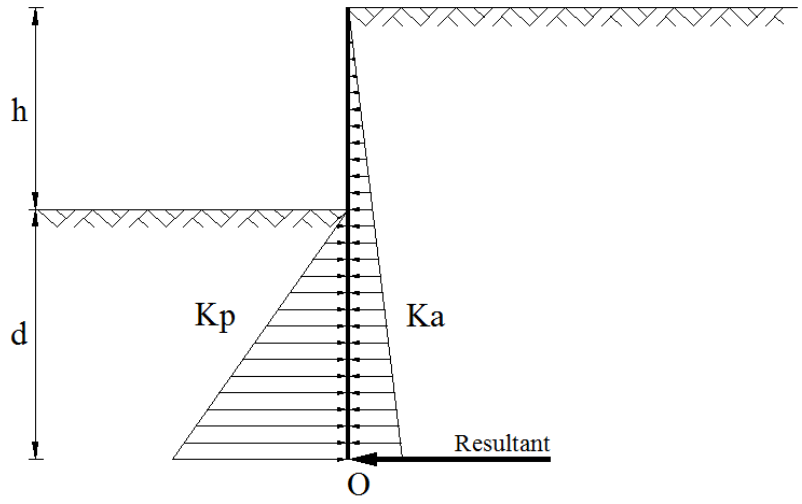

Figure 0.3.Simplified method. The thrust below the rotation point O is replaced by a concentrated force R

Gradual method

A slightly different approach was made by Krey (1932), and later reviewed by Bowles (1988), which does not involve the hypothesis of a sudden change in the earth pressure distribution. The assumption made in this method is to consider a transition zone where the net earth pressure gradually changes its direction from the front to the back of the wall, as shown in Figure 0.4. This transition occurs around the rotation point and is assumed to be linear. The earth pressure at the bottom of the wall is known (see Figure 0.4), so the incognita to obtain the embedment depth is the height *z*. The gradual method is known as USA method as well.

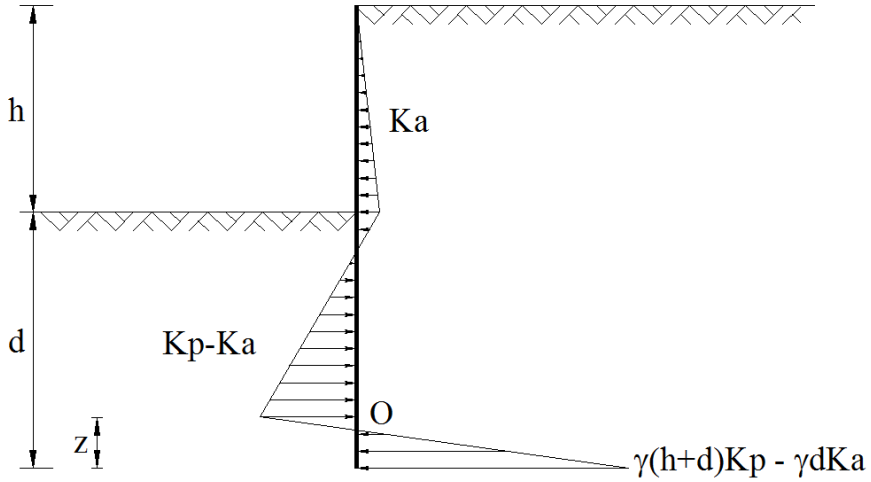

Figure 0.4. Gradual method, shown in net pressures

Earth pressure distributions in anchored walls

Anchored walls with a single row of anchors are able to achieve the equilibrium without considering a passive reaction at the bottom of the back of the wall. The tie rod position, its inclination and its load are the subject of continuous studies, such as those carried out by Plant (1972), Schriver&Valsangkar (1996) or Ma, Berggren, Bengtsson, Stille and Hintze (2009).

Free earth support method

This method is based on the assumption that movements on the embedded zone of the wall are sufficient to mobilize the active and passive thrust behind and in front of the wall respectively. The passive pressure is assumed to act only in front of the wall through the depth *d* (Figure 0.5). The bottom of the wall has therefore free movement, and a minimum reference embedment depth, to satisfy equilibrium, is obtained.

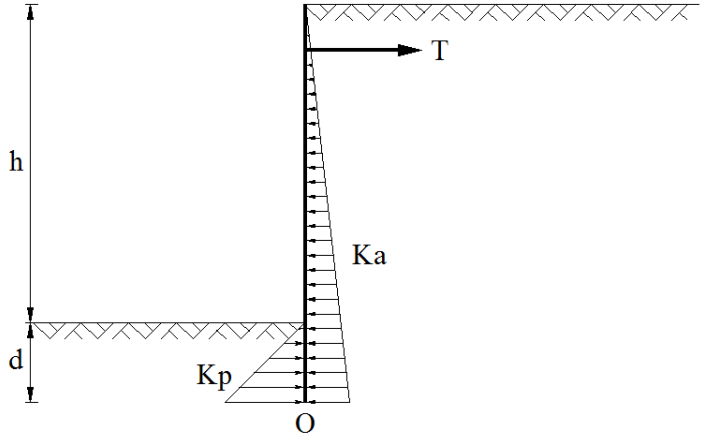

Figure 0.5. Free earth support method. The equilibrium involves movement of the bottom

Fixed earth support method

Increasing the embedment depth, an overturn in the normal earth pressure is achieved, until the deflected shape at the bottom becomes approximately vertical. Hence, the earth pressure distribution is essentially equal to the cantilever casewith the simplified distribution (see Figure 0.6), and the wall behaves like a partially built-in beam subjected to bending moments (United States Steel, 1984).

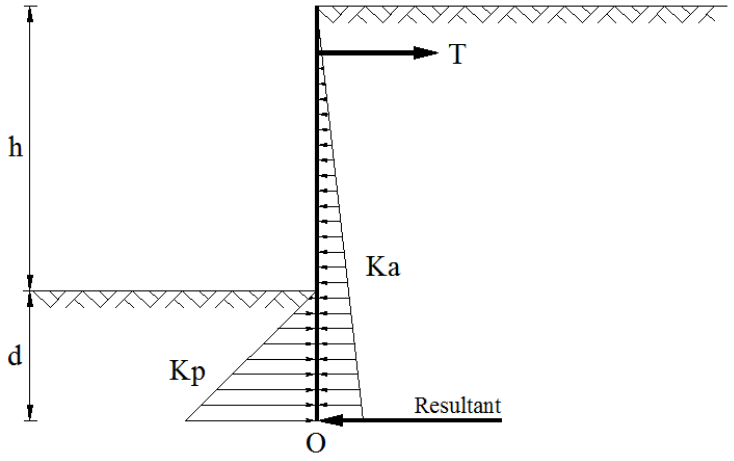

Figure 0.6. Fixed earth support method (simplified distribution)

This method leads to a maximum reference embedment depth. It requires an additional equation which is usually defined estimating where the zero net pressure point (inflection point *O*; zero bending moment) is located. It is frequent to locate such point in the middle of the embedment depth, though other assumptions have been proposed. Blum (1931) showed a dependence relationship between the distance from the inflection point to the dredge level and K_a.

Numerical analysis

In order to study the prediction of the classical methods, a Finite Element analysis has been developed, assuming that its results are closer to the real behaviour of a sheet pile wall. The software used was Plaxis 8.2., a 2-D Finite Element program. A homogeneous single layer of dry soil has been modelled by an elastic perfectly-plastic law under plane strain conditions. The element type is the 15-node triangle and the failure criterion is Mohr-Coulomb.

The domain of the model is 75m to 90m length per 30m high, as seen in Figure 0.7 and Figure 0.8. A sufficient size of the domain has been used, and it has been checked that increasing its size the results remain unchanged. The boundary conditions are vertical fixities on both sides of the geometry, and a total fixity on the bottom, reproducing the most truthful field conditions. The specific weight of the soil is 17 kN/m^3, its elastic modulus $1.3 \cdot 10^5$ kN/m^2 and its Poisson coefficient 0.3, according to the drained conditions. The soil is assumed to be cohesionless. When the effect of cohesion is studied, the value considered is 10 kN/m^2. The soil-structure interaction is modelled by the element interface, which is assumed to be rigid. The soil resistance is therefore not reduced between the soil and the wall. The K_0 coefficient is assumed to be 0.5 in all the cases studied. Further studies showed that for moderate values of K_0 (0.4 to 1.7)results do not differ significantly from those given for K_0=0.5.

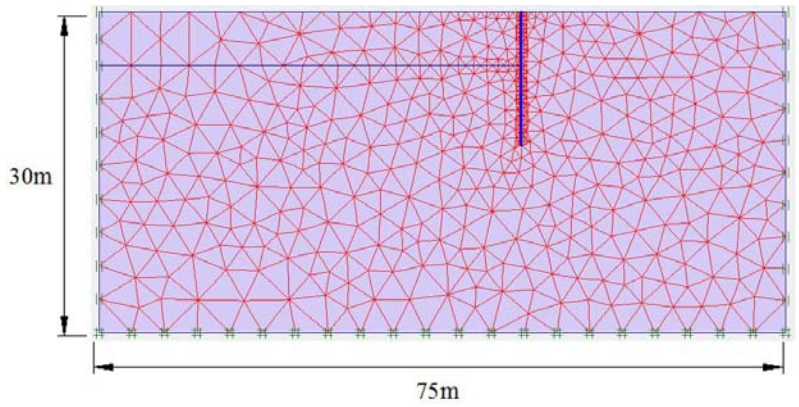

Figure 0.7. Finite Element mesh in a cantilever wall

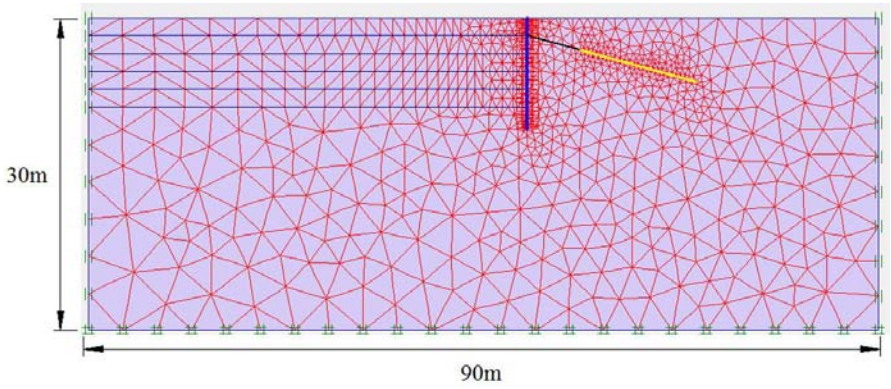

Figure 0.8. Finite Element mesh in an anchored wall

The sheet pile wall is represented by an elastic element, which is a reasonable approximation, as they are usually designed to have an elastic response. The elastic modulus is $3.5 \cdot 10^7$ kN/m^2, the wall thickness 40 cm, leading to an axial stiffness of $1.4 \cdot 10^7$kN/m and a bending stiffness of $1.867 \cdot 10^5$kN/m. The specific weight of the reinforced concrete is 28 kN/m^3.

The grout body of the anchor is modelled through a geogrid element, a slender structure with no bending stiffness, and an axial stiffness of 3.3·104 kN/m. The anchor rod (free length) is modelled through a node-to-node anchor with an axial stiffness of $5.8 \cdot 10^4$ kN and a spacing of 1.75 m. These values are commonly used for the design of sheet pile walls and are summarized in Table 2.

Properties of the soil	
Specific weight	17 kN/m^3
Elastic modulus	$1.3 \cdot 10^5$ kN/m^2
Poisson coefficient	0.3
Cohesion	0 kN/m^2
K_0	0.5
Properties of the sheet pile wall	
Specific weight	28 kN/m^2
Elastic modulus	$3.5 \cdot 10^7$ kN/m^2
Thickness	40 cm
Axial stiffness	$1.4 \cdot 10^7$kN/m
Bending stiffness	$1.867 \cdot 10^5$kN/m
Properties of the anchors	

Grout body axial stiffness	$3.3 \cdot 10^4$kN/m
Anchor rod axial stiffness	$5.8 \cdot 10^4$kN
Spacing	1.75 m

Table 2. Summary of soil, wall and anchor properties

While designing through classical methods, a value of the reference embedment depth *d* is obtained to satisfy equilibrium, starting from a value of *h* and the soil strength parameters. In the Finite Element analysis conducted, a different procedure has been followed. The limit state is reached for each case studied by drawing the geometry, with a known total wall length and embedment depth. The actual soil properties (including soil friction angle) are considered to be those corresponding to the application of the classical methods. The soil friction angle is then reduced successively until the collapse of the soil body is achieved. This procedure enables the comparison between classical methods and numerical methods, and –assuming numerical methods to represent the real behaviour– allows evaluating the safety of the assumptions made in the classical methods.

Bearing in mind that, in the numerical model, when collapse occurs, the soil-structure equilibrium is not guaranteed, the solution must be an approximation to the limit state, and this is assumed to be reached in the case just before collapse.

Near the limit state, numerical difficulties are found out, hindering the choice of the minimum soil friction angle supported. Eventually, equilibrium is achieved for a soil friction angle lower than in a case where it is not. Due to this, a criterion of choice has been established, based on selecting the first angle for which the equilibrium is not fulfilled, in a phi-reduction procedure. In most cases, the numerical difficulties are found to be related to the instantaneous excavation, which are, at least partially, solved with a staged excavation.

Cases considered

Six cases are studied, including cantilever and anchored cases. This represents an adequate, to be meaningful, range of cases. Five cases are studied in cantilever walls with excavation depths of 3 m and 5 m, and embedment depths within 3 m and 7.5 m. A case considering the effect of cohesion is included. A single case of anchored wall is studied, with 10 m of retained height and 2.5 m of embedment depth. Cases are summarized in Table 3 below:

Cantilever sheet pile walls	*h*:3m *d*:3m
	h:3m *d*:4.5m
	h:5m *d*:5m
	h:5m *d*:7.5m
	h:5m *d*:7.5m *c*:10kN/m^2
Anchored sheet pile walls	*h*:10m *d*:2.5m

Table 3. Cases studied

Cantilever walls

In the first place, and starting form the established geometry, the soil friction angle is calculated for each analytical method –simplified and gradual methods– considering all the possible combinations of embedment increase and passive reduction, in order to assess each effect separately. Consequently, 8 values of soil friction angle are obtained from the analytical methods for each geometry. On the other hand, a phi-reduction procedure through the Finite Element analysis is done with the same geometry. The procedure leads to 2 values of soil friction angle, the first considering the original wall geometry and the second considering the embedment increment. Table 4 summarizes the terminology of the different angles calculated. Hence, 10 values of soil friction angle are obtained; 4 from the simplified method, 4 from the gradual method and 2 from the numerical method.

Results are given on Table 5. Note that $\phi_g^P > \phi_s^P > \phi g > \phi s > \phi FE$. The effect of cohesion is found to be, as expected, very beneficial for the stability.

20% Embedment increase	2/3 Passive pressure reduction	Simplified method	Gradual method	Numerical method (ϕ reduction)
No	No	ϕ_s	ϕ_g	ϕ_{FE}
No	Yes	ϕ_s^P	ϕ_g^P	
Yes	No	ϕ_s^E	ϕ_g^E	ϕ_{FE}^E
Yes	Yes	ϕ_s^{PE}	ϕ_g^{PE}	

Table 4. Soil friction angles obtained in cantilever walls

CASES		ANGLE OF SOIL FRICTION									
h	d	ϕ_s	ϕ_g	ϕ_s^E	ϕ_g^E	ϕ_s^P	ϕ_g^P	ϕ_s^{PE}	ϕ_g^{PE}	ϕ_{FE}	ϕ_{FE}^E
3	3	28.5	30.1	25.2	26.7	33.5	35.0	30.3	31.7	25.0	22.0
3	4,5	21.4	22.8	18.7	19.9	26.7	28.0	24.1	25.3	18.0	16.0
5	5	28.5	30.1	25.2	26.7	33.5	35.0	30.3	31.7	26.5	23.4
5	7,5	21.4	22.8	18.6	19.9	26.7	28.0	24.1	25.3	21.0	18.0
5(c)	7.5(c)	11.9		10.3		16.6		15.4		8.0	7.0

Table 5. Cantilever walls. Soil friction angles in the limit state from the classical methods and Finite Element. In the last row, (c) indicates cohesion of 10 kN/m^2. Angles in degrees, *h* and *d* in meters.

Anchored walls

As in cantilever walls, different combinations of the analytical methods with embedment increase and passive reduction are considered. Consequently, for the same geometry, eight soil friction angles are obtained from the classical methods and 4 from the Finite Element analysis.

In the case of anchored walls, the variation of the soil friction angle supported depending on the anchor force has been studied. The anchor force, known as the thrust to be resisted by the anchor, is found starting from the free earth support method, without passive pressure reduction. For the geometry considered, with a retained height of 10 m and an embedment of 2.5 m, the anchor force resulting from the free earth support method is 138 kN/m. This value, and its double amount, are considered in the numerical model, and provide two different soil friction angles.

Table 6 summarizes the nomenclature of the different angles calculated. The two latter represent 100% and 200% of the anchor force, in relation to that obtained from the free earth support method with no passive earth pressure reduction.

Results are given on Table 7. The reduction of the passive earth pressure causes, as expected, an increase of the soil friction angle with respect to the reference case. At the same time, the embedment increase of 20% causes a decrease of the soil friction angle with respect to the reference case. The variation of the anchor force, from 100% to 200% with respect to the theoretical value, provides a lower soil friction angle. Numerical results afford, at first sight, lower values of the soil friction angle.

20% Embedment increase	2/3 Passive pressure reduction	Free earth support method	Fixed earth support method	Numerical method: 100% anchor force	Numerical method: 200% anchor force
No	No	ϕ_f	ϕ_{fx}	ϕ_{FE100}	ϕ_{FE200}
Yes	No	ϕ_f^E	ϕ_{fx}^E	ϕ_{FE100}^E	ϕ_{FE200}^E
No	Yes	ϕ_f^P	ϕ_{fx}^P		
Yes	Yes	ϕ_f^{PE}	ϕ_{fx}^{PE}		

Table 6. Soil friction angles obtained in anchored walls

CASE	ANGLE OF SOIL FRICTION											
d	ϕ_f	ϕ_{fx}	ϕ_f^E	ϕ_{fx}^E	ϕ_f^P	ϕ_{fx}^P	ϕ_f^{PE}	ϕ_{fx}^{PE}	ϕ_{FE100}	ϕ_{FE200}	ϕ_{FE100}^E	ϕ_{FE200}^E
2.5	37.1	38.5	34.0	37.0	41.6	42.9	38.7	41.5	37.0	31.0	30.0	28.0

Table 7. Anchored walls. Soil friction angles in the limit state for the reference and design embedment depth from the classical methods and Finite Element. Angles in degrees, *d* in meters. Retained height *h*=10m

Results

Results: Cantilever walls

The stress state near the limit state described by the numerical method is broadly in agreement with the predictions of the classical methods, as shown in Fig.10. However, clear differences in the principal stresses are found between the numerical solution and the classical methods, especially in the back of the wall around the bottom. The stress state at this point should be theoretically close to the passive state. The numerical results show that even though a turn in the principal stresses occurs, these are still relatively far from the passive state (see Figure 0.9). It should be noted, that the classical methods assume perfect plasticity and that the principal stresses can only be vertical or horizontal. The numerical net pressure law differs as well in front of the wall immediately below the dredge level, staying above the prediction of the classical methods (see Figure 0.10 and Figure 0.11).This overpressure is due to the 3-D stress state existent in Plaxis, which increases the confinement, so a greater resistance to deformation is produced. The overpressure is higher the farther the soil friction angle from the limit state value is. On the other hand, the active pressure provided by the numerical solution matches the classical methods fairly well.

Figure 0.10 shows the evolution of the earth pressure distribution over the wall as the excavation takes place. The limit state is restricted initially to the most superficial zone, and the passive state in the bottom of the wall is reached in the last meters of excavation. As shown by Kray (1932), Bransby& Milligan (1975), Powrie (1996), Day (1999), and more authors, the active and passive pressures are fully mobilised above and immediately below the dredge level respectively.

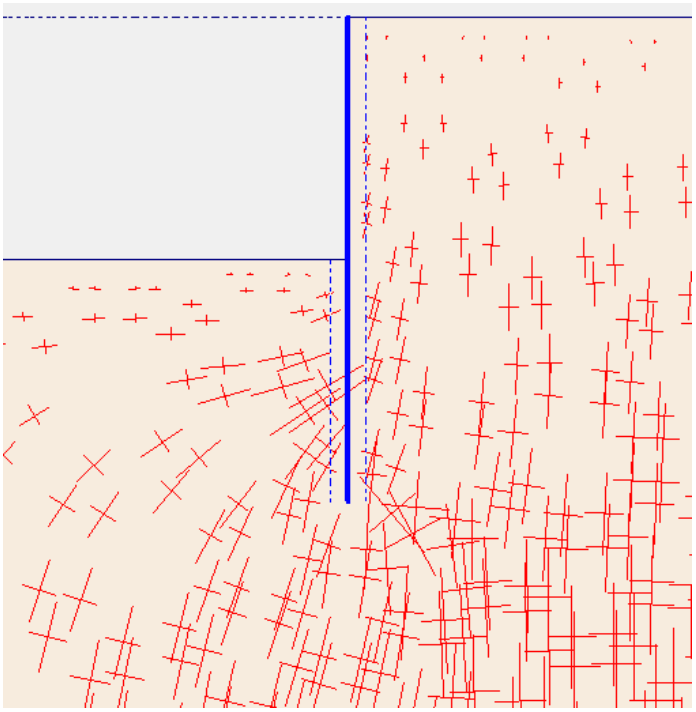

Figure 0.9. Principal stresses represented with crosses near the limit state. The larger line represents the major principal stress

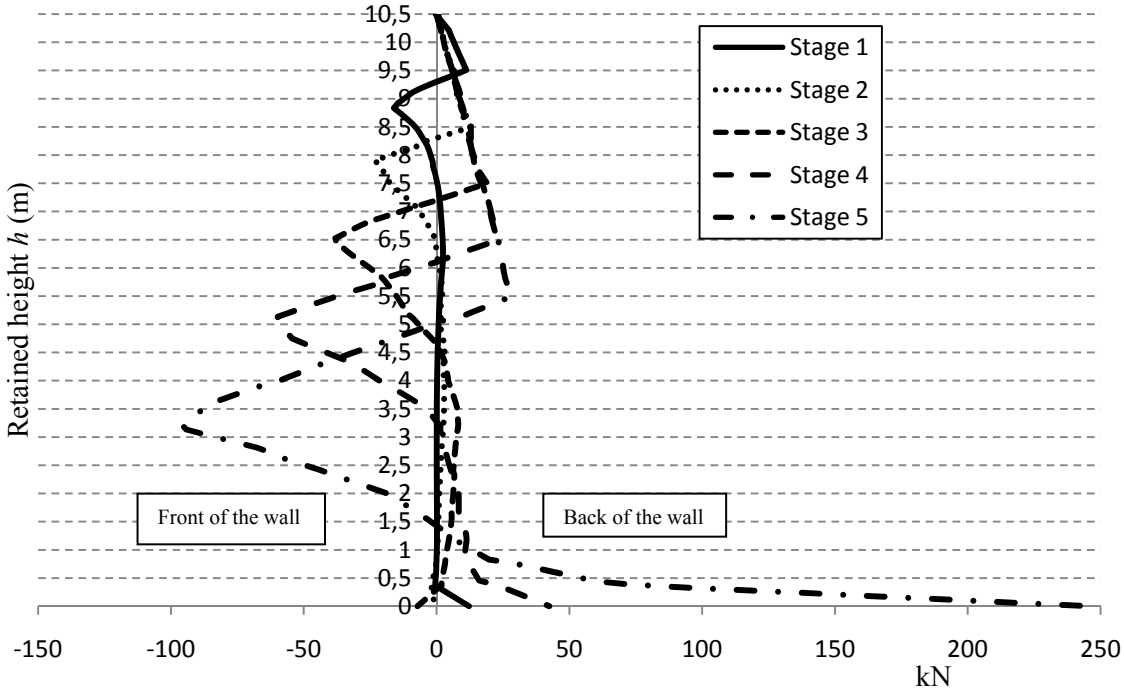

Figure 0.10. Overlay of net earth pressure distributions near the limit state in a cantilever wall, showing the evolution by excavation stages. *h*=5m *d*=5.5m ϕ=25º

Figure 0.11 shows the displacement at the top of the wall growing as the soil friction angle declines. This figure may be used to identify the soil friction angle at failure. A vertical asymptote may be recognised, corresponding to the limit state. Figure 0.11 shows clearly a non linear trend on the displacement as approaching the limit state. The evolution of the earth pressure lawas soil friction angle declines (Figure 0.12) shows that the stresses in the lower zone of the wall are increased as the soil friction angle is reduced.

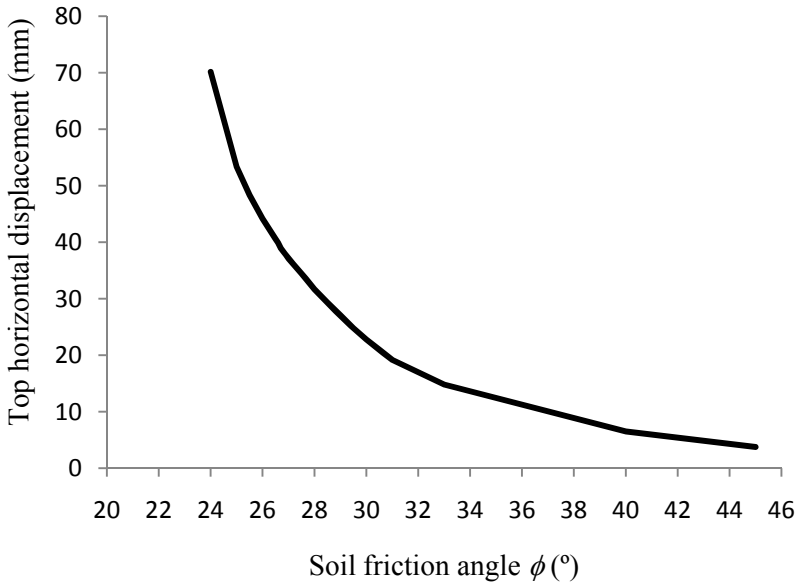

Figure 0.11. Evolution of the horizontal displacement at the top of the wall with the soil friction angle in a cantilever wall. Note the vertical asymptote

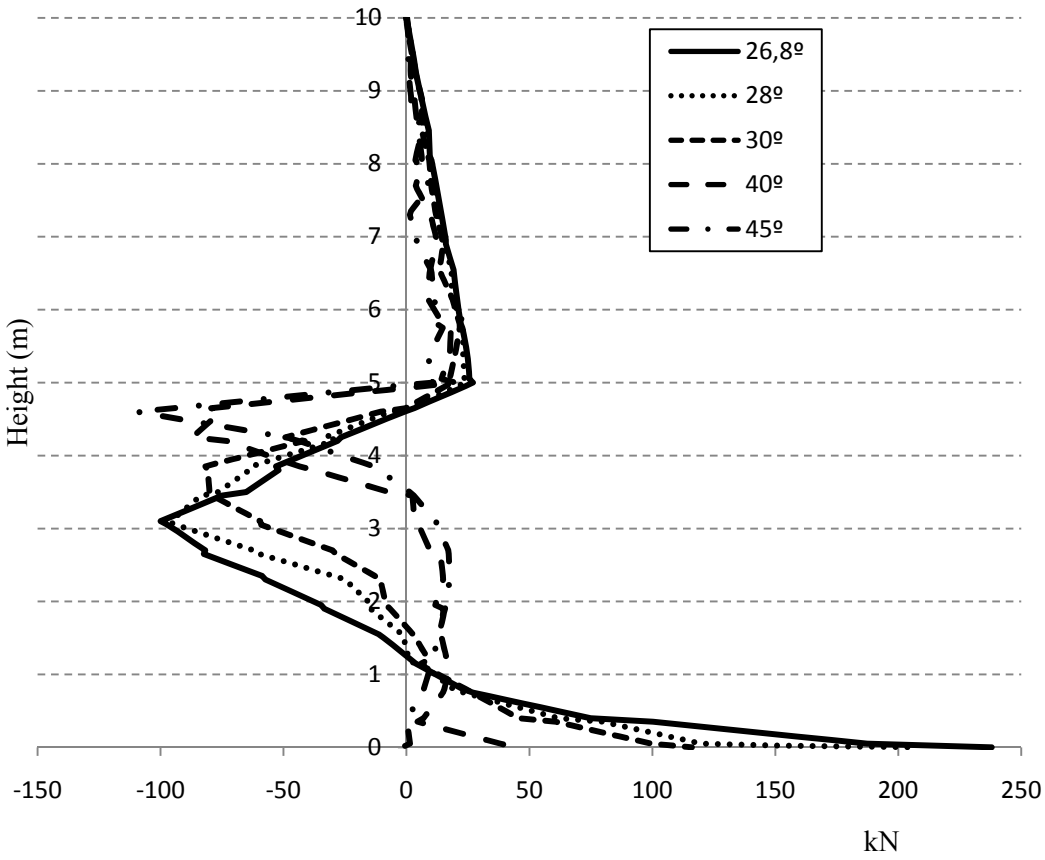

Figure 0.12. Evolution of the net earth pressure law as soil friction angle is reduced in a cantilever sheet pile wall with *h*=5m and *d*=5m

Results: Anchored walls

The analysis of anchored sheet pile walls reveals that the anchor affects the stress state around the top and the bottom of the wall. As seen in Figure 0.1, a trend to generate a passive state in the back of the wall around the anchor is found, as opposed to what is established by the classical methods.

The numerical solution shows a rotation around the anchor point, which is in agreement with the classical methods. However, a passive state in the back and bottom of the wall is generated (see Figure 0.2), not satisfying the free earth support method hypothesis, as it assumes the passive pressure only to act in front of the wall below the dredge level.

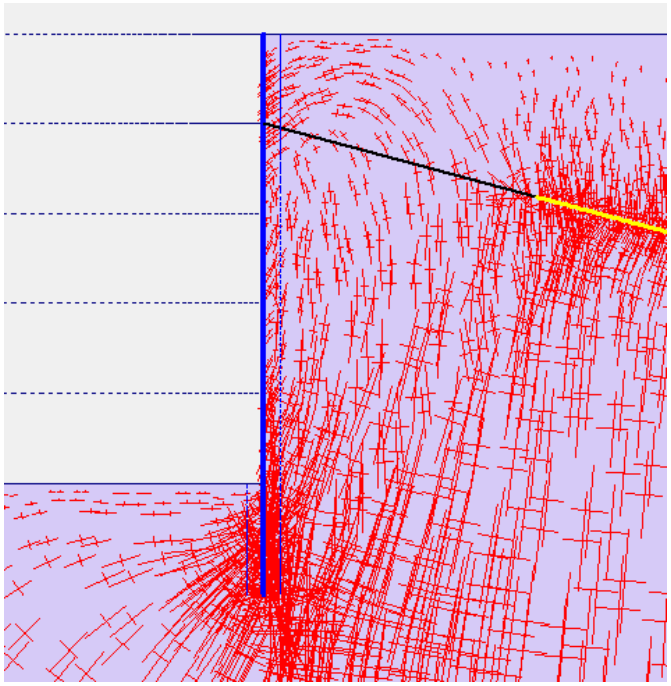

Figure 0.1. Principal stresses around the anchorage

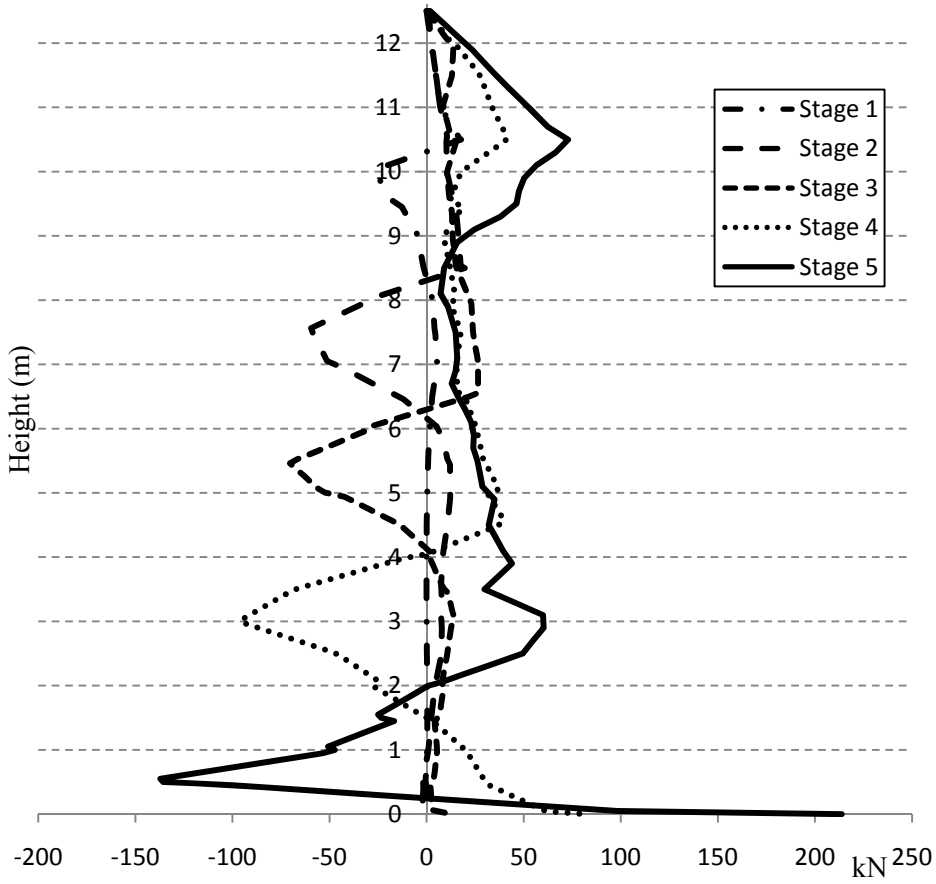

Figure 0.2. Overlay of pressure laws as a staged excavation takes place in an anchored sheet pile wall with *h*=10m and a final *d*=2,5m. ϕ=31º (near the limit sate)

For an equal soil friction angle, the fixed earth support method requires further embedded depth than the free earth support method. Thereby, for an equal embedment

depth, the free earth support method provides a lower value of the soil friction angle as the fixed earth support method. The Finite Element model does not consider the conservative hypotheses of the classical methods, and therefore the limit equilibrium is reached with a lower value of the soil friction angle. The existence of a three-dimensional stress state in Plaxis lets the confinement grow, and therefore the resistance to deformation is increased. The passive pressure is then greater than those calculated from the analytical methods.

Anchor load results

Classical limit state methods provide an anchor force, while establishing equilibrium at failure state. However, they neither consider the interaction with the soil, nor its evolution in service, and the anchor load depends directly on the stages followed.

The anchor prestressing load has been changed from 0% to 300% of the theoretical value. Figure 0.3. Evolution of the anchor load as excavation takes place, for different prestressing loads summarizes the results and shows that the anchor load appears to trend to an equilibrium value.

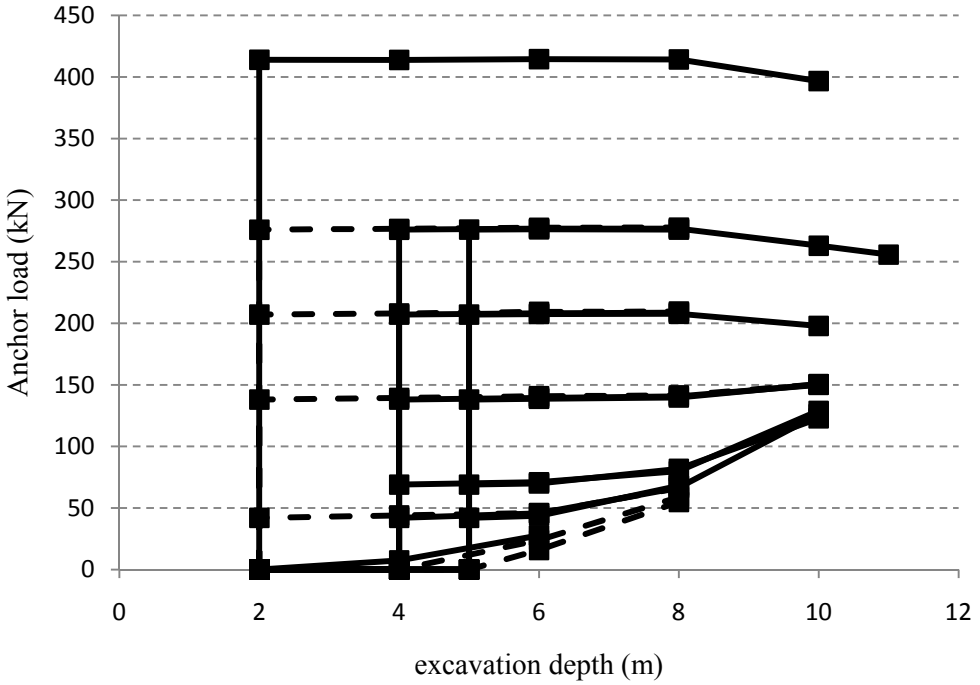

Figure 0.3. Evolution of the anchor load as excavation takes place, for different prestressing loads

Discussion

Cantilever walls

Results from the analytical methods are found to be in disagreement with the numerical predictions. At first sight, the latter provides lower values of the soil friction angle, for the same wall geometry. A comparison between methods can be established in terms of safety factors, in order to asses the safety introduced by those.

Safety factors are typically expressed in terms of embedment depth, moments, passive resistance or strength parameters (Padfield&Mair, 1984). Nonetheless, the value of the factor obtained is not in accordance with the real safety provided. In service conditions, a safety factor on the strength parameters can be defined as:

$$\boldsymbol{SF} = \frac{\tan\boldsymbol{\phi}_{real}}{\tan\boldsymbol{\phi}_{failure}} \tag{4}$$

whereϕ_{real} is the actual value of the soil friction angle and $\phi_{failure}$ is the minimum value supported, immediately before collapse. After increasing the embedment depth by 20%, a lower value of the soil friction angle can be achieved before collapse. Hence, the relationship between the supported friction angle before and after the increase of the embedment depth gives an estimation of the distance to the limit state –predicted by the method– due to this practice, as seen below:

$$\boldsymbol{SF} = \frac{\tan\boldsymbol{\phi}_{reference\ embedment}}{\tan\boldsymbol{\phi}_{embedment+20\%}} \tag{5}$$

Starting from ($\boldsymbol{SF}= \frac{\tan\phi_{reference\ embedment}}{\tan\phi_{embedment+20\%}}$ (**5**), a first group of safety factors (SF1 to SF5 on Table 8) reveals the safety provided by the increase of the embedment depth by 20% for each method. Results show that this practice barely provides a safety factor of 1.15, or lower.

The way to establish a more realistic safety factor must include the classical limit equilibrium methods and the numerical methods. The safety factor can be decomposed on successive multiplicative sub-factors that enable to rate each effect separately.An accurate evaluation of the real safety of both simplified and gradual method can be defined as follows:

$$\boldsymbol{SF} = \frac{\tan\boldsymbol{\phi}}{\tan\boldsymbol{\phi}_{FE}} \cdot \frac{\tan\boldsymbol{\phi}_{FE}}{\tan\boldsymbol{\phi}^{E}_{FE}} = \frac{\tan\boldsymbol{\phi}}{\tan\boldsymbol{\phi}^{E}_{FE}} \tag{6}$$

Where tanϕ refers to the minimum soil friction angle supported by the sheet pile wall, calculated using the gradual method (tanϕ_g) or the simplified method (tanϕ_s). See SF6 to SF9 on Table 9. Results show that the real safety provided by the classical methods comprises a range between 1.2 and 1.8. The lower safety factor calculated corresponds to the simplified method, while the greatest values are obtained for the gradual method with passive earth pressure reduction.

The safety provided by the classical methods by ignoring the cohesionis known to be favourable, and can be evaluated by adding the effect of cohesion on ($\boldsymbol{SF}= \frac{\tan\phi}{\tan\phi_{FE}} \cdot \frac{\tan\phi_{FE}}{\tan\phi^{E}_{FE}} = \frac{\tan\phi}{\tan\phi^{E}_{FE}}$ (**6**) as follows:

$$\boldsymbol{SF} = \frac{\tan\boldsymbol{\phi}}{\tan\boldsymbol{\phi}^{C}} \cdot \frac{\tan\boldsymbol{\phi}^{C}}{\tan\boldsymbol{\phi}^{C}_{FE}} \cdot \frac{\tan\boldsymbol{\phi}^{C}_{FE}}{\tan\boldsymbol{\phi}^{CE}_{FE}} = \frac{\tan\boldsymbol{\phi}}{\tan\boldsymbol{\phi}^{CE}_{FE}} \tag{7}$$

where the superscript *C* indicates cohesion. Table 10 shows the effect of ignoring the cohesion in the simplified method. SF10 compares the soil friction angle calculated with the simplified method versus the prediction of the Finite Element method considering cohesion. SF11 on Table 10 further consider the reduction of the passive resistance. Results show that ignoring, when existing, the cohesion turn out to be an especially

conservative practice. Otherwise, considering a wrong value of cohesion may have severe consequences.

		SAFETY FACTORS				
		SF1 $\frac{\tan\phi_s}{\tan\phi_s^E}$	SF2 $\frac{\tan\phi_g}{\tan\phi_g^E}$	SF3 $\frac{\tan\phi_s^P}{\tan\phi_s^{PE}}$	SF4 $\frac{\tan\phi_g^P}{\tan\phi_g^{PE}}$	SF5 $\frac{\tan\phi_{FE}}{\tan\phi_{FE}^E}$
CASE	*h*:3m *d*:3m	1.16	1.16	1.13	1.13	1.15
	h:3m *d*:4,5m	1.16	1.16	1.13	1.12	1.13
	h:5m *d*:5m	1.16	1.15	1.13	1.13	1.15
	h:5m *d*:7,5m	1.16	1.16	1.12	1.12	1.18
	h:5m *d*:7.5m *c*:10kN/m^2	1.16		1.08		1.14

Table 8. Safety factors related to cantilever walls. Effect of increasing the reference embedment depth by 20% for each method

		SAFETY FACTORS			
		SF6 $\frac{\tan\phi_s}{\tan\phi_{FE}^E}$	SF7 $\frac{\tan\phi_g}{\tan\phi_{FE}^E}$	SF8 $\frac{\tan\phi_s^P}{\tan\phi_{FE}^E}$	SF9 $\frac{\tan\phi_g^P}{\tan\phi_{FE}^E}$
CASE	*h*:3m *d*:3m	1.4	1.4	1.6	1.7
	h:3m *d*:4,5m	1.4	1.5	1.8	1.8
	h:5m *d*:5m	1.3	1.3	1.5	1.6
	h:5m *d*:7,5m	1.2	1.3	1.6	1.6
	h:5m *d*:7.5m *c*:10kN/m^2	1.7		2.4	

Table 9. Safety factors related to cantilever walls. Safety provided by the classical methods. Reduction of the passive pressure is evaluated for both methods non SF8 and SF9

	SAFETY FACTORS	
CASE	SF10 $\frac{\tan\phi_s}{\tan\phi_{FE}^{CE}}$	SF11 $\frac{\tan\phi_s^P}{\tan\phi_{FE}^{CE}}$
h:5m *d*:7.5m *c*:10kN/m^2	3.2	4.1

Table 10. Safety factors related to cantilever walls. Safety provided by the classical methods when cohesion of 10 kN/m^2 is ignored in addition

Anchored walls

The same relation as shown in ($\boldsymbol{SF}=\frac{\tan\phi_{reference\ embedment}}{\tan\phi_{embedment+20\%}}$ (5)) is appropriate for anchored walls, and the values of SF12 to SF16 (see Table 11) express the safety provided by the increase of the embedment depth by 20% for each method. This practice leads to a safety factor of barely 1.1, depending on the method and on the anchor force. Therefore, the embedment increase in anchored walls has less influence on the safety than in cantilever walls.

The real safety of both free and fixed earth support method can be defined as in (3). Safety factors SF17 to SF20, shown in Table 12, make out the situations of passive earth reduction and two different anchor forces, in relation to the numerical prediction including the increase of 20% on the reference embedment depth. Safety factors comprise a range between 1.3 and 1.7, depending on the method and the anchor force. As expected, safety factors grow from SF17 to SF20, and the fixed earth support method with passive earth pressure reduction is found to be the most conservative. In addition, note that an anchor force increase of 200% does not lead into a double safety factor. The anchor force should trend to the equilibrium force when all the soil is at failure, and so the safety factor considering 100% or 200% of the anchor force may not differ greatly.

The analysis of the anchor force shows that when considering its theoretical value, the behaviour of the wall is well predicted by the classical methods. Instead, when increasing the anchor force by the double amount, the passive pressure may not be fully mobilised and the failure mechanism differs form the classical predictions. In addition, the anchor effect involves significant changes in the global stress state. Passive pressure appears between the grout body and the wall, which creates a confined zone around the anchor rod. This effect is not taken into account by the classical methods.

SAFETY FACTORS					
SF12 $\frac{\tan\phi_f}{\tan\phi_f^E}$	SF13 $\frac{\tan\phi_{fx}}{\tan\phi_{fx}^E}$	SF14 $\frac{\tan\phi_f^P}{\tan\phi_f^{PE}}$	SF15 $\frac{\tan\phi_{fx}^P}{\tan\phi_{fx}^{PE}}$	SF16a $\frac{\tan\phi_{FE100}}{\tan\phi_{FE100}^E}$	SF16b $\frac{\tan\phi_{FE200}}{\tan\phi_{FE200}^E}$
1.1	1.1	1.1	1.1	1.3	1.1

Table 11. Effect of increasing the reference embedment depth by 20% for each method in anchored walls.*h*=10m, *d*=2,5m

SAFETY FACTORS							
SF17a $\frac{\tan\phi_f}{\tan\phi_{FE100}^E}$	SF17b $\frac{\tan\phi_f}{\tan\phi_{FE200}^E}$	SF18a $\frac{\tan\phi_{fx}}{\tan\phi_{FE100}^E}$	SF18b $\frac{\tan\phi_{fx}}{\tan\phi_{FE200}^E}$	SF19a $\frac{\tan\phi_f^P}{\tan\phi_{FE100}^E}$	SF19b $\frac{\tan\phi_f^P}{\tan\phi_{FE200}^E}$	SF20a $\frac{\tan\phi_{fx}^P}{\tan\phi_{FE100}^E}$	SF20b $\frac{\tan\phi_{fx}^P}{\tan\phi_{FE200}^E}$
1.3	1.4	1.4	1.5	1.5	1.7	1.6	1.7

Table 12. Safety provided by the classical methods in anchored walls. *h*=10m, *d*=2,5m

Conclusions

An evaluation of the safety provided by the classical methods on the design of sheet pile walls has been carried out. The analytical results of six cases, comprising cantilever and anchored walls, have been compared with the Finite Element model Plaxis.

The simplification of reality done by the classical methods allows us to generally understand the behaviour of the whole body wall-soil. Nonetheless, the hypotheses in which these are based on are found to be conservative. For instance, the hypothesis of considering that both active and passive pressure are fully mobilised over the whole length of the wall provides a lower embedment depth for the same soil friction angle. Additionally, there are other effects that the classical methods ignore. Classical methods may underestimate the passive pressure, as they do not take into account the confinement in depth due to the three-dimensional stress state. Classical methods for anchored walls neither take into account the confinement around the free length of the anchor rod that increases the passive pressure.

The Finite Element numerical model requires knowing additional parameters, whose influence needs to be known. Its interpretation requires understanding of the studied phenomenon.

In cantilever walls, the real safety factor of each method comprises a range between 1.2 and 1.8, depending on the method. The most conservative is found to be the gradual method with passive earth pressure.

In anchored walls, the real safety factor provided by the classical methods comprises a range between 1.3 and 1.7 depending on the method and the anchor force.

For both cantilever and anchored walls, the traditional increase of 20% on the reference embedment depth does not lead into the same amount on the safety factor. For each method, the embedment increase of 20% provides a safety factor about 1.15 for cantilever walls, and slightly less for anchored walls.

The active earth pressure is fully mobilised on the back of the wall above the dredge level, even with soil friction angles far from the limit state. In contrast, the earth pressure distribution on the back of the wall below the dredge level resembles the at-rest state, with soil friction angles far from the limit state or with shallow depth of excavation. The passive earth pressure is fully mobilised immediately below the dredge level. However, its range and value increases with retained height, and exceeding the theoretical value, due to the confinement caused by a three-dimensional stress state.

The failure wedge obtained by the classical methods and the Finite Element analysis are not identical, even so they maintain a close similarity.

Even though the anchor force is increased, the overall stability is barely increased. An anchor force increase of 200% does not lead into a double safety factor. For a theoretical anchor force value, the classical methods predict the behaviour of the wall fairly well. On the other hand, when the anchor force is increased, the stress state of the soil is altered and the failure mechanism differs from the classical methods prediction. Regardless of the anchor prestressing force, the final anchor load appears to trend to an equilibrium load.

After comparing numerical results with the classical methods in anchored walls, the failure mechanism given by the Finite Element analysis suggests an intermediate failure state, where the sheet pile wall describes a translation movement on the deep zone, and at the same time a rotation movement around the anchor point.

Small variations of the cohesion lead to a significant rise of the safety factor. Consequently, ignoring this parameter provides reliability, but considering it wrongly may have severe consequences.

References

36. BARDEN, L. (1974) "Sheet pile wall design based on Rowe's method". Part III of "A comparison of quay wall design methods". CIRIA Technical Note 54.
37. BICA, A. V. D. & CLAYTON, C. R. I. (1989) "Limit equilibrium design methods for free embedded cantilever walls in granular materials". ICE Proceedings, Part 1, 86, 879-898.
38. BLUM, H. (1931) Einspannungsverhältnisse bei Bohlwerken. W. Ernst & Sohn. Berlin.
39. BOWLES, J. E. (1988) "Foundation analysis and design". McGraw-Hill, 4th Edition. New York.
40. BRANSBY, P. L. & MILLIGAN, G. W. E. (1975) "Soil deformations near cantilever sheet pile walls". Géotechnique 25, No. 2, 175-195.
41. CHERUBINI, C., GARRASI, A., PETROLLA, C. (1992) "The reliability of an anchored sheet pile wall embedded in a cohesionless soil". Canadian Geotechnical Journal, 29, 426-435.
42. CHUGH, A. K. & LABUZ, J. F. (2011) Numerical simulation of an instrumented cantilever wall". Canadian Geotechnical Journal, 48, 1303-1313.
43. DAY, R. A. & POTTS, D. M. (1993) "Modelling sheet pile retaining walls". Computers and Geotechnics, 15, 125- 143.
44. DAY, R. A. (1999) "Net pressure analysis of cantilever sheet pile walls". Géotechnique, 49, No.2, 231-245.
45. DAY, R. A. (2001) "Earth pressure on cantiléver walls at design retained heights". ICE Proceedings Geotechnical Engineering, 149, Issue 3, 167-176.
46. FOURIE, A. B. & POTTS, D. M. (1989) "Comparison of a finite element and limiting equilibrium analyses for an embedded cantilever retaining wall". Géotechnique 39, No.2, 175-188.
47. HANNAH, T. H. (1987) "Ground anchorages: anchor testing - measuring absolute movement". ICE Proceedings, 82, Part 1, 639-644.
48. KING, G. J. W. (1995) "Analysis of cantilever sheet-pile walls in cohesionless soil". Journal of Geotechnical Engineering, Vol. 121, No.9.
49. MA, J., BERGGREN, B., BENGTSSON, P., STILLE, H., HINTZE, S. (2009) "Behaviour of anchored walls in soils overlying rock in Stockholm". International Journal of Geoengineering Case Histories Vol. 2, Issue 1, 1-23.
50. MILLIGAN, G. W. E. (1983) "Soil deformations near anchored sheet-pile walls". Géotechnique 33, No.1, 41-55.
51. OSMAN, A. S. & BOLTON, M. D. (2004) "A new design method for retaining walls in clay". Canadian Geotechnical Journal, 41, 451-466.

52. PADFIELD, C. J. &MAIR, R. J. (1984) “Design of retaining walls embedded in stiff clay”. CIRIA Report 104.
53. PLANT, G. W. (1972) “Anchor inclination - its effect on the performance of a laboratory scale tied-back retaining wall”. ICE Proceedings, Part 2.
54. Plaxis 8.2. (www.plaxis.nl)
55. POTTS, D. M. & FOURIE, A. B. (1984) “The behaviour of a propped retaining wall: results of a numerical experiment”. Géotechnique 34, No.3, 383-404.
56. POWRIE, W. (1996) “Limit equilibrium analysis of embedded retaining walls”. Géotechnique, 46, No.4, 709-723.
57. RICHARDS, D. J. & POWRIE, W. (1994) “Finite element analysis of construction sequences for propped retaining walls”. ICE Proceedings, 107, 207-216.
58. ROWE, P. W. (1952) “Anchored sheet-pile walls”. ICE Proceedings. Part I, Vol. I.
59. ROWE, P. W. (1955) “A theoretical and experimental analysis of sheet-pile walls”. ICE Proceedings. Part I, Vol. I.
60. ROWE, P. W. (1955) “Sheet-pile walls encastré at the anchorage”. ICE Proceedings. Part I, Vol. I.
61. ROWE, P. W. (1956) “Sheet-pile walls at failure”. ICE Proceedings.
62. ROWE, P. W. (1957) “Sheet-pile walls subject to line resistance above the anchorage”. ICE Proceedings.
63. ROWE, P. W. (1957) “Sheet-pile walls in clay”. ICE Proceedings. Part I, Vol. I.
64. SCHRIVER, A. B. &VALSANGKAR, A. J. (1996) “Anchor rod forces and maximum bending moments in sheet pile walls using the factored strength approach”. Canadian Geotechnical Journal, 33, 815-821.
65. SIMPSON, B. (2000) “Partial factors: where to apply them?” International Workshop on Limit State Design in Geotechnical Engineering. Melbourne, Australia.
66. ŠKRABL, S. (2006) “Interactional approach of cantilever pile walls analysis”. ActaGeotechnicaSlovenica, 2006/1.
67. USS (1975) “Steel Sheet Piling Design Manual”. United States Steel.
68. VALSANGKAR, A. J. &SCHRIVER, A. B. (1991) “Partial and total factors of safety in anchored sheet pile design”. Canadian Geotechnical Journal, 28, 812-817.
69. YOUSSEF, Y. G. (2003) “Berms for stabilizing earth retaining structures”. Faculty of Engineering of Cairo University. Fayoum, Egypt.

ANEEX II: BIBLIOGRAPHIC REVIEW

A summary of the most relevant literature is presented below.

Author	Design method	Theory	Factor of safety	Wall friction	Depth increase
Engels	Engels	Rankine	Allowable stress	-	Not necessary
Krey	Krey	Coulomb	1-3 on lower end	2ϕ/3 to ϕ 0 passive lower end	Not necessary
Jacoby	Krey	Rankine	1.2 embedment	-	Not necessary
Lee	Krey	Rankine corrected for friction	1.43 embedment	O active, 17º to ϕ/2 passive	Not necessary
US Steel	Krey	Caquot and Kerisel	1.2-1.4 on embedment	17º for sand and steel	Not necessary
Blum	Blum	Rankine corrected for friction	1.0	Up to 0.4ϕ	Approximated by wall friction correction
Schmidt	Blum	Rankine active, 2 Rankine passive	1.0	2ϕ/3	Approximated by 1.2d’
Verdeyen and Roisin	Blum	Rankine active, 2 Rankine passive	1.1-1.5 for ϕ>25º	-	Approximated by 1.2d’
Costet and Sanglerat	Blum	Caquot and Kerisel	2 on Kp	2ϕ/3 active, 0.7ϕ passive	Approximated by 1.2d
CP-2	Blum	Packshaw	2 on Kp	15º active, 7.5º passive	-
Padfield and Mair-Fp	Blum	Caquot and Kerisel	1.2-1.5 on Kp	2ϕ/3 active, ϕ/2 passive	Approximated by 1.2d
Padfield and Mair-Fs	Blum	Caquot and Kerisel	1.2 on tanϕ	2ϕ/3 active, ϕ/2 passive	Approximated by 1.2d
Padfield and Mair-Fr	Blum	Caquot and Kerisel	1.5	2ϕ/3 active, ϕ/2 passive	Approximated by 1.2d
Lechner		Coulomb	1.0	2ϕ/3	Approximated by 1.2d’
Clayton and Milititsky	Blum	Mayniel active, Caquot and Kerisel passive	1.5 on Kp	ϕ/2 active, 2ϕ/3 passive	Approximated by 1.2d
Rowe	Rowe	Coulomb	1.5 on safe d, And 1 for M_{max}	O for safe d, 2ϕ/3 for M_{max}	No
Hong Kong GCO	Rowe	Caquot and Kerisel	3 on tan ϕ and tanδ for Kp	ϕ72	No
Danish Geotechnical Institute	Brinch Hansen	Brinch Hansen	1.2 to 1.3 on tanϕ	ϕ, but mobilized value might	Not necessary

				be smaller	
Canadian Geotechnical Society	Blum	Rankine active (see ref.44 for Kp)	1.0	O active, $\phi/2$-$2\phi/3$ passive	No

Design methods for free embedded cantilever walls based on limit equilibrium analyses

ANNEX III: STUDY OF THE K_0 INFLUENCE

Cantilever sheet pile wall with 5 m of retained height and 5 m of embedment depth (h = 5 m, d = 5 m)

Results from software Plaxis

	ϕ (°)	Stages	U_x (10^{-3}m)	M_{max} (kNm)	ΣMstage	State	1-ΣMstage	Steps
K_0=0,3	45	1	6,39	61,92	0,9995	ok	0,0005	67
	40	1	14,62	86,73	1	ok	0	104
	35	1	20,87	115,05	1	ok	0	130
	30	1	32,74	162,09	0,9997	ok	0,0003	88
	27	1	46,04	200,13	1	ok	0	93
	26	1	52,39	218,49	0,9999	ok	1E-04	148
	25	1	60,04	236,91	0,9995	ok	0,0005	165
	24	1	73,76	257,86	0,9995	ok	0,0005	238
	23	1	101,19	278,12	0,9967	col	0,0033	271
	22	1	108,49	278,92	0,9742	col	0,0258	282
	21	1	103,47	273,06	0,9444	col	0,0556	225
	Staged Excavation							
	26	5	43,25	201,18	0,9329	col	0,0671	337
	25	5	56,54	235,64	0,9994	ok	0,0006	422
	24	5	61,49	243,4	0,9415	col	0,0585	489
	23	5	49,29	219,06	0,697	col	1	368
	22	5	76,1	259,74	0,7933	col	0,2067	506

	ϕ (°)	Stages	U_x (10^{-3}m)	M_{max} (kNm)	ΣMstage	State	1-ΣMstage	Steps
K_0=1	45	1	6,81	63,01	0,9998	ok	0,0002	91
	40	1	9,11	80,84	0,9991	ok	0,0009	59
	35	1	13,2	110,5	1	ok	0	53
	30	1	19,97	154,9	1	ok	0	54
	27	1	28,4	200,93	1	ok	0	55
	26	1	31,91	213,7	0,9994	ok	0,0006	60
	25	1	36,79	234,8	0,9994	ok	0,0006	62
	24	1	43,77	257,09	1	ok	0	67
	23	1	56,39	284,43	1	ok	0	62
	22	1	126,21	310,17	0,9994	ok	0,0006	74
	21,5	1	96,13	300,17	0,986	col	0,014	87
	21	1	98,86	294,96	0,9741	col	0,0259	79
	20	1	214,43	288,27	0,951	col	0,049	76
	Staged Excavation							
	25	5	36,84	235,45	1	ok	0	116
	24	5	43,45	256,04	0,9998	ok	0,0002	144
	23	5	54,16	280,47	0,9995	ok	0,0005	202
	22	5	73,54	300,04	0,9634	col	0,0366	267
	21	5	69,3	292,97	0,8151	col	0,1849	169

	ϕ (º)	Stages	U_x (10^{-3}m)	M_{max} (kNm)	ΣMstage	State	1-ΣMstage	Steps
	45	1	7,21	44,63	0,8557	col	0,1443	34
	40	1	19,58	88,13	0,9991	ok	0,0009	107
	35	1	25	108,8	0,9999	ok	1E-04	64
	30	1	34,56	153,31	0,9995	ok	0,0005	69
	27	1	45,51	199,81	1	ok	0	59
	26	1	50,2	212,7	0,9999	ok	1E-04	56
	25	1	57,17	237,08	1	ok	0	57
K_0=2	24	1	64,87	256,24	0,9996	ok	0,0004	55
	23	1	79,96	283,78	1	ok	0	60
	22	1	161,78	309,33	0,9993	ok	0,0007	68
	21	1	266,18	294,42	0,9821	col	0,0179	85
	Staged Excavation							
	25	5	56,09	234,95	0,9995	ok	0,0005	245
	24	5	65,21	256,64	0,9997	ok	0,0003	291
	23	5	77,89	280,92	0,9993	ok	0,0007	322
	22	5	99,4	296,16	0,9481	col	0,0519	432
	21	5	90,01	285,03	0,7825	col	0,2175	340

	ϕ (º)	Stages	U_x (10^{-3}m)	M_{max} (kNm)	ΣMstage	State	1-ΣMstage	Steps
	45	1	2,439	-29,74	0,1504	col	0,8496	13
	40	1	1,906	-33,54	-0,0361	col	1,0361	4
	35	1	3,055	-25,34	0,091	col	0,909	5
	30	1	49,42	156,28	1	ok	0	92
	27	1	54,61	197,74	0,9998	ok	0,0002	77
	26	1	58,25	210,95	0,9994	ok	0,0006	79
	25	1	63,58	235,55	0,9994	ok	0,0006	75
	24	1	70,42	256,9	1	ok	0	77
K_0=5	23	1	**83,62**	281,38	0,9997	ok	0,0003	75
	22	1	139,92	305,79	0,9987	col	0,0013	101
	21	1	149,04	289,66	0,9835	col	0,0165	81
	Staged Excavation							
	26	5	59,55	217,41	0,9993	ok	0,0007	273
	25	5	63,46	235,72	1	ok	0	278
	24	5	70,81	256,17	0,9992	ok	0,0008	310
	23	5	83,54	280,85	0,9998	ok	0,0002	342
	22	5	100,45	293,64	0,9412	col	0,0588	427

Case form A. Cuadrardo (2010)

	ϕ (º)	Stages	U_x (10^{-3}m)	M_{max} (kNm)	ΣMstage	State	1-ΣMstage	Steps
	45	1	3,76	56,67	0,9997	ok	0,0003	60
	40	1	6,51	78,55	1	ok	0	64
	33	1	14,81	127,15	1	ok	0	73
	31	1	19,18	143,94	0,9994	ok	0,0006	71
	30,5	1	20,99	150,77	1	ok	0	105
	30	1	22,76	156,65	0,9995	ok	0,0005	81
	29,5	1	24,74	164,41	0,9997	ok	0,0003	67
	29	1	27,07	174,09	1	ok	0	92
	28,5	1	29,34	181,6	0,9999	ok	1E-04	87
	28	1	31,67	187,95	0,9991	ok	0,0009	86
	27,5	1	34,46	195,21	0,9993	ok	0,0007	105
	27	1	37,11	199,97	0,9997	ok	0,0003	140
	26,9	1	37,79	201,03	0,9995	ok	0,0005	91
	26,8	1	38,35	202,25	0,9993	ok	0,0007	100
K_0=0,5	26,7	1	38,94	203,13	0,9995	ok	0,0005	136
	26,6	1	39,9	206,11	0,9996	ok	0,0004	116
	26,5	1	40,59	208	0,9993	ok	0,0007	140
	26	1	44,17	217,22	0,9995	ok	0,0005	134
	25,5	1	48,36	226,8	0,9992	ok	0,0008	148
	25	1	53,38	235,8	0,9992	ok	0,0008	153
	24	1	70,17	256,57	0,9992	ok	0,0008	258
	23	1	83,48	265,09	0,9867	col	0,0133	259
	22	1	94,92	269,52	0,968	col	0,032	283
	Staged Excavation							
	27	5	35,35	197,71	1	ok	0	277
	26	5	42,05	214,08	1	ok	0	329
	25	5	51,7	234,98	0,9993	ok	0,0007	425
	24	5	67,2	255,25	0,9994	ok	0,0006	552
	23	5	74,86	260,41	0,9191	col	0,0809	555
	22	5	70,54	255,29	0,7687	col	0,2313	477

	ϕ (º)	Stages	U_x (10^{-3}m)	M_{max} (kNm)	ΣMstage	State	1-ΣMstage	Steps
	45	1	5,09		1	ok	0	80
	40	1	7,2		1	ok	0	79
	35	1	10,96		1	ok	0	66
	30	1	18,07		1	ok	0	56
	27	1	26,25		1	ok	0	81
	26	1	30,96		1	ok	0	64
	25	1	36,73		1	ok	0	70
K_0=0,75	24	1	46,1		0,9996	ok	0,0004	74
	23	1	64,13		1	ok	0	83
	22	1	95,46		0,9907	col	0,0093	194
	21	1	79,15		0,9612	col	0,0388	134
	Staged Excavation							
	25	5				ok	1	
	24	5				ok	1	
	23	5				ok	1	
	22	5				col	1	
	21	5				col	1	

	ϕ (º)	Stages	U_x (10^{-3}m)	M_{max} (kNm)	ΣMstage	State	1-ΣMstage	Steps
K_0=1,5	45	1	9,53		0,9775	col	0,0225	111
	40	1	14,15		0,9994	ok	0,0006	100
	35	1	18,98		1	ok	0	59
	30	1	26,8		0,999	ok	0,001	62
	27	1	36,78		1	ok	0	51
	26	1	40,98		1	ok	0	51
	25	1	47,13		1	ok	0	52
	24	1	54,24		0,9991	ok	0,0009	57
	23	1	69,98		0,9998	ok	0,0002	59
	22	1	150,48		0,9996	ok	0,0004	66
	21	1	369,76		0,9808	col	0,0192	85
	Staged Excavation							
	25	5				ok	1	
	24	5				ok	1	
	23	5				ok	1	
	22	5				col	1	
	21	5				col	1	

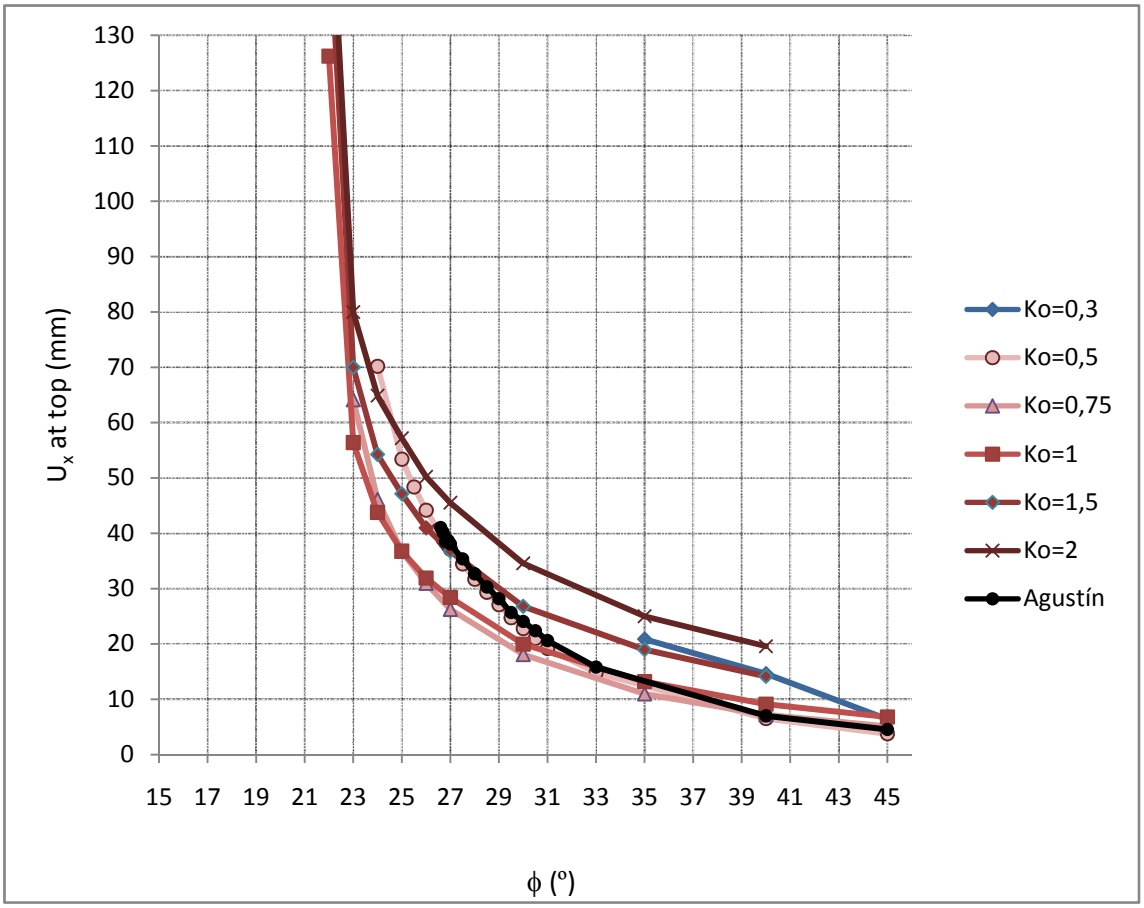

Evolution of the movement of the top of the wall when soil friction angle is decreased for the geometry *h* = 5 m, *d* = 5 m

Results for the same geometry h = 5 m d = 5 m. Relation between K_0 and U_x for a given friction angle.

K_0	ϕ (º)	Stages	U_x (10^{-3}m)	M_{max} (kNm)	ΣMstage	State	1-ΣMstage	Steps	Ux/max
0,25	30	1	32,71	161,96	0,9999	ok	1E-04	119	31,7%
0,5	30	1	21,71	156,15	0,9998	ok	0,0002	72	21,1%
0,7	30	1	17,79	154,68	1	ok	0	64	17,3%
0,75	30	1	18,07	156,01	1	col	0	56	17,5%
0,8	30	1	18,18	155,19	1	ok	0	68	17,6%
1	30	1	19,97	154,9	1	ok	0	54	19,4%
1,25	30	1	23,41	155,8	1	ok	0	56	22,7%
1,5	30	1	26,8	153,66	0,999	ok	0,001	62	26,0%
1,75	30	1	30,85	154,4	1	ok	0	64	29,9%
2	30	1	34,56	153,31	0,9995	ok	0,0005	69	33,5%

K_0	ϕ (º)	Stages	U_x (10^{-3}m)	M_{max} (kNm)	ΣMstage	State	1-ΣMstage	Steps	Ux/max
0,405	25	1	60,23	237,59	0,9994	ok	0,0006	174	58,4%
0,5	25	1	51,88	235,65	0,9991	ok	0,0009	176	50,3%
0,7	25	1	38,33		1	ok	0	85	
0,75	25	1	36,73	235,49	1	ok	0	70	35,6%
0,85	25	1	35,92		1	ok	0	82	
1	25	1	36,79	234,8	0,9994	ok	0,0006	62	35,7%
1,25	25	1	41,84	236,59	1	ok	0	57	40,6%
1,5	25	1	47,13	136,46	1	ok	0	52	45,7%
1,75	25	1	51,95	236,2	1	ok	0	55	50,4%
2	25	1	57,17	237,08	1	ok	0	57	55,4%

K_0	ϕ (º)	Stages	U_x (10^{-3}m)	M_{max} (kNm)	ΣMstage	State	1-ΣMstage	Steps	Ux/max
0,25	35	1	21,16	114,01	0,9996	ok	0,0004	75	20,5%
0,5	35	1	10,72	106,51	1	ok	0	60	10,4%
0,75	35	1	10,96	108,49	1	ok	0	66	10,6%
1	35	1	13,2	110,5	1	ok	0	53	12,8%
1,25	35	1	15,65	110,11	1	ok	0	75	15,2%
1,5	35	1	18,98	113,5	1	ok	0	59	18,4%
1,75	35	1	22,11	113,45	0,9997	ok	0,0003	53	21,4%
2	35	1	25	108,8	0,9999	ok	1E-04	64	24,2%

Viability of cases depending on the initial stress state:

ϕ (º)	Ka	Kp	K0=0,3	K0=0,485	K0=1	K0=2	K0=5
45	0,1716	5,8284	OK	OK	OK	OK	OK
44	0,1802	5,5500	OK	OK	OK	OK	OK
43	0,1891	5,2893	OK	OK	OK	OK	OK
42	0,1982	5,0447	OK	OK	OK	OK	OK
41	0,2077	4,8150	OK	OK	OK	OK	NO
40	0,2174	4,5989	OK	OK	OK	OK	NO
39	0,2275	4,3955	OK	OK	OK	OK	NO
38	0,2379	4,2037	OK	OK	OK	OK	NO
37	0,2486	4,0228	OK	OK	OK	OK	NO
36	0,2596	3,8518	OK	OK	OK	OK	NO
35	0,2710	3,6902	OK	OK	OK	OK	NO
34	0,2827	3,5371	OK	OK	OK	OK	NO
33	0,2948	3,3921	OK	OK	OK	OK	NO
32	0,3073	3,2546	NO	OK	OK	OK	NO
31	0,3201	3,1240	NO	OK	OK	OK	NO
30	0,3333	3,0000	NO	OK	OK	OK	NO
29	0,3470	2,8821	NO	OK	OK	OK	NO

28	0,3610	2,7698	NO	OK	OK	OK	NO
27	0,3755	2,6629	NO	OK	OK	OK	NO
26	0,3905	2,5611	NO	OK	OK	OK	NO
25	0,4059	2,4639	NO	OK	OK	OK	NO
24	0,4217	2,3712	NO	OK	OK	OK	NO
23	0,4381	2,2826	NO	OK	OK	OK	NO
22	0,4550	2,1980	NO	OK	OK	OK	NO
21	0,4724	2,1171	NO	OK	OK	OK	NO
20	0,4903	2,0396	NO	NO	OK	OK	NO
19	0,5088	1,9655	NO	NO	OK	NO	NO
18	0,5279	1,8944	NO	NO	OK	NO	NO
17	0,5475	1,8263	NO	NO	OK	NO	NO
16	0,5678	1,7610	NO	NO	OK	NO	NO
15	0,5888	1,6984	NO	NO	OK	NO	NO
14	0,6104	1,6383	NO	NO	OK	NO	NO

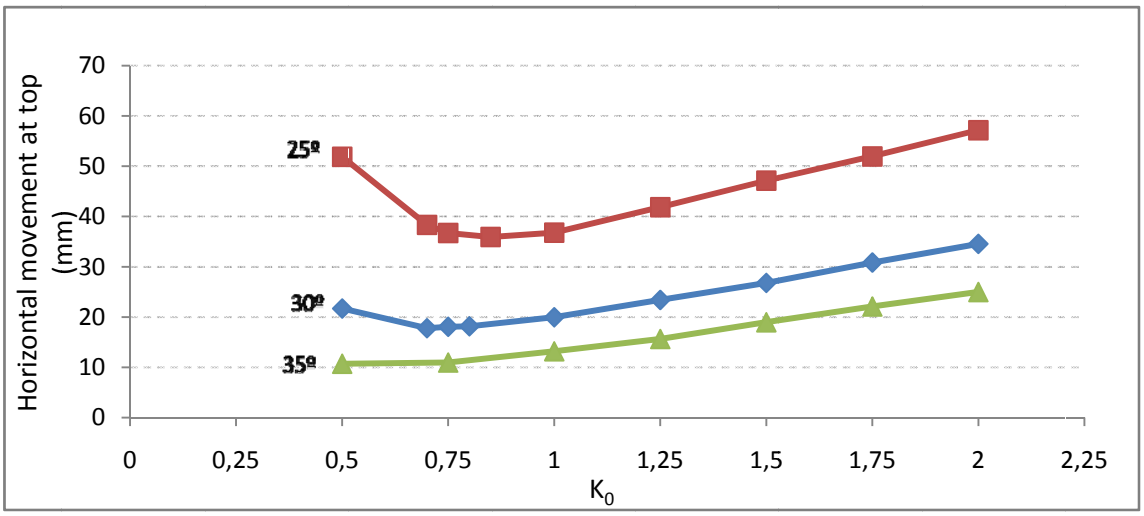

Relation between K_0 and horizontal movement

Cantilever sheet pile wall with 3 m of retained height and 5,4 m of embedment depth (h = 3 m, d = 5,4 m).

	Stages	ϕ (º)	U_x (10^{-3}m)	M_{max} (kNm)	ΣMstage	Estado	1-ΣMstage	Steps
K_0=0,25	1	35	2,78	25,01	1	ok	0	9
	1	30	4,23	36,65	1	ok	0	28
	1	25	7,98	53,74	0,9999	ok	1E-04	72
	1	23	9,81	63,3	1	ok	0	94
	1	21	11,95		0,999	-	0,001	93
	1	20	13,38	83,39	0,9994	ok	0,0006	107
	1	19	15,21	92,16	0,9996	ok	0,0004	143
	1	18	17,72	103,32	1	ok	0	146
	1	17	21,35	116,82	0,9997	ok	0,0003	141
	1	16	28	132,49	1	ok	0	56
	1	15	45,14	150,44	0,9991	-	0,0009	184
	1	14	166,95	159,15	0,9784	col	0,0216	79
	Staged Excavation							
	3	15	45,14	150,44	0,9991	-	0,0009	225
	3	14	166,95	159,15	0,9784	col	0,0216	125

	Stages	ϕ (º)	U_x (10^{-3}m)	M_{max} (kNm)	ΣMstage	Estado	1-ΣMstage	Steps
K_0=0,5	1	40		18,53	0,9997	ok	0,0003	15
	1	35		23,14	0,9991	ok	0,0009	17
	1	30	1,565	33,6	1	ok	0	24
	1	25	4,38	51,67	0,9997	ok	0,0003	39
	1	23	7,11	62,44	1	ok	0	77
	1	21	10,99	75,65	1	ok	0	94
	1	20	12,94	83,6	0,9997	ok	0,0003	110
	1	19	15,08	92,45	1	ok	0	121
	1	18	17,5	103,32	0,9997	ok	0,0003	128
	1	17	21,11	116,95	0,9995	ok	0,0005	146
	1	16	27,41	132,16	0,9994	ok	0,0006	163
	1	15	45,41	150,8	1	ok	0	66
	1	14	4180	160,58	0,9811	col	0,0189	304
	Staged Excavation							
	3	15	45,41	150,8	1	ok	0	103
	3	14	4180	160,58	0,9811	col	0,0189	337

	Stages	ϕ (º)	U_x (10^{-3}m)	M_{max} (kNm)	ΣMstage	Estado	1-ΣMstage	Steps
K_0=0,75	1	35	1,141	27,03	1	ok	0	17
	1	30	1,79	34,66	1	ok	0	25
	1	25	3,13	50,1	1	ok	0	33
	1	23	4,14	60,28	0,9998	ok	0,0002	33
	1	21	5,68	73,85	1	ok	0	39
	1	20	6,761	82,07	1	ok	0	45
	1	19	8,26	91,49	1	ok	0	46
	1	18	10,32	103,23	1	ok	0	45
	1	17	13,29	116,03	0,9998	ok	0,0002	51
	1	16	18,52	131,82	1	ok	0	53
	1	15	31,51	150,39	0,9996	ok	0,0004	60
	1	14	496,72	160,3	0,9808	col	0,0192	78
	Staged Excavation							
	3	15	31,51	150,39	0,9996	ok	0,0004	93
	3	14	496,72	160,3	0,9808	col	0,0192	117

	Stages	ϕ (º)	U_x (10^{-3}m)	M_{max} (kNm)	ΣMstage	Estado	1-ΣMstage	Steps
	1	35	0,679	23,17	1	ok	0	16
	1	30	1,62	33,71	1	ok	0	24
	1	25	4,9	51,97	1	ok	0	51
	1	20	13,26	83,5	1	ok	0	127
	1	19	15,14	92,65	1	ok	0	52
	1	18	17,46	103,15	0,9993	ok	0,0007	125
K_0=0,485	1	17	21,01	116,4	0,9996	ok	0,0004	147
	1	16	27,31	131,78	0,9993	ok	0,0007	155
	1	15	45,36	150,74	1	ok	0	65
	1	14	151,54	158,88	0,9786	col	0,0214	76
	Staged Excavation							
	3	16	27,31	131,78	0,9993	ok	0,0007	189
	3	15	45,36	150,74	1	ok	0	94
	3	14	151,54	158,88	0,9786	col	0,0214	108
	3	13	351,99	151,49	0,9282	col	0,0718	116

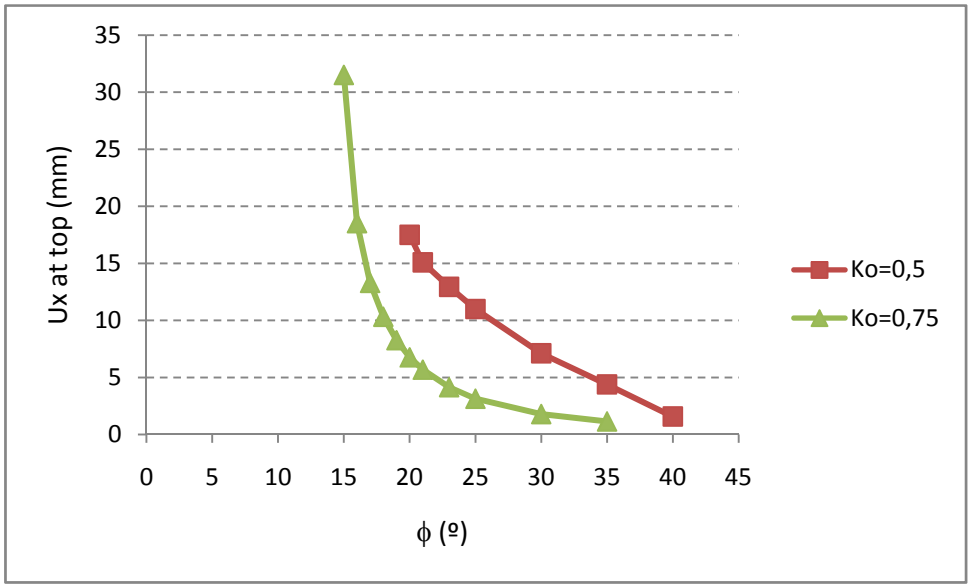

Evolution of the horizontal movement as soil friction angle is decreased for the geometry *h* = 3 m, *d* = 5.4 m

ANNEX IV: MULTIPLE-ANCHORED SHEET PILE WALLS

Results form Plaxis for the three-level-anchored sheet pile wall. Retained height h = 12m. Embedment depth d = 3 m.

Tables below show all the cases considered and the stages followed in Plaxis. In the right column are the results.

CASE 1 "Ah12d3-simultaneoETAPAS-Ko1-36"		M_{MAX}	Displ.Hzt.$_{MAX}$
STAGE 1	Excavation 1 m	530,44	83,83
STAGE 2	Excavation 1 m	location (from top)	location (from top)
STAGE 3	Pre-stress 125 kN/m upper anchor	10	6,5
STAGE 4	Excavation 1 m		
STAGE 5	Excavation 1 m	Displ.Hzt.$_{TOP}$	Displ.Hzt.$_{TOE}$
STAGE 6	Excavation 1 m	68	16,86
STAGE 7	Excavation 1 m		
STAGE 8	Excavation 1 m	$M_{upper\ anchor}$	$M_{lower\ anchor}$
STAGE 9	Pre-stress 125 kN/m lower anchor	44	145,55
STAGE 10	Excavation 1 m		
STAGE 11	Excavation 1 m		
STAGE 12	Excavation 1 m		
STAGE 13	Excavation 1 m		
STAGE 14	Excavation 1 m		

CASE 2 "Ah12d3-CASE2-Ko1-36"		M_{MAX}	Displ.Hzt.$_{MAX}$
STAGE 1	Excavation 1 m	533,25	89,44
STAGE 2	Excavation 1 m	location (from top)	location (from top)
STAGE 3	Excavation 1 m	10	6
STAGE 4	Pre-stress 125 kN/m upper anchor		
STAGE 5	Excavation 1 m	Displ.Hzt.$_{TOP}$	Displ.Hzt.$_{TOE}$
STAGE 6	Excavation 1 m	75,78	16,66
STAGE 7	Excavation 1 m		
STAGE 8	Excavation 1 m	$M_{upper\ anchor}$	$M_{lower\ anchor}$
STAGE 9	Excavation 1 m	47,32	160,19
STAGE 10	Pre-stress 125 kN/m lower anchor		
STAGE 11	Excavation 1 m		
STAGE 12	Excavation 1 m		
STAGE 13	Excavation 1 m		
STAGE 14	Excavation 1 m		

CASE 3 "Ah12d3-CASE3-Ko1-36"		M_{MAX}	Displ.Hzt.$_{MAX}$
STAGE 1	Excavation 1 m	525,96	101,96
STAGE 2	Excavation 1 m	location (from top)	location (from top)
STAGE 3	Excavation 1 m	10	5
STAGE 4	Excavation 1 m		
STAGE 5	Pre-stress 125 kN/m upper anchor	Displ.Hzt.$_{TOP}$	Displ.Hzt.$_{TOE}$
STAGE 6	Excavation 1 m	93,28	16,16
STAGE 7	Excavation 1 m		
STAGE 8	Excavation 1 m	$M_{upper\ anchor}$	$M_{lower\ anchor}$
STAGE 9	Excavation 1 m	46,73	187,39
STAGE 10	Excavation 1 m		
STAGE 11	Pre-stress 125 kN/m lower anchor		
STAGE 12	Excavation 1 m		
STAGE 13	Excavation 1 m		
STAGE 14	Excavation 1 m		

CASE 4 "Ah12d3-CASE4-Ko1-36"		M_{MAX}	Displ.Hzt.$_{MAX}$
STAGE 1	Excavation 1 m	546,64	133,51
STAGE 2	Excavation 1 m	location (from top)	location (from top)
STAGE 3	Excavation 1 m	10	3,125
STAGE 4	Excavation 1 m		
STAGE 5	Excavation 1 m	Displ.Hzt.$_{TOP}$	Displ.Hzt.$_{TOE}$
STAGE 6	Pre-stress 125 kN/m upper anchor	130,7	15,16
STAGE 7	Excavation 1 m		
STAGE 8	Excavation 1 m	$M_{upper\ anchor}$	$M_{lower\ anchor}$
STAGE 9	Excavation 1 m	48,58	239,05
STAGE 10	Excavation 1 m		
STAGE 11	Excavation 1 m		
STAGE 12	Pre-stress 125 kN/m lower anchor		
STAGE 13	Excavation 1 m		
STAGE 14	Excavation 1 m		

CASE 5 "Ah12d3-CASE5-Ko1-36"		M_{MAX}	Displ.Hzt.$_{MAX}$
STAGE 1	Excavation 1 m		
STAGE 2	Excavation 1 m	location (from top)	location (from top)
STAGE 3	Excavation 1 m		
STAGE 4	Excavation 1 m	Displ.Hzt.$_{TOP}$	Displ.Hzt.$_{TOE}$
STAGE 5	Excavation 1 m		
STAGE 6	Pre-stress 125 kN/m upper anchor		COLLAPSE
STAGE 7	Excavation 1 m + P1	$M_{upper\ anchor}$	$M_{lower\ anchor}$
STAGE 8	Excavation 1 m + P1		
STAGE 9	Excavation 1 m + P1		
STAGE 10	Excavation 1 m + P1		
STAGE 11	Excavation 1 m + P1		
STAGE 12	Pre-stress 125 kN/m lower anchor		
STAGE 13	Excavation 1 m + P1 + P2		
STAGE 14	Excavation 1 m + P1 + P2		

CASE 6 "Ah12d3-CASE6-Ko1-36"		M_{MAX}	Displ.Hzt.$_{MAX}$
STAGE 1	Excavation 1 m	499,24	183,47
STAGE 2	Excavation 1 m	location (from top)	location (from top)
STAGE 3	Excavation 1 m	9,875	0
STAGE 4	Excavation 1 m		
STAGE 5	Excavation 1 m	Displ.Hzt.$_{TOP}$	Displ.Hzt.$_{TOE}$
STAGE 6	Excavation 1 m	183,47	14,47
STAGE 7	Pre-stress 125 kN/m upper anchor		
STAGE 8	Excavation 1 m	$M_{upper\ anchor}$	$M_{lower\ anchor}$
STAGE 9	Excavation 1 m	48,99	176,16
STAGE 10	Excavation 1 m		
STAGE 11	Excavation 1 m		
STAGE 12	Pre-stress 125 kN/m lower anchor		
STAGE 13	Excavation 1 m		
STAGE 14	Excavation 1 m		

CASE 7 "Ah12d3-CASE7-Ko1-36"		M_{MAX}	Displ.Hzt.$_{MAX}$
STAGE 1	Excavation 1 m	670,66	305,25
STAGE 2	Excavation 1 m	location (from top)	location (from top)
STAGE 3	Excavation 1 m	9,375	0
STAGE 4	Excavation 1 m		
STAGE 5	Excavation 1 m	Displ.Hzt.$_{TOP}$	Displ.Hzt.$_{TOE}$
STAGE 6	Excavation 1 m	305,25	11,48
STAGE 7	Excavation 1 m		
STAGE 8	Pre-stress 125 kN/m upper anchor	$M_{upper\ anchor}$	$M_{lower\ anchor}$
STAGE 9	Excavation 1 m	46,78	463,95
STAGE 10	Excavation 1 m		
STAGE 11	Excavation 1 m		
STAGE 12	Excavation 1 m		
STAGE 13	Pre-stress 125 kN/m lower anchor		
STAGE 14	Excavation 1 m		

CASE 8 "Ah12d3-CASE8-Ko1-36"		M_{MAX}	Displ.Hzt.$_{MAX}$
STAGE 1	Excavation 1 m		
STAGE 2	Excavation 1 m	location (from top)	location (from top)
STAGE 3	Excavation 1 m		
STAGE 4	Excavation 1 m	Displ.Hzt.$_{TOP}$	Displ.Hzt.$_{TOE}$
STAGE 5	Excavation 1 m		
STAGE 6	Excavation 1 m	COLLAPSE	
STAGE 7	Excavation 1 m	$M_{upper\ anchor}$	$M_{lower\ anchor}$
STAGE 8	Excavation 1 m		
STAGE 9	Pre-stress 125 kN/m upper anchor		
STAGE 10	Excavation 1 m		
STAGE 11	Excavation 1 m		
STAGE 12	Excavation 1 m		
STAGE 13	Excavation 1 m		
STAGE 14	Pre-stress 125 kN/m lower anchor		

CASE 6.1 "Ah12d3-CASE6.1-Ko1-36"		M_{MAX}	Displ.Hzt.$_{MAX}$
STAGE 1	Excavation 1 m		
STAGE 2	Excavation 1 m	location (from top)	location (from top)
STAGE 3	Excavation 1 m		
STAGE 4	Excavation 1 m	Displ.Hzt.$_{TOP}$	Displ.Hzt.$_{TOE}$
STAGE 5	Excavation 1 m	COLLAPSE	
STAGE 6	Excavation 1 m		
STAGE 7	Pre-stress 125 kN/m upper anchor	$M_{upper\ anchor}$	$M_{lower\ anchor}$
STAGE 8	Excavation 1 m		
STAGE 9	Excavation 1 m		
STAGE 10	Excavation 1 m		
STAGE 11	Excavation 1 m		
STAGE 12	Excavation 1 m		
STAGE 13	Pre-stress 125 kN/m lower anchor		
STAGE 14	Excavation 1 m		

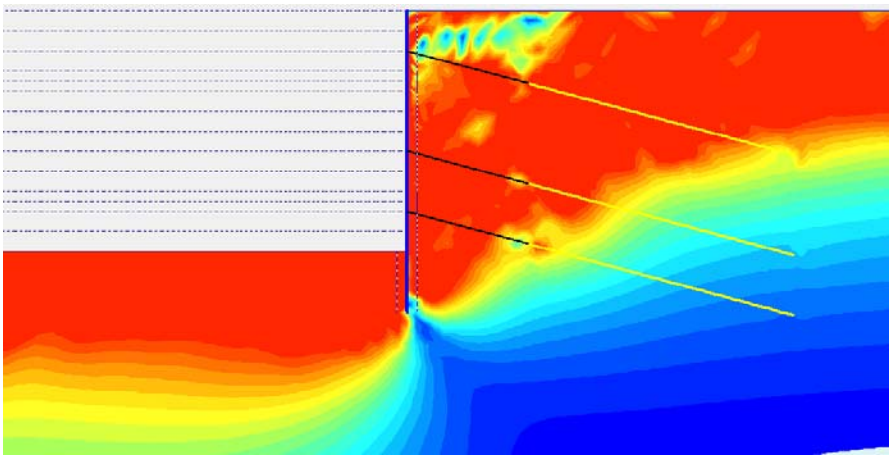

Relative shear stresses around a three-level-anchored sheet pile wall. Dark and clear shadings represent lower and higher values of stress respectively.

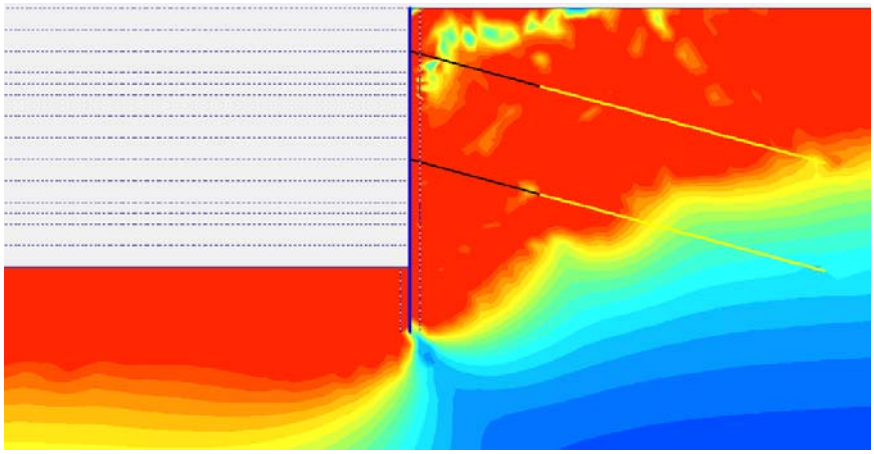

Relative shear stresses around a two-level-anchored sheet pile wall

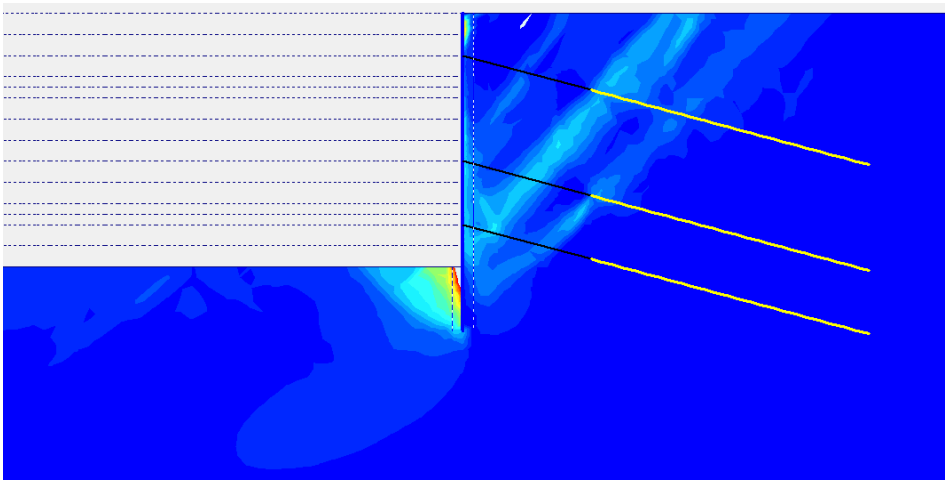

Shear strains around a three-level-anchored sheet pile wall. Dark and clear shadings represent lower and higher values of strain respectively. Maximum strain 7,04% scale 0% to 3,6%

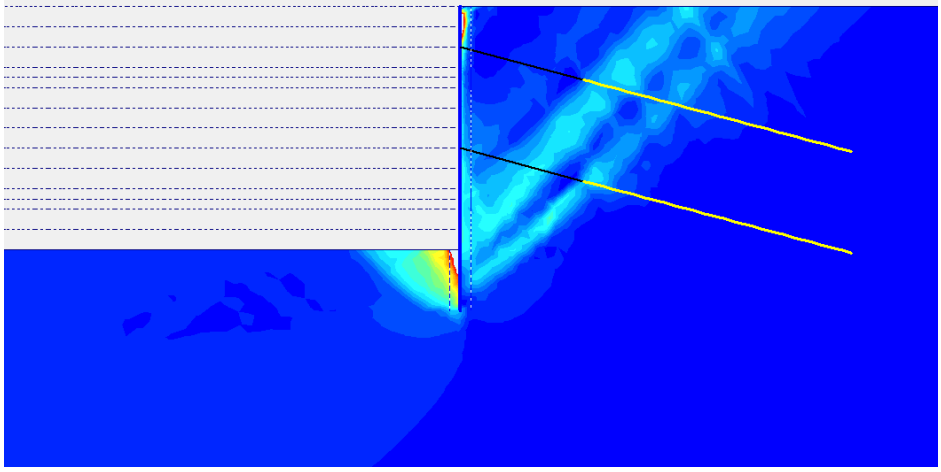

Shear strains around a two-level-anchored sheet pile wall. Maximum strain 8,46% 0% to 3,6%